

الجمهورية الجزائرية الديمقراطية الشعبية

REPUBLIQUE ALGERIENNE DEMOCRATIQUE ET POPULAIRE

وزارة التعليم العالي والبحث العلمي

Ministère de l'Enseignement Supérieur et de la Recherche Scientifique

جامعة أبي بكر بلقايد - تلمسان

Université Aboubakr Belkaïd – Tlemcen –

Faculté de TECHNOLOGIE



THESE

Présentée pour l'obtention du **grade de DOCTORAT 3^{ème} Cycle**

En : Génie Biomédical

Spécialité : Télémedecine

Par : BENABDALLAH Hadjer

Sujet

**La Bioimpédancemétrie Appliquée au diagnostic médical :
Application au Signal ICG**

**The Bioimpedancemetry Applied in Medical Diagnosis:
The ICG Signal Application**

Soutenue publiquement, le 06/ 07 / 2022, devant le jury composé de:

M Hamza CHERIF Lotfi	Professeur	Univ. Tlemcen	Président
M KERAI Salim	MCA	Univ. Tlemcen	Directeur de thèse
Mme SOUFI Yamina	Professeur	Centre universitaire de Maghnia	Examineur 1
M BENALI Redouane	MCA	Univ. Tlemcen	Examineur 2

NB : les membres du jury doivent être classés conformément au P.V d'autorisation de soutenance.

Dedications

*It is with genuine gratitude and warm regard that I
dedicate this Thesis:*

*To my loving **parents** with a special feeling of
gratitude,*

*To my dearest **husband**,*

*To my beloved **brother** and **sisters**,*

*To all my **family**,*

*To my **teachers** and **colleagues** at the University of
Tlemcen, Algeria,*

I give special thanks to everyone I love.

*This dissertation is dedicated to each person who
encouraged me to pursue my dreams and supported me
to finish my research.*

Acknowledgement

In the first step, I would thank god for helping me in my research. I would like to express my gratitude to several people who helped me releasing my thesis.

*I would like to thank the entire teachers' team (Abou Bekr Belkaid) I would also like to thank the members of the **Biomedical Engineering Laboratory (GBM)**, where this work was carried out and finalised.*

*I would like to express my gratitude to my supervisor **Dr. KERAI Salim**. Many thanks to him because he oriented, helped, and advised me.*

I would also like to thank all my professors for the help and advice they gave me for the missions mentioned in this thesis.

I would particularly like to thank the jury members:

***Mr. Hamza CHERIF Lotfi** professor at the University of Tlemcen,
Mrs. SOUFI Yamina professor at Maghnia University Center,
Mr BENALI Redouane MCA at University of Tlemcen.*

To all contributors, I extend my respect, gratitude, and thanks.

Abstract

Thanks to advances in the biomedical technology field, Hemodynamic monitoring can be carried out with non-invasive methods such as impedance cardiography. This technique is reliable, safe, simple, secure, and less expensive; it is used for the diagnosis and continuous monitoring of cardiovascular diseases.

The non- invasive ICG technique comes to solve the complexity problem for measurement and analyzing heart diseases based on the thoracic electrical impedance change assessment that is due to blood velocity and resistivity changes in order to estimate several hemodynamic parameters.

This type of signal is altered by artefacts' which distort the significant information of the signal. This distortion will cause clinicians to misdiagnose or monitor the pathological state of patients, for whom it is important to find techniques to eliminate noises without destroying the varied morphology of the signal. For this reason, the signal processing field developed several denoising technique applied to respiratory and motion artifacts suppression without corrupting the shape of the signal.

Our three denoising methodologies are based on several comparative studies between different type of adaptive filters and Savitzky-Golay (SG) filtering, singular value decomposition (SVD) with least mean squares (LMS), the orthogonal wavelet family: Daubechies wavelets (db) and Symlet (sym) with several types of thresholding such as Shrinkage, NeighBlock and classical threshold as Rigrsure and Sqrtwolog; they are all compared with linear filters as well as with the LMS-based adaptive filter. The evaluation was done on 10 subjects and the results showed efficiency, where the best method in terms of noise reduction is sym8 wavelets at level 5, and the most optimal thresholding technique is the Rigrsure technique with a mean error rate (MER) equal to 0.0001 %.

The automatic detection of the characteristic points allowed us to calculate the cardiac indices and subsequently to extract significant information on the condition of each patient. In our work we developed an algorithm under Matlab for the processing and identification of characteristic points on the 10 ICG signals. This new algorithm aims to detect B, C and X points by using a simple mathematical model based on two bells to study ICG signals for 26 cycles; the pre-ejection and the ejection waves. The results significantly improve the efficacy and accuracy of LVET estimation for beat-to-beat estimation under conditions.

The detection is realised on ICG signals from 10 healthy subjects. The calculations results show effectiveness and accuracy; when compared with the normal range for a healthy person. To estimate cardiac indices and time intervals, we are finding a solution that is effective and simple. We have developed an application of automatic access to help the clinics to analyse ICG and electrocardiogram (ECG) signals, either locally or remotely.

This application aims to make available all necessary information to doctors that help them to establish a fast and reliable diagnosis either locally or remotely. This application is automatic access to the real-time application used to optimise the quality of care and speed of diagnosis, whatever their geographical location. It is performed according to two criteria: information storage and data manipulation. This application is based on three softwares: Java Netbeans, Matlab, and WAMP / EASYPHP (MySQL) for web development.

Keywords-- *ICG, ECG, Hemodynamic monitoring, Non-invasive, Denoising concept, Automatic detection, Automatic access application.*

Résumé

Grâce aux avancées dans le domaine de la technologie biomédicale, la surveillance hémodynamique peut être effectuée à l'aide des méthodes non invasives telles que la cardiographie par impédance. Cette technique est fiable, sûre, simple, sécurisée et moins coûteuse ; elle est utilisée pour le diagnostic et la surveillance continue des maladies cardiovasculaires.

La technique non invasive d'ICG vient pour résoudre le problème de complexité de la mesure et de l'analyse des maladies cardiaques, basant sur l'évaluation de changement d'impédance électrique thoracique qui est due aux changements de vitesse et de résistivité du sang afin d'estimer plusieurs paramètres hémodynamiques. Ce type de signal est altéré par des artefacts qui ruinent l'information significative du signal. Cette distorsion pousse les cliniciens vers un mauvais diagnostic et une mauvaise surveillance de l'état pathologique des patients, dans lesquels il est important de trouver des techniques pour éliminer les bruits sans détruire la morphologie de notre signal.

Pour cette raison, le domaine du traitement du signal a développé plusieurs techniques de débruitage appliquées à la suppression des bruits respiratoires et de mouvement sans déformer la forme du signal. Nos trois méthodologies de débruitage sont basées sur plusieurs études comparatives entre différents types de filtres adaptatifs et le filtrage Savitzky-Golay (SG), la décomposition en valeurs singulières (SVD) avec des carrés moyens maigres (LMS), la famille des ondelettes orthogonales : ondelettes de Daubechies (db) et Symlet (sym) avec plusieurs types de seuillage tels que Shrinkage, NeighBlock et seuil classique comme Rigrsure et Sqtwolog ; ils sont tous comparés aux filtres linéaires ainsi qu'au filtre adaptatif basé sur LMS. L'évaluation a été faite sur 10 sujets et les résultats ont montré une efficacité, où la meilleure méthode en termes de réduction de bruit est les ondelettes sym8 au niveau 5, et la technique de seuillage la plus optimale est la technique Rigrsure avec un taux d'erreur moyen (MER) égal à 0,0001 %.

La détection automatique des points caractéristiques nous a permis de calculer les indices cardiaques et par la suite d'extraire des informations significatives sur l'état de chaque patient. Dans notre travail, nous avons développé un algorithme sous Matlab pour le traitement et l'identification de points caractéristiques sur les 10 signaux ICG. Ce nouveau algorithme vise à détecter les points B, C et X en utilisant un modèle mathématique simple basé sur deux cloches pour étudier les signaux ICG pendant 26 cycles ; les ondes de pré-éjection et d'éjection. Les résultats améliorent considérablement

l'efficacité et la précision de l'estimation LVET pour l'estimation battement par battement dans certaines conditions.

La détection est réalisée sur les signaux ICG de 10 sujets sains. Les résultats des calculs montrent une efficacité et une précision ; par rapport à la plage normale d'une personne en bonne santé (saine). Pour estimer les indices cardiaques et les intervalles de temps, nous trouvons une solution efficace et simple. Nous avons développé une application d'accès automatique pour aider les cliniques à analyser les signaux ICG et électrocardiogramme (ECG), soit localement, ou à distance.

Cette application a pour objectif de mettre à disposition des médecins toutes les informations nécessaires pour les aider à établir un diagnostic rapide et fiable soit localement soit à distance. Cette application est un accès automatique en temps réel permettant d'optimiser la qualité des soins et la rapidité du diagnostic, quelle que soit leur situation géographique. Elle est réalisée selon deux critères : le stockage de l'information et la manipulation des données. Cette application est basée sur trois logiciels : Java Netbeans, Matlab, et WAMP/EASYPHP (MySQL) pour le développement web.

***Mots clés**-- ICG, ECG, Surveillance hémodynamique, Non invasif, Concept de débruitage, Détection automatique, Application d'accès automatique.*

الملخص

بفضل التقدم في التكنولوجيا الطبية الحيوية ، يمكن إجراء مراقبة الدورة الدموية باستخدام طرق غير جراحية مثل تخطيط القلب بالمقاومة. هذه التقنية موثوقة وأمنة وبسيطة وأمنة وأقل تكلفة ؛ يتم استخدامه للتشخيص والمراقبة المستمرة لأمراض القلب والأوعية الدموية. تأتي تقنية ICG السطحية لحل مشكلة تعقيد قياس وتحليل أمراض القلب ، بالاعتماد على تقييم تغير المعاوقة الكهربائية الصدرية والذي يرجع إلى التغيرات في سرعة الدم والمقاومة لتقدير العديد من معايير الدورة الدموية. يتم تغيير هذا النوع من الإشارات من خلال الاثار التي تدمر المعلومات المهمة للإشارة. يدفع هذا التشويه الأطباء نحو التشخيص الخاطئ والمراقبة السيئ لحالة المرضى ، حيث من المهم إيجاد تقنيات للقضاء على الضوضاء دون تدمير مورفولوجية إشارتنا. لهذا السبب ، طور مجال معالجة الإشارات العديد من تقنيات لتقليل الضوضاء المطبقة على قمع التنفس وضجيج الحركة دون تشويه شكل الإشارة. تعتمد منهجياتنا الثلاثة لتقليل الضوضاء على العديد من الدراسات المقارنة بين أنواع مختلفة من المرشحات التكيفية Savitzky - (SG) وتصفية وتحلل القيمة المفرد SVD مع المربعات المتوسطة الهزيلة LMS والأسرة الموجية المتعامدة (db)Daubechies وموجات letSym مع عدة أنواع من العتبات مثل الانكماش ، والكتلة المجاورة والعتبات الكلاسيكية مثل Rigrsure، تتم مقارنتها جميعاً بالمرشحات الخطية وكذلك المرشح التكيفي القائم على LMS. تم إجراء التقييم على 10 أشخاص وأظهرت النتائج كفاءة ، حيث كانت أفضل طريقة من حيث تقليل الضوضاء هي موجات Sym 8 عند المستوى 5 ، وأفضل تقنية عتبية هي تقنية Rigrsure مع معدل خطأ متوسط يساوي 0.0001%. سمح لنا الاكتشاف التلقائي للنقاط المميزة بحساب مؤشرات القلب وبالتالي استخراج معلومات مهمة عن حالة كل مريض. في عملنا ، قمنا بتطوير خوارزمية تحت Matlab للعلاج وتحديد النقاط المميزة في إشارات ICG العشر. تهدف هذه الخوارزمية الجديدة إلى اكتشاف النقاط B_iCX باستخدام نموذج رياضي بسيط يعتمد على جرسين لدراسة إشارات ICG لمدة 26 دورة ؛ موجات القذف والقذف. النتائج تحسن بشكل كبير كفاءة ودقة تقديري LVET ر نبضة تلو الأخرى في ظل ظروف معينة

يتم الكشف على إشارات ICG لـ 10 أشخاص أصحاء. تظهر نتائج الحسابات الكفاءة والدقة ؛ مقارنة بالنطاق الطبيعي للشخص السليم (السليم). لتقدير مؤشرات القلب والفترات الزمنية ، نجد حلاً فعالاً وبسيطاً. لقد قمنا بتطوير تطبيق وصول تلقائي لمساعدة العيادات على تحليل إشارات ICG وتخطيط القلب EGC إما محلياً أو عن بُعد. يهدف هذا التطبيق إلى تزويد الأطباء بجميع المعلومات اللازمة لمساعدتهم على إجراء تشخيص سريع وموثوق سواء محلياً أو عن بُعد. هذا التطبيق هو وصول تلقائي في الوقت الحقيقي لتحسين جودة الرعاية وسرعة التشخيص ، بغض النظر عن موقعهم الجغرافي. يتم تنفيذه وفقاً لمعيارين: تخزين المعلومات ومعالجة البيانات. يعتمد هذا التطبيق على ثلاثة برامج:

Wamp/EasyPHP(MYSQL), Matlab ,Java Netbeans

الكلمات الرئيسية-- GCE ,GCI , مراقبة الدورة الدموية ، مفهوم عدم التوغل ، مفهوم تقليل الضوضاء ، الكشف التلقائي ، تطبيق الوصول التلقائي.

Table of content

General Introduction	1
Chapter I: Hemodynamic Monitoring	
I. Introduction.....	8
II. Hemodynamic Monitoring Techniques and Systems.....	9
a. Non Invasive.....	9
b. Minimally Invasive or Less_Invasive.....	11
c. Invasive.....	14
III. Discussion and conclusions.....	15
REFERENCES.....	16
Chapter II: The Electrical Bioimpedance	
I. Introduction.....	18
II. The Electrical Bioimpedance.....	19
1. Definition	19
2. Biological Tissues.....	20
3. The Dielectric Properties of Biological Tissues.....	22
4. The Dispersion Windows.....	22
a. A dispersion.....	23
b. β dispersion.....	23
c. γ dispersion.....	23
d. δ dispersion.....	23
5. The Electric Cellular Models.....	23
a. Frick-Morse mode.....	23
b. Debye model.....	24
c. Cole model.....	25
III. The Bioimpedance Measurement Methods.....	26
a. The two electrode method or the bipolar method.....	26
b. The three electrode method.....	27
c. The four-electrode method or the four-pole or Kelvin method.....	27
d. The five electrode method.....	28
IV. The Bioimpedance in Diagnosis.....	28
a. Bioelectrical Impedance Analysis (BIA)	29
b. The electrical impedance spectroscopy (EIS)	29
c. The electrical impedance plethysmography (IPG).....	30
d. The impedance cardiography (ICG).....	30
e. The electrical impedance tomography (EIT)	31
V. Materials used for Bioimpedance Measurement.....	31
VI. Conclusion.....	35
REFERENCES.....	36
Chapter III: The Impedance Cardiography Technique	
I. Introduction.....	41
II. Principal Methodology.....	42
1. Definition	42
2. ICG Features Extraction.....	43
3. Signal Processing.....	46
III. Conclusion.....	48
REFERENCES.....	49

Chapter IV: Denoising methods Applied for ICG signal Analysis	
I. Introduction.....	54
II.Method 1.....	57
III.Method 2.....	60
IV. Method 3.....	63
V.Conclusion	73
REFERENCES.....	74
Chapter V: Results obtaining from Denoising Techniques	
I. Introduction.....	79
II.Results of Method 1.....	79
• Validation step.....	83
III.Results of Method 2.....	85
• Discussion.....	87
IV.Results of Method 3.....	89
• Discussion.....	92
V.Conclusion.....	97
REFERENCES.....	98
Chapter VI: Feature Point Extraction from ICG waveform	
I. Introduction.....	100
II.Background of Detection Methods.....	101
• Discussion.....	105
III.A novel algorithm for B C X Points extraction.....	106
• Results and Discussion... ..	110
IV.Conclusion.....	113
REFERENCES.....	114
Chapter VII: Telemedicine Application of ICG Signals	
I. Introduction.....	119
II.Network Background.....	120
III.Our Developed Application.....	122
• MySQL connection with Matlab	124
• MySQL connection with Java Netbeans	126
IV.Results and Discussions.....	126
• Login interface	128
• Menu interface	128
• Users interface	128
• The ICG images storage	129
• Signals interface	129
• Results interface	129
V.Conclusion.. ..	135
REFERENCES.....	135
General Conclusion.....	136

Figures List

General Introduction

Figure 1: The typical ICG signal.	3
--	---

Chapter II: The Electrical Bioimpedance

Figure 2 : Fricke-Morse model [9].	23
Figure 3: The Debye circuit with an ideal component [7].	24
Figure 4: The Cole circuit [7].	25
Figure 5: The principal of Bioimpedance measurement.	26
Figure 6: The typical ICG signal [6].	31

Chapter III: The Impedance Cardiography Technique

Figure7: The Electrode configuration for ICG signal measurement [9] [10].	43
Figure 8: The characteristic extraction of the ICG waveform [5].	44
Figure 9: The typical ICG and ECG waveform [10].	44

Chapter IV: Denoising methods Applied for ICG signal Analysis

Figure 10 : The ICG signal cycles for subject 1.	55
Figure 11 : The cycles of ICG signal for subject 1 from 1 to 10cycles.	56
Figure 12: The adaptive filter structure.	57
Figure 13: The interpretable diagram of our processed methodology.	64
Figure 14: The signal wavelet decomposition.	66
Figure 15: Schematic diagram method.	71
Figure 16: Interpretable diagram algorithm.	72

Chapter V: Results obtaining from Denoising Techniques

Figure 17: Estimated the error results from the original and reconstructed signal after applying the adaptive filters as well as SavitzkyGolay filters on 10 ICG signals at different SNR _i , where (a) with $\mu=0.004$, (b) with $\mu=0.008$, and (c) with $\mu=0.01$	81
Figure 18: The reconstructed signal of each denoising technique.	82
Figure 19: LMS based method for ICG signal denoising.	85
Figure 20: SVD based method for ICG signal denoising.	86
Figure 21: Comparison between two methods: SVD and LMS for the denoising of the ICG signal.	86
Figure 22: The estimation parameters evaluation for all 10 subjects.	87
Figure 23: Comparison results between different types of thresholds at different SNR _i values.	90
Figure 24: Comparison results of performance parameters evaluation for Gaussian filter, LMS adaptive filter and various wavelets thresholds at different SNR _i values.	91
Figure 25: The ICG signal reconstructed after each technique applied for subject 1 for each technique.	93
Figure 26: The ICG signal samples reconstructed after applying the best denoising technique for all participants: subjects 1 to 10.	94

Chapter VI: Feature Point Extraction from ICG waveform

Figure 27: The characteristic feature points of the ICG waveform.	102
Figure 28: Extraction of the BCX point from ejection, pre-ejection and original signal for cycles from 1 to 7.	111

Chapter VII: Telemedicine Application of ICG Signals

Figure 29: The principle of our developed application.	120
Figure 30: (a) The local area network topology, (b) The wide area network topology.	121

Figure 31: The connection of Matlab and MySQL. (a) connect to database, (b) enter the IP address and port number, (c) test the connection, (d) MySQL database appeared in Matlab.	125
Figure 32: Login interface.	130
Figure 33: Menu interface.....	130
Figure 34: User's management interface; (a) search according to id, (b) add bottom option from the user interface, (c) add option saved to the server under the database..	131
Figure 35: (a), (b), (c) and (d) The images storage interface from Netbeans to the MySQL database in table 'icg_signal'	132
Figure 36: Signals interface. (a) search option with category id, (b) tables in the interface that presents the characteristics points of ICG and ECG signal processing in Matlab, (c) ecg table in the server, (d) icg table in the server.	133
Figure 37: The Results interface. (a) search with category id, (b) print option, (c) complete impression of the results presented in texfields, (d) results table.	134

Tables List

Chapter II: The Electrical Bioimpedance	
Table 1: The ions concentration in living tissue [13].	22
Table 2: Comparison between ANALYCOR and XITRON.	34
Chapter V: Results obtaining from Denoising Techniques	
Table 3: SNR, MSE estimation parameters results after simulation for 10 subjects at SNR _i 10 dB.	80
Table 4: Estimated MER results from the original and reconstructed signal after applying the adaptive filters with $\mu=0.01$, as well as Savitzky-Golay filters on 10 ICG signals at different SNR _i s.	83
Table 5: Estimated MER results from the original and reconstructed signal after applying the adaptive filters with $\mu=0.004$, as well as Savitzky-Golay filters on 10 ICG signals at different SNR _i .	84
Table 6: Estimated MER results from the original and reconstructed signal after applying the adaptive filters with $\mu=0.008$, as well as SavitzkyGolay filters on 10 ICG signals at different SNR _i .	84
Table 7: The C Point Coordinates of The Original Signal and The Reconstructed Signals of The LMS and The SVD Techniques.	88
Table 8: Estimation parameters of linear filters applied to 10 subjects.	89
Table 9: Detection of peak amplitudes C (Ohms) from original noise-free ICG signals.	95
Table 10: Mean error rate (%) of denoising methods for 10 subjects at different SNR _i (ranging from 0 to 35 dB).	96
Chapter VI: Feature Point Extraction from ICG waveform	
Table 11: The ICG parameters used for our algorithm.	109
Table 12: The LVET calculation for each cycle of ICG signal.	112
Chapter VII: Telemedicine Application of ICG Signals	
Table 13: Feature points extraction for ECG signal.	127
Table 14: Feature points extraction for ICG signal.	127
Table 15: Time intervals and hemodynamic parameters values.	128

Abbreviations

Z	Impedance
SV	Stroke volume, ml
SVI	Stroke volume index
SVV	Stroke Volume Variation
CO	Cardiac output, L/min
LVET	the left ventricle ejection time
VET	The ventricular ejection time
MAP	Mean arterial pressure
PPV	pulse pressure variation
SP	Systolic blood pressure
DP	Diastolic blood pressure
PP	Pulse blood pressure
PEP	Preejection period
TFC	Thoracic fluid content
HRV	Heart rate variability
IVRT	Isovolumic relaxation time
FT	Ventricular filling time
CWT	The continuous wavelet
DWT	The discrete wavelet transformation
IDWT	The inverse discrete wavelet transformation
ECG	Electrocardiogram
EEG	Electroencephalogram
VC	Volume clamp
PWA	Pulse wave analysis
PCA	Pulse contour analysis
RNV	Radionuclide angiography
RVG	Radionuclide ventriculography
ICU	Intensive care units
TTE	Transthoracic Doppler echocardiography
TPTD	Transpulmonary thermodilution
PAC	Pulmonary artery catheter
TBW	Total body water
FFM	Fat-free mass
BMI	Body cell mass index
BMR	Basal metabolic rate
BCM	Body cell mass
ECM	Extracellular mass
ICW	Intracellular water
ECW	Extracellular water
BIA	Bioelectrical impedance analysis
EIS	Electrical impedance spectroscopy
IPG	Impedance plethysmography
ICG	Impedance cardiography
EIT	Electrical impedance tomography

DC	Direct current
AC	Alternating current
ICF	intracellular fluid
ECF	Extracellular fluid
DUT	Device under test
SG	Savitzky-Golay
LMS	Least mean squares
NLMS	Normalised least mean squares
LLMS	Leaky least mean squares
SLMS	Sign least mean squares
SRLMS	Signed regressor least mean squares
SSLMS	Sign-sign least mean squares
RLS	Recursive least square
SVD	Singular value decomposition
db	Daubechies
sym	Symlet
FIR	Finite impulse response
SNR	Noise ratio output, dB
SNR _i	Noise ratio input, dB
SNR _{imp}	Noise ratio improvement, dB
SE	Square error
RMSE	Root mean square error
MSE	Mean square error
PRD	Percent difference root mean square, %
MER	Mean error rate %
LAN	Local area network
WAN	Wide area network

General Introduction

General Introduction

Scientific research progress has led to hemodynamic monitoring techniques from invasive to minimally invasive to non-invasive that became the most recommended in the field.

The application of the appropriate type of monitoring depends on the risk rate on patients under condition [1]. So, to ensure the safety of patients, an alternative technique has been developed called Bioimpedance that is the main purpose of researcher's nowadays, it is applied for cardiovascular monitoring and body composition analysis. The bioimpedance is the resistance of biological tissues, where the simulation is made by a low intensity current through electrodes.

The measurement of bioimpedance provides information on anatomy, tissue physiology and pathology such as cardiac output, stroke volume, heart rate and blood pressure, gender, age, weight and height, the total body water (TBW), bone mineral content, fat-free mass (FFM) and others.

There are multiple non invasive electrical impedance analysis and characterization techniques including:

- Bioelectrical Impedance Analysis (BIA)
- The electrical impedance spectroscopy (EIS)
- The electrical impedance plethysmography (IPG)
- The electrical impedance tomography (EIT)
- The impedance cardiography (ICG)

The ICG is a novel technique, non invasive, safe, simple, reliable, painless, and cheaper method to measure the blood volume variations inside the thorax during each cardiac cycle, widely used mainly in clinical for non-invasive cardiac functions, and is based on a theoretical model of the thorax.

The ICG signal is an interesting indicator for the monitoring and diagnosis of cardiovascular diseases [2], it is based on the application of a low electric current field at the level of the thorax [3] using a Tetrapolar ICG electrode configuration system. The aortic blood volume and its velocity variations cause changes in impedance which

General Introduction

subsequently causes a voltage difference, dZ/dt is the first derivative that presents the maximum rate of ICG waveform [4] [5]. Kubicek et al. developed the four-electrode for ICG measurement [6].

ICG (dZ/dt) presented in Figure 1 is in the range between 0.8Hz and 20 Hz range signal, it is retrieved after acquisition, it presents the first derivative of Z, where its max peak presents the ventricular ejection (dZ/dt)_{max}.

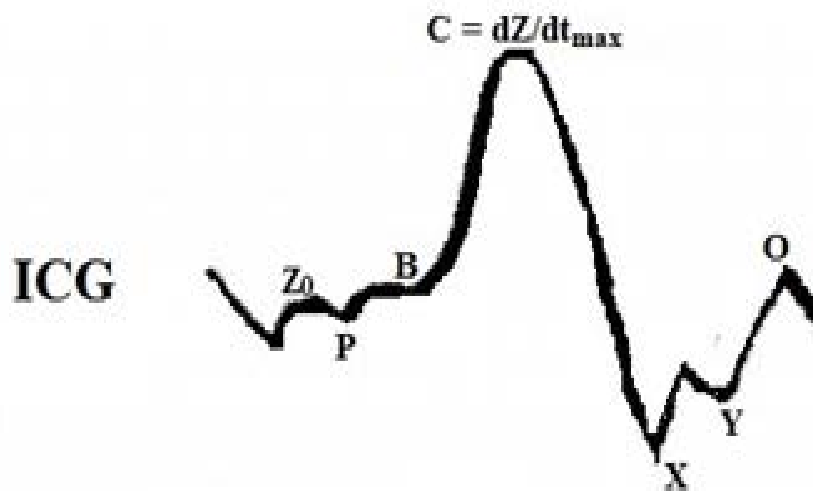


Figure 1: The typical ICG signal.

The recuperated ICG signal is drastically distorted by some noises due to physiological changes and others as respiratory in the range of 0.4 to 2 Hz, motion artifacts in the range of 0.1 to 10 Hz [7] that caused baseline drift, power frequency interference, and myoelectricity interference [8].

These factors make evaluation of cardiac indices calculation inaccurate as well as the diagnosis and monitoring of the patient state.

The signal analysis is necessary for noise removal to have better detection of the characteristic A, B, C, X, Y, O points that give us medical information. Where A coincides with P of electrocardiogram signal (ECG), B corresponds to the aortic and pulmonary valve opening, C the peak maximum in the ICG signal corresponds to the

General Introduction

ventricular contraction, X is the aortic valve closing, Y the pulmonary valve closing, and O is the opening of the mitral valve.

It is highly necessary to use artifact suppression methods as filtering, adaptive filter, ensemble averaging, coherent ensemble averaging, and wavelet-based methods. These approaches are powerful to estimate the constitutive characteristics points and for assessment of several hemodynamic parameters such as SV, and CO defined in equations (1) and (2) for the diagnosis and monitoring the healthy state of the patient with cardiac disorder [9].

$$SV = \rho_b \left(\frac{L}{Z_0}\right)^2 \left(\frac{dZ}{dt}\right)_{max} \times LVET \quad (1)$$

$$CO = SV \times HR \quad (2)$$

Where ρ_b is the resistivity, Z_0 is the base impedance, dZ/dt is the 1st derivate of ICG, LVET is left ventricular ejection time between B point and X point, and the values of heart rate (HR) expressed in (L / min) for men and women are respectively 5.6 and 4.9.

The impedance cardiography can be measured by some systems like BioZ and Niccomo, which are the most popular system.

The acquired signal is altered by artifacts; for this purpose the signal processing field is used to overcome the problem of noises that disturb the signals, where our studies are establish to solve this problem.

In the next chapters, we will discuss denoising methodology applied on ICG signals. The first method is to find the best method that performs well between adaptive filters and Savitzky-Golay (SG) filtering. The second method is based on the application of both techniques: singular value decomposition (SVD) and least mean squares (LMS). The third denoising tools based on the wavelets concept using several types of thresholding such as Shrinkage, NeighBlock as well as classical threshold and compared it with and LMS-based adaptive filter and linear filters such as: Butterworth, Elliptical,

General Introduction

Bessel, Gaussian, Chebychev1, and Chebychev2. All results are tested and evaluated thanks to the hemodynamic parameters calculation.

After that, we will explain the developed detection algorithm for features points' extraction to estimate time intervals as LVET. At the end, we will present our developed automatic application for ICG and ECG signals.

REFERENCES

- [1] B. Saugel and J.-L. Vincent, 'Cardiac output monitoring: how to choose the optimal method for the individual patient', *Current opinion in critical care*, vol. 24, no. 3, pp. 165–172, 2018.
- [2] R. L. Summers, W. C. Shoemaker, W. F. Peacock, D. S. Ander, and T. G. Coleman, 'Bench to bedside: electrophysiologic and clinical principles of noninvasive hemodynamic monitoring using impedance cardiography', *Academic emergency medicine*, vol. 10, no. 6, pp. 669–680, 2003.
- [3] J. M. Gayes, 'Transthoracic electrical bioimpedance: a noninvasive measurement of cardiac output.', *Journal of Post Anesthesia Nursing*, vol. 4, no. 5, pp. 300–305, 1989.
- [4] A. P. DeMarzo, R. M. Lang, R. Priemer, and C. E. Korcarz, 'Computer method of predicting the reliability of impedance cardiography stroke volume measurements', in *Computers in Cardiology 1995*, 1995, pp. 497–500.
- [5] M. Snajdarova, S. Borik, and I. Cap, 'Features extraction from impedance cardiography signal', in *2017 11th International Conference on Measurement*, 2017, pp. 225–228.
- [6] W. G. Kubicek *et al.*, 'The Minnesota impedance cardiograph-theory and applications', *Bio-Medical Engineering*, vol. 9, no. 9, pp. 410–416, 1974.
- [7] V. K. Pandey and P. C. Pandey, 'Cancellation of respiratory artifact in impedance cardiography', in *Proc. 27th Annual Conference on Engineering in Medicine and Biology*, 2005, pp. 5503–5506.
- [8] S. Liu, K. Yue, H. Yang, L. Liu, X. Duan, and T. Guo, 'Study on cardiac impedance signal feature point extraction', in *2017 IEEE 3rd Information Technology and Mechatronics Engineering Conference (ITOEC)*, 2017, pp. 790–793.
- [9] S. Kerai, 'The impedance cardiography technique in medical diagnosis', *Medical Technologies Journal*, vol. 2, no. 3, pp. 232–244, 2018.

Chapter .I

Introduction

Hemodynamic monitoring is essential for the therapeutic decision and the early detection of diseases, especially for patients who suffer from cardiovascular diseases. It is confirmed that monitoring is mandatory according to the decree of law n°94-1050 of December 5, 1994 [1], even for patients who suffer from less critical diseases, especially for normal and critical cases, we find its application simple in anaesthesia and increasingly complicated in intensive care and perioperative [2].

Its purpose is to ensure the safety of patients who dispose of them at very high risk because it reduces the mortality rate. It is used to detect heart rhythm disorders and abnormalities. This feature helps doctors to prevent incidents and accidents. The hemodynamic monitors are always clinically tested to validate them to acquire the accuracy and precision of the measured values. Scientific researchers must always be encouraged and funded in order to find alternative methods replacing invasive methods. Thanks to advances in the biomedical technology field, monitoring can be carried out with non-invasive methods instead of minimally invasive and invasive methods. The continuous measurement of hemodynamic parameters such as blood pressure, cardiac output, stroke volume, and other cardiac functions pose a great danger to the patient because invasive hemodynamic monitors are too complicated in their use [3].

Thermodilution is the reference method that requires the placement of a central venous catheter to extract precise and reliable information; this method is annihilation because it presents a real danger to the patient [4].

The scientific research progress has led to hemodynamic monitoring techniques from invasive to minimally invasive to non-invasive, which is nowadays the most recommended. Although, the choice of the appropriate method is dependent on factors according to setting, cost, comorbidities, and risk rate on patients [5].

The risk varies from low to medium to high risk. The patient with a low risk can benefit from standard monitoring. The patient with a medium risk can benefit from non-invasive monitoring using contour analysis pulse wave and thoracic bioimpedance methods, or benefits from invasive pulse wave analysis as ProAQT/FloTrac or even

Chapter I: Hemodynamic Monitoring

esophageal Doppler for arterial catheterization that requires a professional acquainted with the technique. If the risk increases, it is necessary to use a more appropriate technology which is transpulmonary thermodilution [1].

II. Hemodynamic Monitoring Techniques and Systems

a. Non Invasive

- Oscillometric is the oldest method; its disadvantage includes its low reliability [3].
- Applanation tonometry: (AT) Its implementation is based on a transducer attached to a flattened artery which provides the transmural pressure to zero with a bone below. It allowed us to measure systolic and diastolic blood pressure and central vascular pressure. DMP-Life system utilise AT method and TL-300 system showed reliability for the category of patients who had undergone colon surgery. This system can be used to monitor Blood pressure (BP) intraoperatively better than invasive systems [3].
- VC method : volume clamp method [6] used finger cuffs to measure blood pressure (BP), it is implemented in two systems:
 - Clear-Sight (Edwards Lifesciences, Irvine, CA): (exist in the hemodynamic platform EV1000) is based on the modified Peñáz principle, it uses Nexfin technology, it measures blood pressure continuously, heart rate, SV, CO, CI, SVI, SVV, SVR, and SVR index. In this system, the calibration is not necessary because it does it automatically after 5 to 70 beats.
 - CNAP (CNSystems Medizintechnik, Graz, Autriche): Used fot PB measurements, it provides beat-to-beat blood pressure readings, it has a good accuracy for severe cases (Smolle et al.), but it is sensitive to movement, and it needs a great device for pulse pressure measurement [3]. It is a type of system called finger cuff; it has shown good results in surgery for patients with non-critical cases [6].

Chapter I: Hemodynamic Monitoring

- Bioimpedance and bioreactance, carbon error 42% for CO values [4]. Among the disadvantages are noises such as respiratory artifacts, skin-electrodes contact, and electrocoagulation of the scalpel, Its validity is limited compared to clinical gold standard techniques [4] [7]. For example the **Niccomo system** is based on impedancemetry.
- Dioxide (CO₂)-rebreathing/partial CO₂-rebreathing, has an error rate of 40% [4]. The carbon dioxide metabolism is calculated with partial rebreathing technology. Pulmonary disease can affect the accuracy of measurement. This technique is not recommended for pulmonary hypertension or increased intracranial pressure cases. It needs an intubated and vented CO₂ charge.
- Pulse wave analysis PWA has a pulse transit time PTT this tech has an error of 62%. This method is sensitive to noises and has limitations in its application. It can also be considered less invasive , systems such as Finapres (FINger Arterial PRESsure) based on non-invasive pulse wave analysis. in the CNAP monitor (CNSystems Medizintechnik AG, Graz, Austria) the Continuous Noninvasive Arterial Pressure (CNAP®) monitor Based on non-invasive pulse wave analysis [4] [7].
- The LIDCO system integrates indicator dilution monitoring system and continuous arterial waveform analysing system [3]. The advantage of this system is based on the ability to recalibrate every eight hours or to be calibrated if one of the hemodynamic parameters has changed as CO, mean arterial pressure (MAP), SVR, SV, SVV, pulse pressure variation (PPV).
- LIDCOrapid(LIDCO,London,UK) is considered also minimally invasive, and uses a pulse wave analysis algorithm called PulseCOTM, based on a mathematical analysis of pulse pressure.
- Pulse contour analysis (PCA) for CO monitoring error of 45%. Considered also as a minimally invasive technique [8]. Used an arterial line, Continuous measurement

Chapter I: Hemodynamic Monitoring

Evaluate SVV/PPV. This technique has developed other parameters to be evaluated as Pulse Pressure Variation (PPV) and Stroke Volume Variation (SVV). Its disadvantage is Arterial cannulation. (covered by noninvasive continuous finger cuff/tonometric BP technology), there are several PCA based CO monitoring systems as the Nexfin monitor monitor (BMEYE, Amsterdam, Netherlands) based on finger arterial pulse contour analysis PCA.

- Radionuclide angiography (RNV) or ventriculography (RVG): is a non invasive way of assessing the ventricular function allows estimating the cardiac output by applying the dynamic sampling radioactive counts of the left ventricle technique.
- Transthoracic Doppler echocardiography (TTE) is a non-invasive technique [6].
- Capnography: It allows non-invasive and continuous measurement of CO₂ concentration, indirect measurement of PaCO₂, and production and transport of CO₂ (highly indirect measurement of cardiac output (CO)).
- Pulse oximetry: It it has a respiratory and hemodynamic interest. It measures the oxygenation rate of the blood by the lung and monitors the transport of oxygen to the periphery. Among these systems: Estimated Continuous Cardiac Output (esCCO) (from the Japanese firm NIHON KOHDEN (Cacan, France)) is used to measure cardiac CO from the transit time of the pulse wave (pulse Wave Transit Time or PWTT).

b. Minimillay Invasive or Less_Invasive

- Arterial cannulation can be coupled with systems like FloTrac. Used for direct BP measurement [3].
- Arterial pressure waveform analysis

Chapter I: Hemodynamic Monitoring

- The oesophageal Doppler ((Cardio Q; Deltex Medical, Chichester, UK) allows us to measure the blood flow in the descending aorta by a flexible Doppler probe introduced into the esophagus of patients under anesthesia.

The Doppler transducer at the extremity of a flexible probe allowed the instantaneous measurement of the descending aortic flow velocity. It is introduced into the oesophagus, preferably orally or nasally, until a characteristic aortic flow signal is obtained.

There are two devices for cardiac output calculating: the first one is called Hemosonic, which measures the aortic diameter, and the second is CardioQ which estimates the aortic diameter [4].

- The transesophageal echocardiography is for Stroke volume measurement by introducing a transducer in the descending aorta. This technique is recommended for patients undergoing open-heart and thoracic aortic surgery [5].
- Doppler-derived blood flow measurement is not recommended for long-term use.

Less invasively systems

- FloTrac (Edwards Lifesciences, Irvine, California) is a system that provides hemodynamic values such as different heart functions and blood pressure, often used to obtain frequent blood gas specimens. Also used for the calculation of Stroke volume that requires the standard deviation of the pulse arterial pressure. Recalibration is not necessary for this system. The accuracy of the estimated CO is in the morbidly obese category. It is connected to a general peripheral arterial catheter and a monitor as the Vigileo that displays more precise results for SV, CO, and SVV. It gives good results in intraoperative chemotherapy. Pairs with Vigileo the EV1000 platform
- Vigileo/ Flotrac: used without calibration, estimates arterial compliance and allows the analysis of SV variations according to respiration. This technique is validated for only healthy people [3].

Chapter I: Hemodynamic Monitoring

- PICCO (Pulsion Medical Systems, Munich, Germany) is a system that combines: “pulse contour analysis (PCA)” and “transpulmonary thermodilution” highly recommended in severe cases, it measures CV, SV, AP with recalibration. used two methods:

- Transpulmonary thermodilution: The time taken by a cold bolus injected into the right atrium to reach the arterial sensor is proportional to cardiac output.
- The pulse contour: This is the same technology as Vigileo, but the calibration factor was determined during the first thermodilutions.

Allows continuous monitoring of cardiac output and determination of respiratory variations in SV and PP presented in the equation below:

$$PP=SP-DP \quad (1)$$

With systolic blood pressure (SP), diastolic blood pressure (DP) and pulse blood pressure (PP) [6].

- ProAQT/PulsioFlex system (Pulsion-Getinge, Feldkirchen, Germany: Minimally invasive perioperative cardiac output trend monitoring with ProAQT. Utilize the PCA-based algorithm of the PICCO system. ProAQT ProAQT technology is integrated into the Pulsioflex platform, which can include PiCCO technology. It is a calibration-free technology [1].
- LiDCOTM: Used pulse power analysis. Discontinuously cardiac output measurement using lithium chloride dilution techniques, where the latter is injected in small quantities through a central or peripheral venous catheter.
- the LiDCOTMplus requires calibration using transpulmonary thermodilution by lithium injection.
- The ProAQT sensor (Pulsion Medical systems), the FloTrac sensor (Edwards LifeSciences), and the Most Care monitor (Vytech Health, Padua, Italy) require no calibration and can be adapted to the existing arterial line [1].

Chapter I: Hemodynamic Monitoring

- Pulsio cath technology (Pulsion Medical Systems) of the VolumeView™ catheter (Edwards Life Sciences) and the LiDCO™ system monitor (LiDCO) require calibration by thermodilution or lithium injection, allowing an accurate measurement of cardiac output [1].

c. Invasive

- Pulmonary artery catheterization (PAC) is a gold standard method used for years in surgery and intensive care units (ICU). A pulmonary artery catheter (PAC) with an arterial line is not used in critical cases such as bleeding and infection. Used to measure CO. Serve as the clinical gold standard for CO measurement [3] [7].
- Transpulmonary thermodilution: Serve as the clinical gold standard for CO and SV measurement, based on the insertion of a central venous catheter and an arterial thermistor catheter by injection of a cold fluid bolus into the vena cava system through the central line to have more precision, it is recommended to assess acute circulatory failure. This technique is implemented in PICCO [4].
- Mixed venous oxygen saturation.
- Pulmonary arterial pressures
- ScvO₂: It is the measurement of the Venous Oxygen Saturation of the blood of the Superior Vena Cava. It is realised thanks to the Swan-Ganz pulmonary artery catheter, which gives the oxygen saturation of the venous blood and the values of CvO₂ and DAV_{O₂}. This technique is useful, especially in monitoring septic shock states with associated heart failure. This method is very complicated, but it allows us to determine cardiac output where the measurement is made through a central catheter, continuously through a fibre optic catheter, and discontinuously by sampling blood gases [9].

Chapter I: Hemodynamic Monitoring

- Direct Fick: to measure mixed oxygen concentrations of venous blood in order to estimate cardiac output. NICOT, Respironics is based on Fick's method but it is used in a non-invasive way.
- Indirect Fick: it seems like the direct Fick method, but its specificity is that it uses pulse oximetry to evaluate the arterial oxygen content.

III. Discussion and Conclusions

Monitors based on transpulmonary thermodilution technology such as Pulscath with the Pulsioflex or PICCO2 monitor, the Volume view sensor with the EV 1000 monitor use Cardiac output calibration. These two technologies are not performant in the case of principal intrathoracic volumes determination [10]. For invasive analysis, the FloTRAQ, the ProAQT, the VolumeView, and the PulsioCath have the same performance in predicting the filling response [11].

However, these same performances can be obtained from non-invasive monitors such as ClearSight, CNAP, and NICOM. In this purpose, the researchers are still ongoing for non-invasive technologies.

The error rate of the comparison between Nexfin and ClearSight with transpulmonary thermodilution (TPTD) is 44%. However, CNAP grants the reference values of TPTD [4].

It is important to choose the best method, whether invasive, minimally invasive, or non-invasive, to accurately measure the various hemodynamic parameters such as cardiac output. The most appropriate monitoring method is recommended according to the indications and limitations of each type.

REFERENCES

- [1] A. Ouattara and M. Biaï, *Quel monitoring hémodynamique au bloc opératoire?* Paris, 2014.
- [2] I. N. de Keijzer and T. W. Scheeren, ‘Perioperative Hemodynamic Monitoring: An Overview of Current Methods’, *Anesthesiology clinics*, vol. 39, no. 3, pp. 441–456, 2021.
- [3] I. Pour-Ghaz *et al.*, ‘Accuracy of non-invasive and minimally invasive hemodynamic monitoring: where do we stand?’, *Annals of Translational Medicine*, vol. 7, no. 17, 2019.
- [4] T. W. Scheeren and M. A. Ramsay, ‘New developments in hemodynamic monitoring’, *Journal of cardiothoracic and vascular anesthesia*, vol. 33, pp. S67–S72, 2019.
- [5] B. Saugel and J.-L. Vincent, ‘Cardiac output monitoring: how to choose the optimal method for the individual patient’, *Current opinion in critical care*, vol. 24, no. 3, pp. 165–172, 2018.
- [6] M. R. Pinsky, J.-L. Teboul, J.-L. Vincent, and E. S. of I. C. Medicine, *Hemodynamic monitoring*. Springer, 2019.
- [7] D. A. Reuter and S. A. Haas, ‘Cardiac Output Monitors’, in *Hemodynamic Monitoring*, Springer, 2019, pp. 247–252.
- [8] T. Yamada, S. Vacas, Y. Gricourt, and M. Cannesson, ‘Improving perioperative outcomes through minimally invasive and non-invasive hemodynamic monitoring techniques’, *Frontiers in medicine*, vol. 5, p. 144, 2018.
- [9] M. Durand and P. A. Réanimation, ‘SVO₂, ScVO₂ & Lactate’.
- [10] C. K. Hofer, A. Senn, L. Weibel, and A. Zollinger, ‘Assessment of stroke volume variation for prediction of fluid responsiveness using the modified FloTrac™ and PiCCOplus™ system’, *Critical Care*, vol. 12, no. 3, pp. 1–8, 2008.
- [11] M. Biaï, A. Ouattara, G. Janvier, F. Sztark, and B. Riou, ‘Case scenario: respiratory variations in arterial pressure for guiding fluid management in mechanically ventilated patients’, *The Journal of the American Society of Anesthesiologists*, vol. 116, no. 6, pp. 1354–1361, 2012.

Chapter .II

I. Introduction

Bioelectrical impedance or bioimpedance is a goal of multiple scientific researches of different specialities in medicine; it has been progressively improvised for various clinical applications. It is inexpensive, easy to use, requiring no specialised personnel, applied for cardiovascular monitoring and body composition analysis [1].

The biological tissue stimulation is made using a low intensity current through the electrodes, the voltage is recuperated and complex electrical impedance is involved that depends on the type of tissue, the structure, the tissue composition and its state of health as well as the frequency of the alternative signal [2]. The impedance Z is the some of the resistance and reactance vectors, it measured in an identified time-varying electric field frequency chosen between 20 to 200 KHz, where the instantaneous impedance signal $\Delta Z(t)$ of a human body segment varying according to physiological processes [3].

The measurement of bioimpedance can provide information on anatomy, tissue physiology and pathological Bioimpedance is used on living tissues for 60 years ago [4], since 1950 multiple bioimpedance-based clinical applications is developed and exploited in this field including medical applications such as cancer diagnosis of skin and measurement of pulmonary respiratory activity as well as non-invasive cardiac volume [5].

The electrical impedance implementation provides hemodynamic parameters such as cardiac output, stroke volume, heart rate and blood pressure, it estimate also the total body water (TBW), bone mineral content, body fat (adiposity), fat-free mass (FFM), gender, age weight and height that are measured with several non-invasive electrical impedance methods as bioelectrical impedance analysis (BIA), electrical impedance spectroscopy (EIS), impedance plethysmography (IPG), impedance cardiography (ICG), and electrical impedance tomography (EIT), used for the pathological condition diagnosis and monitoring of the patient's tissues, as well as the treatment in different clinical situations as operative and post-perioperative, cardiovascular pathologies, and pregnant women [6].

Chapter II: The Electrical Bioimpedance

In this section, we have discussed the bioimpedance measurement purpose, its principle, its applications, its techniques, and multiple models of equivalent circuits of a cell.

II. The Electrical Bioimpedance

1. Definition

In 1886, the word impedance was invented by Oliver Heaviside, it comes from the English word "impede". In the sinusoidal mode, the impedance Z (Ω) is a complex number which consists of a real and an imaginary one, it is defined by Ohm's law which is the ratio between the voltage V and the current I as in equation 1 [7]:

$$V=Z.I \quad (1)$$

Where,

V expressed in Volt: it is a voltage measured at the terminals of electrodes,

I expressed in Ampere: it is the current injecting through the body.

It applies to both direct current (DC) and alternating current (AC), the use of the latter makes it possible to modify the frequency. The Admittance is the opposite of impedance expressed in Siemens (S) defined in equation 2 as follow:

$$Y= K (\sigma+ j\omega\epsilon_r\epsilon_0) \quad (2)$$

It is a complex conductance where G is the conductance and B is the susceptance. Immittance is the combined term for impedance and admittance, whilst the better and the more generic term than bio-impedance is bio-immittance [7]. In continuous mode as in equation 3 as defined follow:

$$Z=R \quad (3)$$

The electrical properties depend on all the physical or chemical parameters which determine their concentration or mobility.

Chapter II: The Electrical Bioimpedance

The temperature, the viscosity, and the conductivity in the biological environment are factors that contribute to resistance changes, subsequently to bioimpedance.

In addition to that, the distance, location, and type of electrodes affect the bioimpedance measurement.

The impedance is a complex depending on the resistance (R) as real part which is inversely proportional to conductance, and the reactance (X) as imaginary which is inversely proportional to the capacitance [8].

The latter varies according to the frequency used; it is introduced by capacitors or inductors in the circuit. The formula is defined in the Cartesian form and the Polar form as in equation 4, where the impedance equation is shown in equation 5, and the phase ϕ is presented in equation 6. The impedance is resistive when ϕ equal to 0° , and it is capacitive when ϕ is equal to 90° [9].

$$Z = R + jX = |Z|e^{j\phi} \quad (4)$$

$$Z = \sqrt{|Z|^2} = \sqrt{R^2 + X^2} \quad (5)$$

$$\phi = \arctan(X/R) \quad (6)$$

2. The Biological Tissues

The bioimpedance related to the tissues properties and the geometric dimensions, the electrical properties of the tissues are constant so it is possible to measure the size and the volume from the detected impedance fluctuations and the data of the electric conductors of the known tissues [7].

The biological tissue groups several cells that have the same function, the whole of a specific tissue forming an organ.

Chapter II: The Electrical Bioimpedance

The living tissue is a set of cells in the body that lives under specific conditions; it can be damaged by electrical energy through three mechanisms: thermic injury, electroporation or fibrillation [10].

The tissues are conjunctive when the cells are separated by an inter-cellular medium. This is the case of blood, bones, muscles or adipose tissue. The epithelium tissues consist of cells such as those of the skin. The cells have a membrane of a thickness of about 7 nm and contain substructures such as the cell nucleus or mitochondria. From an electromagnetic point of view, the biological environment appears as materials at the same time: non-magnetic, ionic conductors, and lossy dielectrics. The current flows through the cell environment. The cell membrane is composed of a lipid bilayer that separates the cell medium and the conductive liquid environment; it has a very poor conductance, considered a dielectric. The total structure formed by the intracellular fluid, plasma membrane and extracellular fluid (conductive-dielectric conductor) behaviour is similar to a capacitor, with an approximate capacity of 0.01 F / m² [11].

Bioparhom's experiments have shown that with a frequency of 100 KHz, the current can easily cross certain extracellular environments [12].

At low frequencies (<1KHz), the ECF is the medium that drives the electrical current that cannot penetrate the membrane, and at high frequencies (> 1MHz), the electric current flows through the membrane and the measurement of the bioimpedance depends on the ECF and the ICF. The extracellular fluid (ECF) contains ions like sodium, chloride and bicarbonate; it also contains carbon dioxide, waste, and nutrients such as oxygen, glucose, fatty acids and amino acids. The intracellular fluid (ICF) also contains ions such as potassium, magnesium and phosphate [13].

As shown in Table, if the frequency increases, the charges of the membrane will be accumulated and the current passes through the cell membranes, and subsequently the intra-extracellular liquids.

Chapter II: The Electrical Bioimpedance

Table 1: The ions concentration in living tissue [13].

Concentration (meq/L)	Body Fluids	
	<i>Intracellular</i>	<i>Extracellular</i>
Na ⁺	10	142
K ⁺	140	4
Ca ⁺⁺	0.0001	2.4
Mg ⁺⁺	58	1.2
Cl ⁻	4	103
HCO ₃ ⁻	10	28
Protein	40	5

3. The Dielectric Properties of Biological Tissues

The purpose of the electrical characterization of biological tissues is to simplify a composite of the characteristics of the constituent cells. The dielectric properties are also influenced by the specific tissue structure, any hardware stores a capacitive energy; it can be classified as a dielectric, they depend on all the physical or chemical parameters that determine their concentration or mobility [14].

such as: (1) the temperature which has an important role in ionic conductance, and ion mobility, however the mobility increases with increasing temperature and resistance decreases, (2) the electrical conductivity of living tissues that is difficult to measure by ultrasonic transducer and magnet with a non-invasive method in vitro of biological tissue, (3) the cellular electrical conductivity, (4) the impedance of tissue,(5) the conduction models of living tissues, (6) electrical permittivity: macroscopic property that describes the response of an environment expressed by farad per metre, (7) The frequency [15] [16].

4. The Dispersion windows

Dispersion is a frequency dependence of permittivity and conductivity functions for living tissue. It is considered as a dispersive medium [8] [17].

Chapter II: The Electrical Bioimpedance

There are three major dielectric dispersions α , β which appear between 10 Hz and tens of MHz and γ , identified and named by HP Schwan in 1957, and the fourth the δ dispersion noted by B. Rajewsky & HP Schwan in 1948 [16], identified and named by H. Schwan in 1994 [15].

- a. **A dispersion:** is based on the ionic species diffusion process, its range interval is varied from 10 Hz to 10 kHz.
- b. **β dispersion** its range interval varying from 10 kHz to 100 MHz, caused by the cellular structure, related to the extracellular and intracellular electrolytes interchanges, the dielectric properties, and the behaviour of the cell membranes. The bioimpedance analysis is released in this range with a single frequency of 50 KHz.
- c. **γ dispersion:** the dielectric properties are attributed to the high water content of the biological species and the presence of small molecules such as proteins and amino acids. Water displays a wide dispersion spectrum from hundreds of MHz to a few GHz.
- d. **δ dispersion:** is located between β and γ dispersion, observed around 100 MHz, (Pethig, 1984) which is provided thanks to the dipole moments of large molecules such as water-bound proteins.

5. The Electric Cellular Models

a. Fricke-Morse model

Fricke-Morse model is presented in Figure 2:

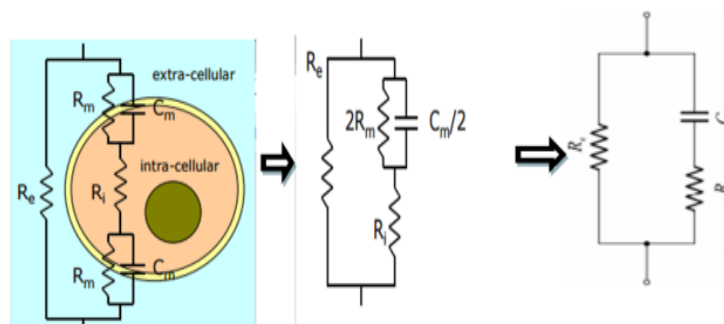


Figure 2 : Fricke-Morse model [9].

Chapter II: The Electrical Bioimpedance

where

$$C^*m=Cm/2 \quad (7)$$

According to the Fricke model [19], the equation of Z is defined in equation (8):

$$Z = \frac{R_e R_i + \frac{R_e}{j\omega C m}}{R_e + R_i + \frac{R_e}{j\omega C m}} \quad (8)$$

Where,

R_e is an electrical resistance of the extracellular environment, R_i is a electrical resistance of the intracellular environment and C_m is a membrane capacity.

b. Debye model

The Debye model is presented in Figure 3.

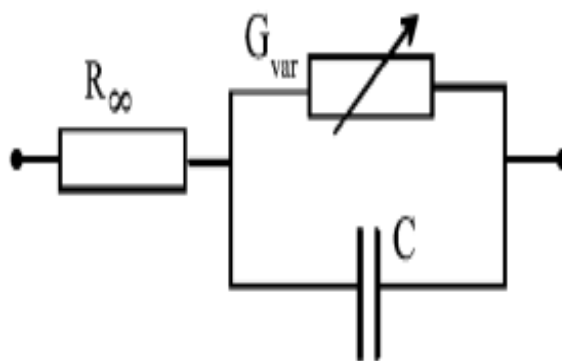


Figure 3: The Debye circuit with an ideal component [7].

Chapter II: The Electrical Bioimpedance

According to the Debye model [20], a phenomena of electrical relaxation is added where the impedance Z equation is shown in equation (9):

$$Z = R_{\infty} + \frac{1}{G_{\text{var}} + j\omega C} \rightarrow Z = R_{\infty} + \frac{1}{G_{\text{var}} + G_{\text{var}}j\omega\tau} \quad (9)$$

Where,

R_{∞} : the environment resistance at very high frequency (Ω);

C : supposedly perfect capacity (F);

G_{var} : independent conductance (Siemens S);

ω : angular frequency (s-1) with $\omega\tau = 1 / \tau z$;

$\tau z = C / G_{\text{var}}$: it is a constant of relaxation time and characteristic of the system corresponding to a characteristic angular frequency, τz is expressed in (s).

c. Col model

The Cole model 1940 [21] as show in Figure 4; it is derived from the Fricke model 1932 and Debye model 1929. Cole's impedance model was introduced in its final form by Kenneth Cole, it took the Debye model, basing on the replacement of the ideal capacitance by "a Constant Phase Element CPE" which is a mathematical concept with Frequency dependent components.

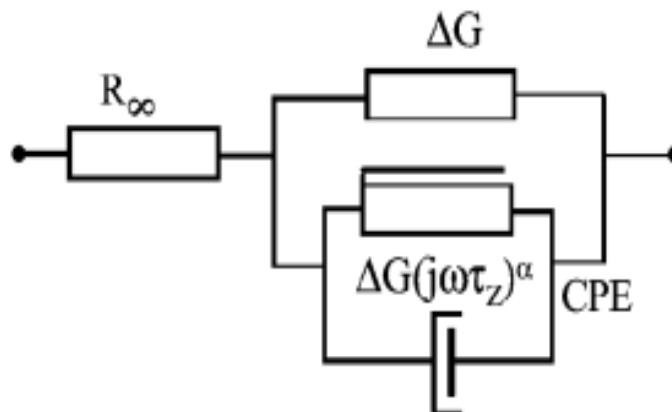


Figure 4: The Cole circuit [7].

Chapter II: The Electrical Bioimpedance

The impedance equation is defined equation (10):

$$Z = \frac{1}{\Delta G + \Delta G(j\omega\tau)^{\alpha}} \quad \text{with } R_0 - R_{\infty} = 1/\Delta G \quad \text{So } Z = \frac{R_0 - R_{\infty}}{1 + (j\omega\tau)^{\alpha}} \quad (10)$$

R_0 : resistance of the environment at very low frequency;

R_{∞} : resistance of the environment to very high frequency;

α : constant such that: $\alpha = \phi_{\text{CPE}} / 90^\circ$ according to Frick's law.

III. The Bioimpedance Measurement Methods

The measurement is based on the electrode contact as shown in Figure 5.

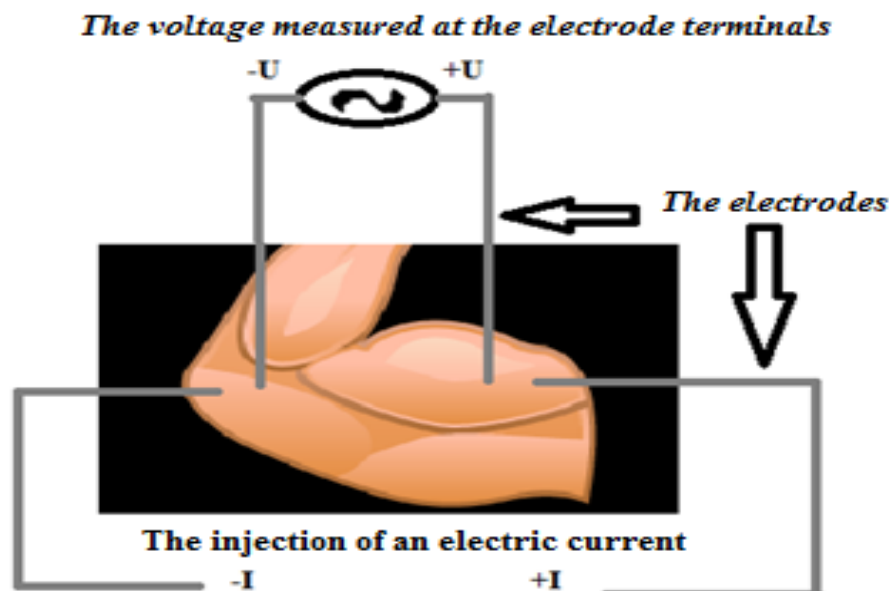


Figure 5: The principal of Bioimpedance measurement.

The methods are as follows:

a. The two electrode method or the bipolar method

It is injecting a known current into the device under test (DUT) through two electrical contacts and measuring the resulting voltage drop between these two contacts from the same electrodes. The bipolar method is used in several applications such as skin [22] or dental in which the impedance of the sample used is much higher than that of the

Chapter II: The Electrical Bioimpedance

electrode. The two-electrode method works if the impedance of the test material is greater than the impedance of the electrode contacts at the working frequency. This method is dysfunctional if a BIS device is used because the impedance at the electrode-electrolyte interface is vulnerable to frequency variations [23].

b. The three electrode method

Used for the measurement of skin resistance at the volume of transdermally extracted interstitial fluid (ISF) extraction point. If the surface of the electrode is sufficient, its interface impedance can be reduced in order to make the electrode unnecessary, and simplify the configuration of the measurement [24].

c. The four-electrode method or the four-pole or Kelvin method

Separate Separate electrode pairs are used to inject current and measure voltage. This method has been used for more than a century. In the late 1800s the four-pole method was used to measure the resistivity of materials, and also used to measure cardiac bioimpedance as well as in electrical impedance tomography (EIT). The electrode-electrolyte interface impedance has no influence on the measurement and if it exists it will be in the low frequencies where their amplitude can be very large; it is in the case where no current passes through the voltmeter which has infinite impedance [25].

The electrode-electrolyte interface impedances are in series with the impedance of the sample, and the measured impedance is the sum of the three impedances. At high frequencies, the parasitic impedances influence on the quality of the results by causing errors that can be studied analytically; we conclude that the purpose is the manner for estimating the error and especially in the case of living tissues. The parasitic capacitances are in the form of capacitances between the electrode wires and input capacitances of the instrumentation. In some cases it is necessary to accept the measurement with two electrodes which makes it necessary to have a large surface ($> 1\text{cm}^2$) and of high frequencies ($> 10\text{ KHz}$) because the impedance of electrode is negligible than the impedance under test [9]. The kelvin method is the most used

Chapter II: The Electrical Bioimpedance

nowadays for the measurement of the bio impedance because if the voltmeter is ideal, the result of the measurement will be the impedance of the tested material [23].

d. The five electrode method

It's a new measurement method based on five electrodes presented and analysed. It serves to minimise errors at low frequencies caused by high electrode-electrolyte interface impedances. This method works, but some limitations are found, therefore, it almost impossible to implement it for live tissue measurements.

IV. The Bioimpedance in Diagnosis

We quote some examples of research: (1) the application of an alternating current (AC) of very low intensity through the thorax, the electrodes of the bioimpedance capture the signal of respiration. This methodology spread during the year 1950 [5]. In 1940, the beginning of research of the thoracic electrical bioimpedance by the National Administration of Aeronautics and Space, (NASA). In 1960, the appearance of the first cardiovascular monitors. In 1962, Thomasett discovered the relationship between the total body water and the bioimpedance. In 1966 the invention of the 1st impedance cardiography monitoring device (thoracic electrical bioimpedance). In the same year, Kubicek replaced the notion of first derivative dZ / dt usable in the ICG method, it represents the rate of the impedance variation, he tested a systolic ejection volume equation according to the bioimpedance. In 1970, the proposition of impedance imaging idea by B.Pullen. In 1978 Henderson applied a voltage and recovered a current by developing an impedance imaging data acquisition system using 144 electrodes. In 1981, Smarek developed a new equation in hemodynamic based on variations in thoracic impedance. In 1983, Barber, Brown and Nyboer, experienced in vivo the first impedance image. In 1987, Kim developed a data acquisition system of 192 electrodes in Impedance Imaging. The Impedance imaging has evolved significantly with Brown in developing a host of clinical applications such as: pulmonary perfusion, blood vessel distension, pelvic congestion, measurement of chest fluids, pulmonary oedema [26].

Chapter II: The Electrical Bioimpedance

E. De Roux et al. developed a new method called the Continuous chronic detection of fibrosis (characterization of tissue modifications) induced by the electrodes of cardiac implants, using Electrical Impedance Spectroscopy (EIS) [27].

M. Gutierrez-Lopez et al. the authors prevent the breast cancer for early diagnosis, the purpose study is to identify carcinoma emulators in preclinical state in breast agar phantoms, and it is based on bioimpedance measurements through eight Ag/AgCl electrodes. They released several experimental clinical trials that show a great promise [28].

A. Hadif et al. the authors used electrical impedance to simultaneously record impedance cardiography and electrocardiogram with five electrodes using Z-RPI device functions; it aimed to extract the characteristics points to hemodynamic parameters calculation [29].

D. Naranjo-Hernandez et al. the authors present a review paper about the Bioimpedance in medical applications, their measurement, concepts, limitations and the most important future challenges for biomedical devices [8].

There are multiple non invasive electrical impedance analysis and characterization techniques including:

a. Bioelectrical Impedance Analysis (BIA)

In 1969, Hoffer et al. [30] used the BIA technique of total body water to predict body water. Lukaski et al. [31] at the USDA in Grand Forks, ND, is the first whose published an article on body composition and BIA. This technique is non-invasive, simple, reliable, safe, painless, acceptable cost, manipulable, fast, secure, no danger on the subject, can calculate body cell mass (BCM), total body water (TBW), intracellular water (ICW) and The extracellular water (ECW). There are multiple BIA devices.

b. The electrical impedance spectroscopy (EIS)

Applied to characterise tissues and cells using a pulsed signal based on EIS instrumentation. This technique estimates the complex impedance ($Z(f)$) and its angle

Chapter II: The Electrical Bioimpedance

(θ (f)) of a subject under test " SUT ", based on the measurement of the surface tension recovered after a current injection. It is used in several fields including biomedical engineering [32].

c. The electrical impedance plethysmography (IPG)

In 1940, it was introduced by Nyboer [33]. IPG is a non-invasive method that measures the change in blood volume for a body segment in terms of electrical impedance e.g. chest, calf . Several researchers studied IPG for digital including instrumentation, systems led by recent software. This technique is non invasive, simple, portable, easy to perform, comprehensive...etc.

d. The impedance cardiography (ICG)

New methods of exploration and medical treatments such as impedance cardiography, abbreviated ICG or ZCG (Impedance Cardiography), it serves to observe the continuity of the left ventricular volume variation and other hemodynamic parameters such as: Stroke Volume (SV), Continuous Cardiac Output (CO), Total Peripheral Resistance (TPR), Ventricular Ejection Time (VET), Pre-ejection Period (PEP), heart rate (HR), and heart rate variability (HRV) that used for the autonomic nervous system assessment. Kubiceket. Al developed the four-electrode method for measuring cardiac impedance [34].

This technique is a non-invasive technique, simple, reliable, safe, painless, low cost, and fast, secure no danger on the subject. It is studied to evaluate transthoracic parameters for cardiac monitoring either ambulatory or continuous long-term in intensive care unit ICU, it is a more advantageous technique than conventional invasive methods. The ICG signal presented in Figure 6 is measured by some systems like BioZ, Niccomo, Osypka, Analogic, CardioScreen 2000 and CardioScreen 1000.

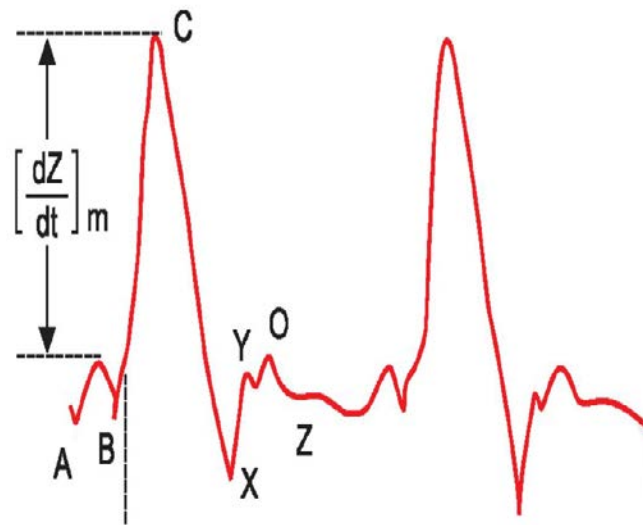


Figure 6: The typical ICG signal [6].

e. The electrical impedance tomography (EIT)

It is a non-invasive technique of tomography image reconstruction used to obtain medical images inside the human body; it is applied in several fields of research such as medical imaging diagnosis. It is inexpensive, portable and easy, fast in data acquisition, non-ionizing and without radiation, an important temporal resolution [35].

V. Materials used for Bioimpedance Measurement

An electrical impedance analyzer from the quantum RNL sciences series called BIA [36] allows us to quickly identify parameters such as Pregnancy, Fat-free mass, Total body water, Lean dry mass, BMR (basal metabolic rate), and DEE (daily energy expenditure). The last intervention of the RNL company is Quantum V Segmental without forgetting the old analyzers of the company: Quantum II, Quantum X, Quantum Desktop, Quantum III, Quantum IV, and Quantum V.

Chapter II: The Electrical Bioimpedance

BIO|ANALOGICS' [37] Health Management System (HMS1000) software and the ElectroLipoGraph Body Composition Analyzer (ELGIII) is a body composition analyzer, it allows making several functions:

- Evaluation of body fat and lean mass
- Have an accuracy normal fat range in percentage and weight
- The fat objective in percentage and weight
- The Body Composition Pie Chart
- Body composition history tracking
- Optional anthropometric measurements

BIA 450 [38] analyzer calculates resistance (R), reactance (X), phase angle (α), body capacitance (C), fat-free mass (FFM), body cell mass (BCM), extracellular mass (ECM), fat mass (FM), ECM/BCM, body mass index (BMI), basal metabolic rate (BMR), total body water (TBW), intracellular water (ICW), extracellular water (ECW), TBW/fat-free mass and TBW/total weight.

The BIA 310 [38] Bioimpedance Analyzer calculates: resistance (R), reactance (X), fat-free mass (or lean body weight), fat mass (or fat body mass), body mass index (BMI), Basal Metabolic Rate (BMR), Total Body Water (TBW), TBW/Body Weight, and TBW/Fat Free Mass.

Bodystat500 [39] is a device that measures at a fixed frequency equal to 50 kHz the following parameters: Impedance, resistance, reactance, and phase angle. There are also devices of the same brand but more sophisticated: the Bodystat1500, the Bodystat1500 touch screen, the Bodystat1500 MDD, the Bodystat Quadscan4000, the Bodystat multiscan5000 used mainly in dialysis where the frequency variance is on a spectrum ranging from 5 kHz to 500 kHz.

BioZ System [40] used to extract features detection and hemodynamic parameters calculation of ECG signal, it also allowed to measure the impedance cardiography changes.

Steorra and CIC-1000 developed by Sorba Medical Systems for cardiology, anesthesiology and research applications.

Chapter II: The Electrical Bioimpedance

Tanita BIA Technology [41]: body composition monitors for electrical impedance analysis. The advantage of this technology is the possibility to analyse the signals at different frequencies.

There are two types of devices [42]: the first is Single frequency devices that measure only overall water and lean mass (tissues containing water with a significant amount), and the second is Multifrequency which allows dry, water, muscle mass, and bone calculation.

- Feet by foot (single frequency) to measure human lower body and overall water lean mass (tissues containing water with a significant amount of 73%);
- hand feet (single or multifrequency) to measure the entire human body; it allows us to calculate and control the level of hydration, dry monitoring, muscle, and bone mass; which makes it more effective and relevant in the case of an obese person, example: Aminostats BIO-ZM II is a multi-frequency device
- hand to hand (single frequency)

A range of BIA products [43]:

- X-Scan Plus II: with frequencies of 1-5-50-250-550-1000 KHz
- IOI 353: with frequencies of 5-50-250 KHz
- Gaia359 Plus: with frequencies of 5-50-250 KHz
- Plusavis 333: with frequencies of 5-50-250 KHz
- Easybody 205: with a frequency of 50 KHz
- Quadscan4000: with frequencies of 5-50-100-200 KHz
- 1500 MDD: with frequencies of 5-50 KHz.

Tanita BC 545 N body composition analyzer: measures body fat and muscle mass.

Tanita BC601 body analysis scale is working as Tanita BC 545 N [44].

Soehnle Professional 7850 balance [45]: allows you to measure impedance by hand contact (and not bare feet)

Tanita RD901/ RD953 body composition analyzer (Bluetooth compatibility): this is the first analyzer from the Tanita brand. Tanita body analysis scales MC 780 MA. Tanita BC587 Body Analysis Scale, Silver [46]

Chapter II: The Electrical Bioimpedance

Garmin Index body fat scale: connected with wifi, allows you to measure weight, body mass index, body fat, muscle mass and others [47].

Soehnle Professional Design 7830 personal scale [48].

FitBit body fat scale Aria 2 [49]

Tanita Professional Scales [50]:

- Tanita SC 240 MA body composition analyzer
- Tanita DC-360 S body composition analyzer
- Tanita DC-360 P body composition analyzer
- Tanita DC-430 MA S Body Composition Analyzer - Class III
- Tanita DC-430 MA P Body Composition Analyzer - Class III
- Tanita MC 980 MA Body Constitution Analyzer

Table 2 presents a comparison between ANALYCOR and XITRON that uses a technique with four silver electrodes, where the first pair is for injecting the current and the other pair is for measuring the potential difference.

Table 2: Comparison between ANALYCOR and XITRON.

UTC study of two devices	ANALYCOR(France)	XITRON 4000B(USA)
Alternating current (mA)	0.5 mA	0.25 mA
Frequency	5, 50, 100 KHz	5 and 1 MHZ

Z-Metrix is a multifrequency device (foot-to-hand) from the French company Bioparhom which works on impedancemetry conception. It has carried out training on bioimpedance which is used to measure the water level and the different body compositions [51].

VI. conclusion

The studies aim to have non-invasive methods with less risk and to have results with the same precision or more with the invasive methods, which will be very useful in diagnosis and monitoring.

The difference between the invasive method (e.g. cardiac catheterization) and non-invasive is low risk of danger, easy to use, less expensive and requires less training. Another disadvantage of invasive techniques is that they are not practical in an outpatient setting for this reason the researchers work on new alternative methods.

The Bioimpedance is one of the non invasive technique analyses that offers valuable information about the tissues' anatomy and physiology. Several studies were about the analysis of the electrical impedance of biological tissues in order to diagnose and study the physiological and pathological state with the non-invasive method.

Nowadays, Bioimpedance is becoming the basis of new non-invasive medical diagnostic devices. For this purpose, we are focused in this party on the principal and the different characterization and analysis techniques of the bioimpedance that use non-invasive techniques, and the different applications applied on the biological tissues in the medical field that assist in the diagnosis and monitoring of pathological state of patients.

Current studies of bio-impedance emphasise instrumentation are already implemented and that can be conducted in the near future by wireless techniques such as Bluetooth.

Several obstacles in this area of research must be overcome such as non-linearity, measurement errors and modelling, errors due to patient positioning or electrodes, the poor performance of the electrodes, the modelling of the system especially in EIT, it must be more precise.

Chapter II: The Electrical Bioimpedance

REFERENCES

- [1] T. K. Bera, 'Bioelectrical impedance methods for noninvasive health monitoring: a review', *Journal of medical engineering*, vol. 2014, 2014.
- [2] J. J. Ackmann and M. A. Seitz, 'Methods of complex impedance measurements in biologic tissue.', *Critical reviews in biomedical engineering*, vol. 11, no. 4, pp. 281–311, 1984.
- [3] Y. Alharbi, A. Alshrouf, and S. Mansouri, 'Heart Rate Monitoring Using Electrical Impedance', in *2021 Seventh International conference on Bio Signals, Images, and Instrumentation (ICBSII)*, 2021, pp. 1–4.
- [4] H. M. Dastjerdi, R. Soltanzadeh, and H. Rabbani, 'Designing and implementing bioimpedance spectroscopy device by measuring impedance in a mouse tissue', *Journal of medical signals and sensors*, vol. 3, no. 3, p. 187, 2013.
- [5] Professor Ørjan, G Martinsen, Head of Electronics Research Group, "Bioimpedance", Department of Physics, University of Oslo 2014.
- [6] J. V. Jethe, A. K. Deshpande, T. S. Ananthakrishnan, and G. D. Jindal, 'Bioelectrical Impedance Analysis and its Clinical Application', 2019.
- [7] S. Grimnes and O. G. Martinsen, *Bioimpedance and bioelectricity basics*. Academic press, 2011.
- [8] D. Naranjo-Hernández, J. Reina-Tosina, and M. Min, 'Fundamentals, recent advances, and future challenges in bioimpedance devices for healthcare applications', *Journal of Sensors*, vol. 2019, 2019. <https://doi.org/10.1155/2019/9210258>
- [9] Ivorra, 'Bioimpedance monitoring for physicians: an overview', *Centre Nacional de Microelectrònica Biomedical Applications Group*, vol. 11, p. 17, 2003.
- [10] M. A. Chilbert, 'High-voltage and high-current injuries', in *Applied Bioelectricity*, Springer, 1998, pp. 412–453.
- [11] L. Bernard and N. B. L. N. J. VASCONCELOS(laurent.nicolas@ec-lyon.fr), 'Electrical characterisation of biological tissues and computing of phenomena induced in the human body by electromagnetic fields below 1 GHz, Caractérisation électrique des tissus biologiques et calcul des phénomènes induits dans le corps humain par des champs électromagnétiques de fréquence

Chapter II: The Electrical Bioimpedance

- inférieure au GHz’, Ecole Centrale de Lyon, Universidade federal de Minas Gerais, 2007. [Online]. Available: <https://tel.archives-ouvertes.fr/tel-00179791>
- [12] <http://www.bioparhom.com/>
- [13] S.-J. E. Hall, ‘Guyton and Hall Textbook of Medical Physiology E-Book, livre ebook’, 2010.
- [14] K. R. Foster, ‘Schwan HP. Dielectric properties of tissues and biological materials’, *Crit Rev Biomed Eng*, vol. 17, p. 25, 1989.
- [15] H. P. Schwan, ‘Electrical properties of tissues and cell suspensions: mechanisms and models’, in *Proceedings of 16th annual international conference of the IEEE engineering in medicine and biology society*, 1994, vol. 1, pp. A70-A71 vol. 1.
- [16] B. Rajewsky and H. P. Schwan, ‘The dielectric constant and conductivity of blood at ultrahigh frequencies’, *Naturwissenschaften*, vol. 35, no. 10, p. 315, 1948.
- [17] P. Bhardwaj, D. V. Rai, M. L. Garg, and B. P. Mohanty, ‘Potential of electrical impedance spectroscopy to differentiate between healthy and osteopenic bone’, *Clinical Biomechanics*, vol. 57, pp. 81–88, 2018.
- [18] H. P. Schwan, ‘Electrical properties of tissue and cell suspensions’, in *Advances in biological and medical physics*, vol. 5, Elsevier, 1957, pp. 147–209.
- [19] H. Fricke, ‘XXXIII. The theory of electrolytic polarization’, *The London, Edinburgh, and Dublin Philosophical Magazine and Journal of Science*, vol. 14, no. 90, pp. 310–318, 1932.
- [20] P. Debye, ‘Polar Molecules, The Chemical Catalog Company’, Inc., New York, pp. 77–108, 1929.
- [21] K. S. Cole, ‘Permeability and impermeability of cell membranes for ions’, in *Cold Spring Harbor symposia on quantitative biology*, 1940, vol. 8, pp. 110–122.
- [22] N. Sekiguchi, T. Komeda, H. Funakubo, R. Chabicovsky, J. Nicolics, and G. Stangl, ‘Microsensor for the measurement of water content in the human skin’, *Sensors and Actuators B: Chemical*, vol. 78, no. 1–3, pp. 326–330, 2001.
- [23] J. Wang, *Design and implementation of an impedance analyzer based on Arduino Uno: A pilot study of bioelectrical impedance analysis*. 2015.

Chapter II: The Electrical Bioimpedance

- [24] Y. Kinouchi, T. Iritani, T. Morimoto, and S. Ohyama, 'Fastin vivo measurements of local tissue impedances using needle electrodes', *Medical and Biological Engineering and Computing*, vol. 35, no. 5, pp. 486–492, 1997.
- [25] L. A. Geddes, 'Who introduced the tetrapolar method for measuring resistance and impedance?', *IEEE Engineering in Medicine and Biology Magazine*, vol. 15, no. 5, pp. 133–134, 1996.
- [26] S. Bayod and A. Hermant, 'Les applications de la bioimpédance', *Projet DESS, UTC*, pp. 98–99, 1999.
- [27] E. De Roux *et al.*, 'Orthogonal Multitone Electrical Impedance Spectroscopy (OMEIS) for the Study of Fibrosis Induced by Active Cardiac Implants', *Journal of Sensors*, vol. 2019, 2019. <https://doi.org/10.1155/2019/7180694>
- [28] M. Gutierrez-Lopez, J. Prado-Olivarez, J. Diaz-Carmona, C. A. Herrera-Ramírez, J. A. Gutierrez-Gnecchi, and C. G. Medina-Sánchez, 'Electrical Impedance-Based Methodology for Locating Carcinoma Emulators on Breast Models', *Journal of Sensors*, vol. 2019, 2019. <https://doi.org/10.1155/2019/8587191>
- [29] A. Hafid, S. Benouar, M. Kedir-Talha, M. Attari, and F. Seoane, 'Simultaneous recording of ICG and ECG using Z-RPI device with minimum number of electrodes', *Journal of Sensors*, vol. 2018, 2018. <https://doi.org/10.1155/2018/3269534>
- [30] E. C. Hoffer, C. K. Meador, and D. C. Simpson, 'Correlation of whole-body impedance with total body water volume.', *Journal of applied physiology*, vol. 27, no. 4, pp. 531–534, 1969.
- [31] H. C. Lukaski, P. E. Johnson, W. W. Bolonchuk, and G. I. Lykken, 'Assessment of fat-free mass using bioelectrical impedance measurements of the human body', *The American journal of clinical nutrition*, vol. 41, no. 4, pp. 810–817, 1985.
- [32] T. K. Bera, J. K. Seo, H. Kwon, and J. Nagaraju, 'A LabVIEW based electrical bio-impedance spectroscopic data interpreter (LEBISDI) for studying the equivalent circuit parameters of biological tissues', in *Proceedings of the 15th International Conference on Electrical Bio-Impedance (ICEBI) and 14th Conference on Electrical Impedance Tomography (EIT)*, 2013, p. 77.

Chapter II: The Electrical Bioimpedance

- [33] J. Nyboer, S. Bango, A. Barnett, and R. H. Halsey, 'Radiocardiograms: electrical impedance changes of the heart in relation to electrocardiograms and heart sounds', *J Clin Invest*, vol. 19, no. 5, pp. 773–8, 1940.
- [34] W. G. Kubicek, 'Development and evaluation of an impedance cardiac output system', *Aerosp Med*, vol. 37, pp. 1208–1212, 1966.
- [35] M. H. Ribeiro, R. W. dos Santos, L. P. S. Barra, and F. C. Peters, 'Simulation study on the determination of cardiac ejection fraction by electrical impedance tomography using a hybrid heuristic approach', *Journal of Medical Imaging and Health Informatics*, vol. 4, no. 1, pp. 113–121, 2014.
- [36] [HTTP://WWW.RJLSYSTEMS.COM/PRODUCTS/ANALYZERS/](http://www.rjlsystems.com/products/analyzers/) 02/03/2022
- [37] [HTTP://BIOANALOGICS.COM/LEADER.CQS](http://bioanalogics.com/leader.cqs) 15/12/2017
- [38] [HTTP://WWW.BIODYNCORP.COM/PRODUCT/PRODUCTS_BIO.HTML](http://www.biodyncorp.com/product/products_bio.html) 02/02/2022
- [39] [HTTPS://WWW.BODYSTAT.COM/](https://www.bodystat.com/) 02/02/2022
- [40] [HTTPS://VERMED.COM/CARDIODYNAMICS/ICG-SENSORS.ASPX](https://vermed.com/CardioDynamics/ICG-Sensors.aspx) 02/03/2022
- [41] [HTTPS://TANITA.EU/TANITA-ACADEMY/BIOELECTRICAL-IMPEDANCE-ANALYSIS](https://tanita.eu/tanita-academy/bioelectrical-impedance-analysis)
- [42] [HTTP://WWW.NUTRILOG.COM/NUTRILOG_FR/AMINOSTATS_DISCOVER.HTM](http://www.nutrilog.com/nutrilog_fr/aminostats_discover.htm) 02/03/2022
- [43] [HTTP://TANITA.FR/BC-545N](http://tanita.fr/BC-545N)
- [44] [HTTP://TANITA.FR/BC-601](http://tanita.fr/BC-601)
- [45] [HTTP://WWW.BALANCE-IMPEDANCEMETRE.COM/BALANCE_SOEHNLE_FITNESS7850.PHP](http://www.balance-impedancemetre.com/balance_soehnle_fitness7850.php) 15/12/2017
- [46] [HTTP://TANITA.FR/](http://tanita.fr/)
- [47] [HTTPS://BUY.GARMIN.COM/EN-GB/GB/P/530464](https://buy.garmin.com/en-gb/gb/p/530464) 02/03/2022
- [48] [HTTPS://WWW.GIRODMEDICAL.COM/FABRICANTS/SOEHNLE/](https://www.girodmedical.com/fabricants/soehnle/)
- [49] [HTTPS://WWW.FITBIT.COM/NL/ARIA2](https://www.fitbit.com/nl/aria2) 15/12/2017
- [50] [HTTP://WWW.BALANCE-IMPEDANCEMETRE.COM](http://www.balance-impedancemetre.com) 26/11/2017
- [51] [HTTP://WWW.ZMETRIX.COM/](http://www.zmetrix.com/)

Chapter .III

I. Introduction

In recent years, cardiovascular disease has increased; consequently the mortality rate also increases. The American Heart Association report has suggested that for near incoming years we will witness an alarming increase [1].

For this reason the researchers are developing new methods to overcome the causes of mortality with less harm. Impedance cardiography ICG known also as transthoracic electrical bioimpedance cardiography based on the intra-thoracic changes of blood volume and measuring changes in electrical resistance during the cardiac cycle [2].

This method is reliable, safe, and does not present any danger to patients because their measurements are released in a non-invasive way and requires four patches attached to the skin of the neck and thoracic wall. It helps to provide information about the physiological activity and pathological changes in the heart and chest.

It is used for hemodynamic metrics extractions that help in the cardiovascular diseases prevention, diagnosis and cardiac monitoring whether ambulatory or continuous long-term in intensive care units and perioperative. The ICG method is an alternative technique to invasive techniques such as thermodilution, pulmonary artery catheter (PAC), and Doppler [3].

Kubicek et al. have developed a model based on the four-electrode method for impedance cardiography measurement. It aims to calculate Stroke volume that includes also the left ventricle ejection time [4].

The electrical impedance has parameters that can be used for the diagnosis and monitoring of the pathological condition of the patient's tissues. Among these parameters: stroke volume, stroke volume index (SV/SVI), cardiac output, cardiac index (CO/CI), left ventricular ejection time (LVET), the preejection period (PEP), thoracic fluid content (TFC) and heart rate variability (HRV).

In 1940, studies using the ICG technique emerged. In 1960, the National Administration of Aeronautics and Space began the research of the thoracic electrical bio-impedance using heart index record [5].

In 1966, Kubicek tested a systolic ejection volume (SV) equation according to the bio-impedance using an electrode location that measured thanks to the four-electrode

Chapter III: The Impedance Cardiography Technique

method developed by Kubicek *et al.* He is the first who used the principal of the first derivative dZ/dt (ICG) of the impedance Z [4].

In the same year, The 1st impedance cardiography monitoring device was developed.

Granerus used the ICG signal for the left ventricular ejection volume computation in 1981 [6], where Sramek developed a new equation in hemodynamic based on the cardiac impedance changes.

In 1986, also Sramek used 8 spot electrodes like standard ECG electrodes. The first pair of electrodes is placed at the beginning of the thorax and the second one at the end of the thorax (the level of the xiphoid process) [7].

In this chapter, aims to review the various studies carried out on this signal type, and to present the multiple methods used for the ICG signal measurement, its shape, , as well as its characteristics which make it possible to calculate hemodynamic parameters for the cardiovascular diseases' diagnosis and a correct analysis

II. Principal Methodology

1. Definition

Impedance Cardiography is the study of the cardiac function by means of thorax electrical impedance measurements with The Tetrapolar electrode system using four-band electrodes or 8 spot electrodes. High frequency (50-100 kHz) is used and in others studies they used a frequency range varying from 20 to 100 KHz, low-intensity current across an outer pair of electrode (0.2-5 mA) is injected through the thorax and recuperated the potential of the impedance change with the sensing inner pair electrodes [8].

There is No risk of physiological effects because various tissues of the human body are not excitable at this frequency and at this low current level (Patterson, 1989).

However, it presents any danger to the patient according to the report of the Association of Advancement of Medical Instrumentation in 2005 and it is applicable without any specialised knowledge.

2. ICG Features Extraction

The measurement (see Figure 7) is based on the skin electrodes contact that generates impedance. In order to eliminate it, the application of pre-gelled highly conductive electrodes is required.

Furthermore, the appearance of electrode-electrolyte impedance can be greater than the impedance tested especially at low frequencies, which are too unstable and unpredictable to think about the measurement [9].

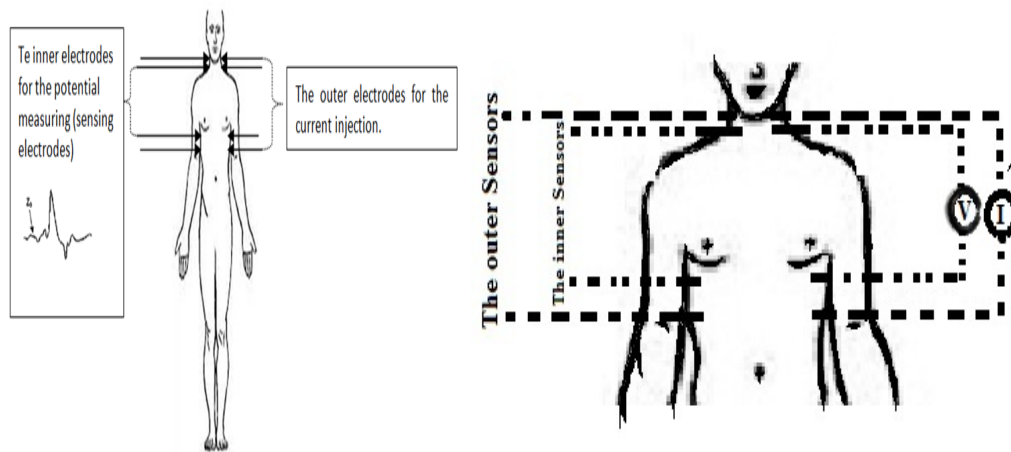


Figure 7: The Electrode configuration for ICG signal measurement [9] [10].

Figure 8 and 9 present the composition of the recuperated ICG waveform, where Z_0 : baseline impedance; where A is the atrial wave coincides with P of the ECG waveform; the point B coincides with the opening of the aortic and pulmonary valves. The point C corresponds to the maximum peak of the dZ/dt (ICG) signal on a heartbeat. It presents the blood ejection rate by the ventricles, which corresponds to the ventricular contraction. The point X is the lowest point after peak C and is associated with the closure of the aortic valve. The point Y : corresponds to the closure of the pulmonary valve. The wave O occurs during the diastole (the passive blood passage between the atriums and the ventricles), its peak is the moment of the mitral valve opening. PEP presents the pre-ejection period. VET is the ventricular ejection time. IVRT is the isovolumic relaxation time, and FT is the ventricular filling time [9].

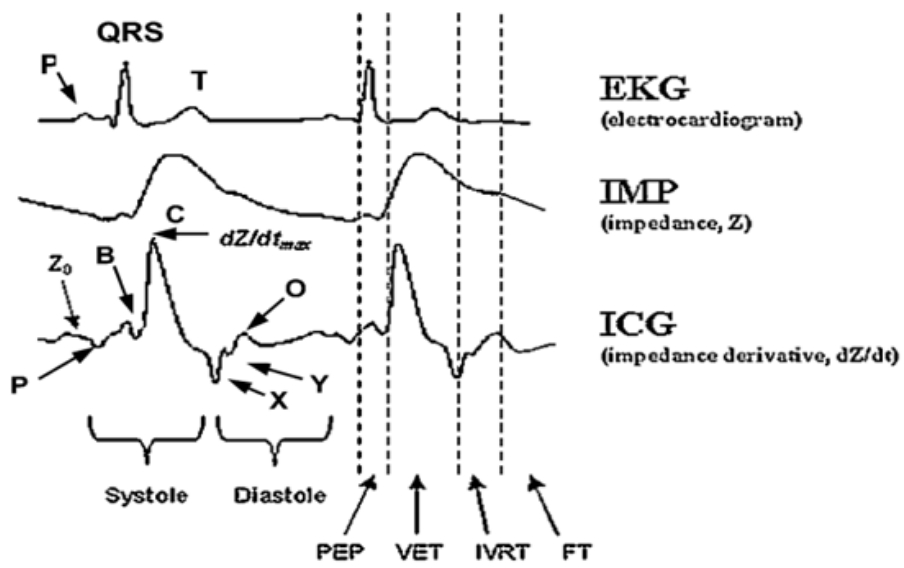


Figure 8: The characteristic extraction of the ICG waveform [5].

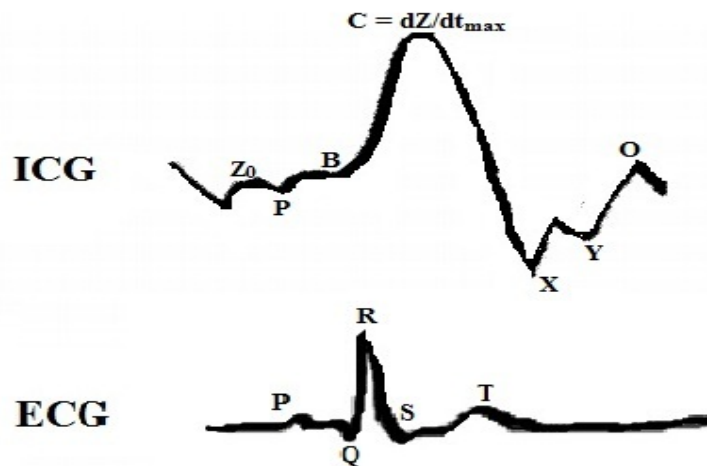


Figure 9: The typical ICG and ECG waveform [10].

The Bioimpedance variation can be used for diagnostic information and for Stroke Volume (SV) and Cardiac output (CO) estimation as well as time intervals measurement.

Chapter III: The Impedance Cardiography Technique

- The term SV indicates the amount of blood pumped by the heart left ventricle in one contraction. The SV equations are for the systolic ejection volume depending on the thoracic impedance variation.

$$SV = \rho \times (L/Z_o)^2 \times \Delta Z \text{ .(Nyboer)} \quad (1)$$

$$SV = \rho_b (L/Z_o)^2 (dZ/dt)_{max} LVET. \text{ (Kubicek [4])} \quad (2)$$

$$SV = \frac{(0.17 H)^3}{4.25} \frac{1}{Z_o} \left(\frac{dz}{dt}\right)_{max} LVET \text{ (Sramek [7])} \quad (3)$$

$$SV = \sigma \frac{(0.17 H)^3}{4.25} \frac{1}{Z_o} \left(\frac{dz}{dt}\right)_{max} LVET \text{ (D.P. Bernstein and Sramek)} \quad (4)$$

$$\text{with } \sigma = \sqrt{BMI_{patient}/24},$$

And the new Bernstein equation is defined as follow:

$$SV = V_c \sqrt{\frac{1}{Z_o} \left(\frac{dz}{dt}\right)_{max}} LVET, \quad (5)$$

Where,

ρ : is a constant specific of the resistivity of blood and variable to person from another person;

ρ_b : is the static specific resistance of blood Ω (cm)= 135 Ω cm [11];

Z_o : is the basic impedance of the thorax (Ω);

$LVET$: is the left ventricular ejection time;

BMI : is the body mass index;

24: is the ideal BMI value assumed by Bernstein ($kg.m^{-2}$);

δ : is the Bernstein Correction Factor [12];

L is the transthoracic length;

V_c is the intrathoracic blood volume (mL);

H is its size in (m).

Chapter III: The Impedance Cardiography Technique

- The cardiac output is the blood ejected by left ventricle at each heart beat; it defined in the equation below:

$$CO_{(L/min \text{ or } mL/min)} = \text{stroke volume} \times \text{heart rate(HR)} \quad (6)$$

The normal range is approximately 5.6 L / min for the man and 4.9L / min for the woman.

3. Signal Processing

The ICG analysis aims to provide a correct diagnosis for cardiovascular disorder thanks to the hemodynamic parameters calculations. For this reason, several algorithms are used to analyse the recuperated ICG signal with range of 0.8 and 20 Hz that is altered by artefacts with low frequencies cause distortions due to multiple causes such as: respiratory and motion artifacts due to patient movement during acquisition, poor electrode placement and electrode material, it caused baseline drift, power frequency interference, myoelectricity interference.

To not erroneously analyse the signal analysis and to not make the analysis inaccurate and very difficult for finding the correct diagnosis, many studies have been done to obtain a better approach to signal segmentation and especially of the highly variable signals.

The noise that reaches the signal pushes towards a bad diagnosis, that is why the Wavelets come to solve this problem, some studies use filters as that of Sarah Ostadabbas 2017. Several models have been created such as that developed by Pinheiro Eduardo et al. in 2011 [13].

The study is based on a heartbeat segmentation method for cardiovascular signals. It uses four parameters that relies on a sliding power window without needing the hypothesis formula including the patient's heartbeat shape or a reference signal to synchronise the points of segmentation.

Its purpose is to transform the cardiac signal and obtain the fundamental frequency of heartbeat oscillation. This model segments highly variable signals as ballistocardiogram

Chapter III: The Impedance Cardiography Technique

(BCG) and ICG, using wavelet filtering and peaks detection. The freely seated wheelchair with a motionless subject is the test condition required to acquire this type of physiological signals in the Pinheiro study.

The second model used a mathematical model based on a process summation effect, the first of which refer to the WpE pre-injection wave and the second referring to the ejection wave WEj.

The important points to detect are the maximum of wave C and the maximum peak of the second derivative is point B [14].

In 2016, Chabchoub et al. use wavelets to denoise the signal, they found that the Daubechies wavelet family (db8) perform better in terms of noise cancellation; it gives better separation between artifact and signal. It allows us to determine the cardiovascular parameters and to diagnose cardiovascular diseases [15].

In 2017, Souhir Chabchoub used the ICG signal to detect mitral insufficiency, heart failure, myocardial infarction, and mitral insufficiency. Their study has an accuracy rate of 98.94% [16].

To reduce noises from ICG waveform, other denoising methods are used as the Savitzky–Golay filter, the median filter; an adaptive filtering based least mean squares (LMS) [17], and others wavelets as Meyer wavelet [18].

The ICG technique accuracy is evaluated and significantly shows the good correlation using the bioimpedance correlation coefficient calculations that are compared with other techniques as conventional invasive methods like Fick, Thermodilution, and aortic Doppler techniques.

In 1996, DeMarzo AP. et al. compared ICG with Aortic Doppler for aortic valve opening detection and found a high correlation equal to 0.996 [19].

In 1996, Belardinelli et al. compared ICG with thermodilution (TD) where he found a good correlation with rate among 0.89 [20].

In 2003, Faddy.S et al. made a comparison between TEB and TD for the population of patients with a right heart catheterization. The results show a good correlation equal to 0.91 [21].

In 2004, Cotter et al. found a good correlation when comparing ICG with thermodilution (TD) in the population of patients suffering with heart failure [22].

Chapter III: The Impedance Cardiography Technique

In 2004, Yung GL et al. found a correlation rate equal to 0.8 when comparing three types of techniques: TD vs ICG and Fick [23].

In 2011, Sharma et al. compared TEB with thermodilution, he found a good correlation [24].

In 2012, Deepak et al. made a comparison between thoracic electrical bioimpedance (TEB), he found a correlation rate equal to 0.9 [25].

Studies have been done to measure the reliability of non-invasive bio-impedance techniques by measuring different hemodynamic parameters that are already calculated by invasive techniques [26].

However, the measurement of this type of physiological signal is influenced by some wave's variations as that contact electrodes with tissue and their positioning on skin, patient weight, pulmonary oedema, biological composition, respiration, noise due to movement or equipment, blood circulation, volume blood from the transthoracic region, tissue fluid volume, sweating skin, and myocardial tissue contraction.

Despite the several advantages of the ICG technique, such as the continuous and real-time hemodynamic monitoring principle in a non-invasive way. It is flexible, simple, reliable, safe, and painless, at low cost, easy and fast. Also it ensures the diagnosis of cardiovascular diseases such as mitral insufficiency and heart failure, it is limited in the field of the valvular heart disease detection as shown in the study of Chabchoub in 2017 [16].

III. Conclusion

Cardiovascular disease is the most popular disorder in the world, for this reason, the ICG study comes to solve the problem of early detection of diseases thanks to the continuous monitoring that the ICG ensures.

The Impedance cardiography (ICG) technique allows obtaining continuous and real-time hemodynamic data measurements as well as the diagnosis and monitoring of cardiovascular diseases, it is advantageous in medical field, it provides a better distribution but is affected by several conditions as the respiration, equipment movements, electrodes emplacement and others. It is a method to obtain the cardiac indexes including cardiac output.

Chapter III: The Impedance Cardiography Technique

This method has many advantages that are non-invasiveness, low cost, and ease of use. However, it has limitations that prevent its implementation in medical practice especially for patients' with critical cases.

Several studies were about the analysis of the electrical impedance of biological tissues in order to diagnose and study the physiological and pathological state with the non-invasive method.

The purpose of the impedance cardiography analysis is the possibility of obtaining important information about the anatomy and tissue physiology.

REFERENCES

- [1] Ghosh, B. P. Chattopadhyay, R. M. Roy, J. Mukherjee, and M. Mahadevappa, 'Estimation of echocardiogram parameters with the aid of impedance cardiography and artificial neural networks', *Artificial Intelligence in Medicine*, vol. 96, pp. 45–58, 2019.
- [2] B. He *et al.*, 'Waveform analysis of differential graphs of reconstructed impedance cardiography from healthy individuals', *Annals of Noninvasive Electrocardiology*, vol. 25, no. 3, p. e12714, 2020.
- [3] B. M. Bonora, S. Vigili de Kreutzenberg, A. Avogaro, and G. P. Fadini, 'Effects of the SGLT2 inhibitor dapagliflozin on cardiac function evaluated by impedance cardiography in patients with type 2 diabetes. Secondary analysis of a randomized placebo-controlled trial', *Cardiovascular diabetology*, vol. 18, no. 1, pp. 1–9, 2019.
- [4] W. G. Kubicek, 'Development and evaluation of an impedance cardiac output system', *Aerosp Med*, vol. 37, pp. 1208–1212, 1966.
- [5] R. L. Summers, W. C. Shoemaker, W. F. Peacock, D. S. Ander, and T. G. Coleman, 'Bench to bedside: electrophysiologic and clinical principles of noninvasive hemodynamic monitoring using impedance cardiography', *Academic emergency medicine*, vol. 10, no. 6, pp. 669–680, 2003. <https://doi.org/10.1197/aemj.10.6.669>. <https://doi.org/10.1111/j.1553-2712.2003.tb00054.x>.
- [6] G. Granerus and R. Elg, 'Stroke volume measurement by impedance cardiography using a formula based on the Δz waveform', *Clinical Physics and*

Chapter III: The Impedance Cardiography Technique

- Physiological Measurement*, vol. 3, no. 2, p. 131, 1982.
<https://doi.org/10.1088/0143-0815/3/2/003>
- [7] B. B. Sramek, 'Status report on BoMed's electrical bioimpedance', *Proceedings of the Annual International Conference of the IEEE Engineering in Medicine and Biology Society*, p. 51 vols1-, 1988.
- [8] H. Shih and T.-C. Lo, 'Electrochemical impedance spectroscopy for battery research and development. Cortech Corporation', CA, Tech. Rep, 31 (9-11), 1996.
- [9] S. Kerai, 'The impedance cardiography technique in medical diagnosis', *Medical Technologies Journal*, vol. 2, no. 3, pp. 232–244, 2018.
- [10] H. Benabdallah and S. Kerai, 'Respiratory and Motion Artefacts Removal from ICG Signal Using Denoising Techniques for Hemodynamic Parameters Monitoring.', *Traitement du Signal*, vol. 38, no. 4, 2021.
<https://doi.org/10.18280/ts.380401>
- [11] A. W. Quail, F. M. Traugott, W. L. Porges, and S. W. White, 'Thoracic resistivity for stroke volume calculation in impedance cardiography', *Journal of Applied Physiology*, vol. 50, no. 1, pp. 191–195, 1981.
- [12] D. P. Bernstein and H. J. M. Lemmens, 'Stroke volume equation for impedance cardiography', *Medical and Biological Engineering and Computing*, vol. 43, no. 4, pp. 443–450, 2005.<https://doi.org/10.1007/BF02344724>
- [13] E. Pinheiro, O. Postolache, and P. Girão, 'Method for segmentation of cardiac signals based on four parameter sine fitting', in *2011 IEEE EUROCON-International Conference on Computer as a Tool*, 2011, pp. 1–4.<https://doi.org/10.1109/EUROCON.2011.5929306>
- [14] V. V. Ermishkin, V. A. Kolesnikov, E. V. Lukoshkova, and R. S. Sonina, 'Simulation of pathologic changes in ICG waveforms resulting from superposition of the preejection and ejection waves induced by left ventricular contraction', in *Journal of Physics: Conference Series*, 2013, vol. 434, no. 1, p. 012007.<https://doi.org/10.1088/1742-6596/434/1/012007>.
- [15] S. Chabchoub, S. Mansouri, and R. B. Salah, 'Impedance cardiography signal denoising using discrete wavelet transform', *Australasian physical &*

Chapter III: The Impedance Cardiography Technique

- engineering sciences in medicine*, vol. 39, no. 3, pp. 655–663, 2016.<https://doi.org/10.1007/s13246-016-0460-z>
- [16] S. Chabchoub, S. Mansouri, and R. B. Salah, ‘Detection of valvular heart diseases using impedance cardiography ICG’, *Biocybernetics and Biomedical Engineering*, vol. 38, no. 2, pp. 251–261, 2018. <https://doi.org/10.1016/j.bbe.2017.12.002>.
- [17] X. Hu *et al.*, ‘Adaptive filtering and characteristics extraction for impedance cardiography’, *Journal of Fiber bioengineering and Informatics*, vol. 7, no. 1, pp. 81–90, 2014.
- [18] V. K. Pandey and P. C. Pandey, ‘Wavelet based denoising for suppression of motion artifacts in impedance cardiography’, 2009.
- [19] A. P. DeMarzo and R. M. Lang, ‘A new algorithm for improved detection of aortic valve opening by impedance cardiography’, in *Computers in Cardiology 1996*, 1996, pp. 373–376. <https://doi.org/10.1109/CIC.1996.542551>.
- [20] R. Belardinelli, ‘Ciampani N, Costantini C, Blandini A, Purcaro A’, *Comparison of impedance cardiography with thermodilution and direct Fick methods for noninvasive measurement of stroke volume and cardiac output during incremental exercise in patients with ischemic cardiomyopathy. Am J Cardiol*, vol. 77, pp. 1293–1301, 1996.[https://doi.org/10.1016/S0002-9149\(97\)89153-9](https://doi.org/10.1016/S0002-9149(97)89153-9).
- [21] S. Faddy, J. Boland, and D. W. M. Muller, ‘Accuracy and reliability of non-invasive cardiac output: the future in cardiology?’, *Computers in Cardiology*, vol. 1, no. 30, pp. 251–254, 2003. <https://doi.org/10.1109/CIC.2003.1291138>
- [22] G. Cotter *et al.*, ‘Accurate, noninvasive continuous monitoring of cardiac output by whole-body electrical bioimpedance’, *Chest*, vol. 125, no. 4, pp. 1431–1440, 2004. <https://doi.org/10.1378/chest.125.4.1431> PMID:15078756.
- [23] G. L. Yung, P. F. Fedullo, K. Kinninger, W. Johnson, and R. N. Channick, ‘Comparison of impedance cardiography to direct Fick and thermodilution cardiac output determination in pulmonary arterial hypertension’, *Congestive heart failure*, vol. 10, pp. 7–10, 2004.<https://doi.org/10.1111/j.1527-5299.2004.03406.x>.

Chapter III: The Impedance Cardiography Technique

- [24] V. Sharma, A. Singh, B. Kansara, and A. Karlekar, 'Comparison of transthoracic electrical bioimpedance cardiac output measurement with thermodilution method in post coronary artery bypass graft patients', *Annals of cardiac anaesthesia*, vol. 14, no. 2, p. 104, 2011. <https://doi.org/10.4103/0971-9784.81564> PMID:21636930.
- [25] P. Barde, A. Bhatnagar, R. Narang, and K. K. Deepak, 'Comparison of non-invasive cardiac output measurement using Indigenous impedance cardiography with invasive fick method', *International Journal of Biomedical Research*, vol. 3, no. 11, pp. 431–434, 2012. <https://doi.org/10.7439/ijbar.v3i11.816>
- [26] P. Chaudhari and M. Panse, 'Measurement of cardiac output using bioimpedance method', *International Journal of Computer Applications*, vol. 975, p. 8887, 2013.

Chapter .IV

Chapter IV: Denoising methods Applied for ICG signal Analysis

I. Introduction

Bioimpedance is a scientifically relevant research area of many researchers which is an alternative method of invasive methods that are painful and very expensive. Through biological tissue stimulation with a low-intensity current through electrodes, the voltage is recuperated and complex electrical impedance is involved that depends on biological tissues.

The different variation in blood volume and low velocity of the ascending aorta during systole and diastole generate the variations of impedance (Z) among their different applications, there are thoracic bioimpedance or impedance cardiography (ICG) technique which is reliable, non invasive and practical method that is widely used in clinical practice for the measurement of multitude hemodynamic parameters and it is a new way for cardiovascular diseases diagnostics and continuous monitoring.

The advantage of this technique is its simplicity of realisation, the speediness of its temporal response, it is cheaper, non-invasive, and safer, it makes continuous monitoring in real-time [1].

The research of ICG [2] is widely used in clinical applications as Hypertension, Surgery, Cardiovascular Diseases, Pregnancy women [3] and others. It emerged in 1940, it is simple, safe, easy to apply, cost-effective and a non-invasive method of diagnostic and medical monitoring that measures the change in blood volume due to impedance variations inside the chest using the electrode system placed on the patient's skin [4].

The result of this measurement is a sensed impedance waveform range between 0.8 and 20 Hz called ICG signal vulnerable to noises such as respiratory and movement artifacts which is due to the motions of patients during the acquisition, the incorrect electrodes positioning, and their manufacturing material. These factors make the evaluation of cardiac indices calculation inaccurate such as; stroke volume (SV) and cardiac output (CO) to diagnose and monitor the patient's condition.

One way to derive several significant parameters is the analysis of this waveform type by denoising which is an important step in the process. The signal processing field is used to overcome the problem of noises that disturb the signals

Chapter IV: Denoising methods Applied for ICG signal Analysis

Many researchers devoted their studies on the algorithm's detection of the characteristic points, but the problem of this ICG signal acquired is the respiratory and motion artefacts which makes its analysis a little delicate, for this purpose, our research contributed to solve this problem.

The samples of the ICG signal (see Figure 10) from 10 participants are recorded with the sampling rate equal to 1000Hz. The ICG device is accomplished in three sections consisting of Howland current injection stage, lock-in amplifier stage for impedance detection and ICG evaluation interface. The bioimpedance measurements were conducted in Tetrapolar configuration based on four electrodes.

In one side, our methodologies based mainly on the denoising process, it is consisted to find the best performing denoising method of the ICG signal without distorting the shape of ICG signals studies, hence we have proposed some filtering techniques such as linear filters, adaptive filters, Savitzky-Golay (SG), singular values decomposition (SVD), and wavelets, and then they are all tested to noise removal and to have more visibility of the ICG waveform. In the other side, we applied some algorithms of detection for features points' extraction.

Ten healthy subjects, recorded by BioLab v.3.0.13 software with the sampling rate equal to 1000 Hz and the code has been developed under Matlab R2014a. During a time period, Figure 10 and 11 present the ten cycles of ICG signal just for subject 1.

In this chapter, the several denoising methods are applied, explained and presented.

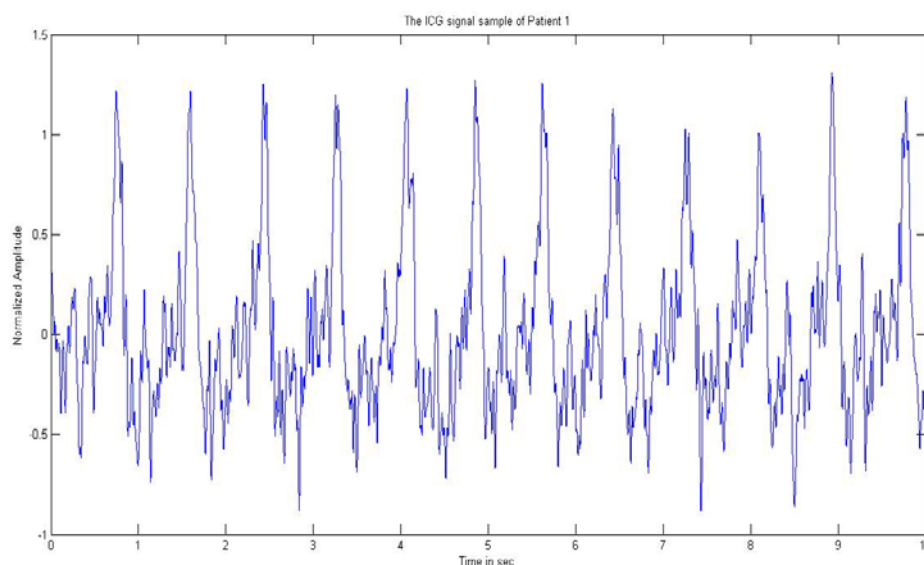


Figure 10 : The ICG signal cycles for subject 1.

Chapter IV: Denoising methods Applied for ICG signal Analysis

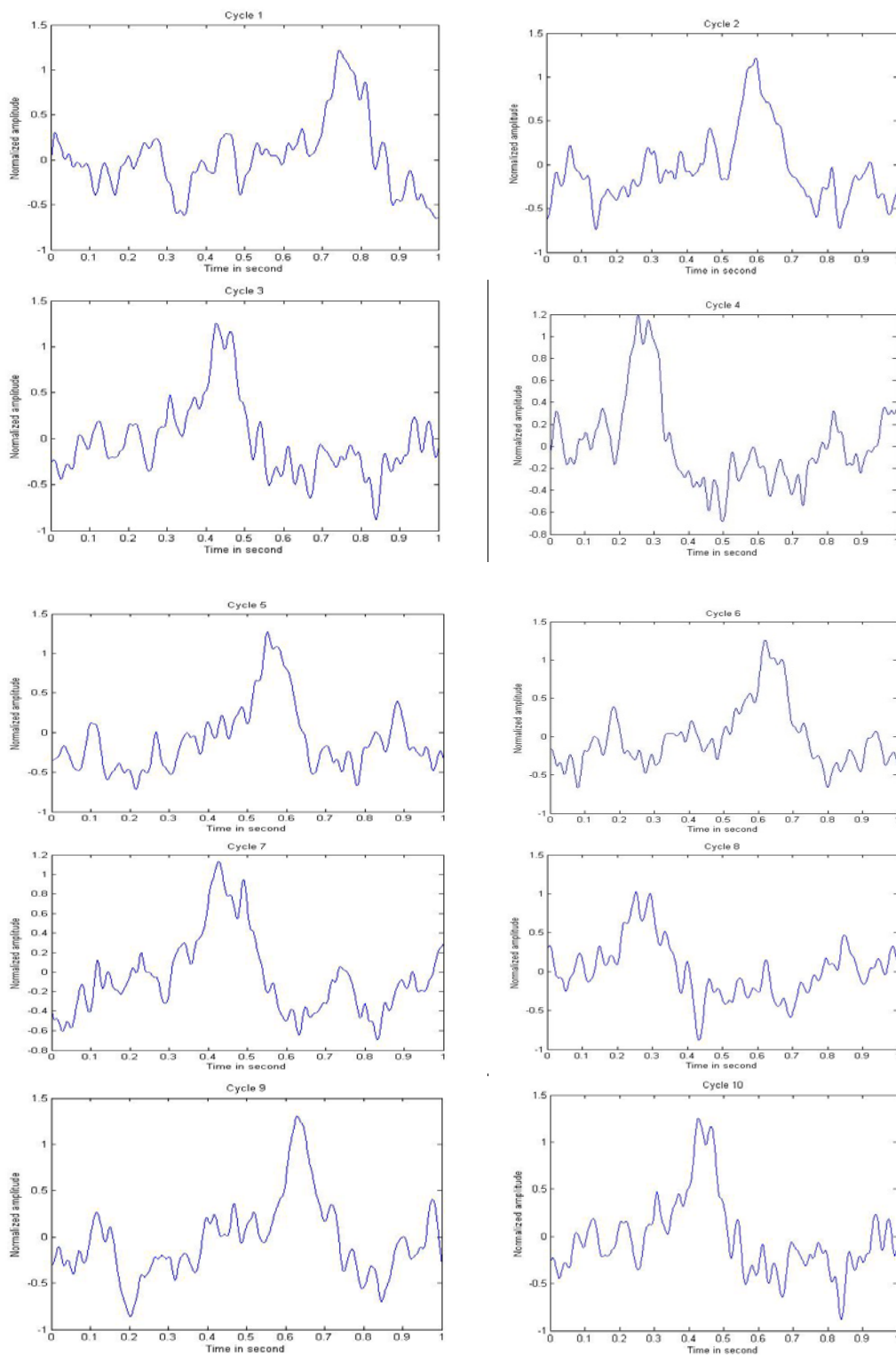


Figure 11 : The cycles of ICG signal for subject 1 from 1 to 10cycles.

Chapter IV: Denoising methods Applied for ICG signal Analysis

II. Method 1

The first method used in the paper under press in Int. J. Medical Engineering and Informatics is based on Adaptive filters and Savitzky-Golay (SG).

Our first research consisted of comparing several types of denoising methods to find that performed well. We used adaptive filter for noise removal of the ICG signal already used by Hu in 2014 [5]; and Pandey in 2011[6] as: on least mean squares (LMS), normalised LMS (NLMS), leaky LMS, signed LMS (SLMS), signed regressor (SRLMS), sign-sign (SSLMS), and recursive least square (RLS), we are also applied Savitzky-Golay filter cited by Chabchoub 2016; Salah and Ouni, 2017 [7] [8].

The adaptive filters are self learned, relying on a feedback mechanism, it is a digital filter employed to reduce or enhance some signal aspects. For cancelling noises that altered the signal under study, the filter parameters are set recursively. The adaptive algorithm has a transfer function used to adjust the adaptive filter weight coefficients $W(i)$ thanks to predefined variable parameters, characterised by filter order M . In our case, it serves to reduce error signal or cost function. The adaptive filter shown in Figure 12 presents a block diagram where $x(i)$ is the input signal throw the adaptive filter that is updated with a weight coefficient $w(i)$ to produce the output signal $y(i)$ [5].

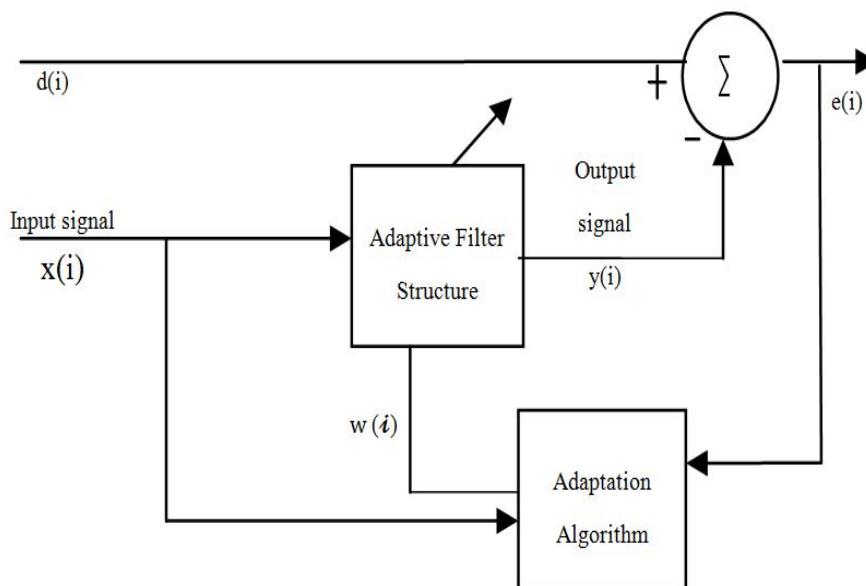


Figure 12: The adaptive filter structure.

Chapter IV: Denoising methods Applied for ICG signal Analysis

LMS based finite impulse response (FIR) filter is the most applied, its implementation is simple and advantageous and it has robust operations. The predefined step size is based on a gradient descent, which is selected at the beginning of the adaptive filter.

The following equations present the basic LMS algorithm steps [9]:

$$x(i) = [x(i), x(i-1), x(i-2), \dots, x(i-M+1)]^T \quad (1)$$

$$x(i) = d(i) + N(i) \quad (2)$$

$$W(i) = [w_i(0), w_i(1), \dots, w_i(M-1)]^T \quad (3)$$

$$y(i) = W(i)^T x(i) \quad (4)$$

$$err(i) = d(i) - y(i) \quad (5)$$

$$W(i+1) = W(i) + \mu x(i) err(i) \quad (6)$$

Where $x(i)$ is the noisy signal, $d(i)$ is the desired signal, $W(i)$ is weight coefficients, $W(i+1)$ is the weight update or the updated filter coefficient, $y(i)$ is the output signal or reconstructed, N is the noise added, M is the order filter, $err(i)$ the signal error for the convergence rate, μ is the step size ($0 < \mu < (2/ T\text{-tap FIR filter})$) for the algorithm convergence, it is varying between 0 and 0.2, where we have selected three values: 0.004, 0.008, and 0.01.

The difference between the several types of LMS is established on the weight update for LMS algorithm types defined in equations below:

NLMS equation defined as follow:

$$w(i+1) = w(i) + 2 \mu err(i) x(i) \quad (7)$$

LLMS equation defined as follow:

$$w(i+1) = v * w(i) + \mu err(i) x(i) \quad (8)$$

Where, v is between 0 and 1, the value is equal to 0.99 in our study.

SLMS equation defined as follow:

Chapter IV: Denoising methods Applied for ICG signal Analysis

$$w(i + 1) = w(i) + \mu \text{sign}(\text{err}(i)) x(i) \quad (9)$$

SRLMS equation defined as follow:

$$w(i + 1) = w(i) + \mu \text{err}(i)\text{sign}(x(i)) \quad (10)$$

SSLMS equation defined as follow:

$$w(i + 1) = w(i) + \mu \text{sign}(\text{err}(i)) \text{sign}(x(i)) \quad (11)$$

The Recursive least squares (RLS) converge faster than LMS that find recursively finds the coefficients of filter, Which minimise a weighted linear least-squares cost function relating to the input signals, the algorithm [10] defined as in the following equations:

$$w(i + 1) = w(i) + e(i).k(i) \quad (12)$$

$$k(i) = \frac{p(i).u(i)}{\lambda + u^T(i)p(i).u(i)} \quad (13)$$

$$p(i) = \delta^{-1}u(i) \quad (14)$$

$$p(i + 1) = \lambda^{-1}p(i) - \lambda^{-1}k(i)u^T(i)p(i) \quad (15)$$

where i is the iterations, $w(i)$ is the filter coefficient vector, $w(i + 1)$ is the weight update, λ is the forgetting factor is between 0 and 1 we choose a value equal to 0.98, δ is the regulation factor, $k(i)$ is the gain factor, $e(i)$ is error signal, $u(i)$ is unity matrix, and $p(i)$ is the inverse correlation matrix of the input signal.

A SavitzkyGolay (SG) filter is a digital filter with a finite impulse response that smoothes the signal data without destroying its shape and makes the information provided on the signal more accurate. It has two settings: the window length and the filter order. Precisely, it can automatically adjust its settings, according to sampling or cut-off frequency [11].

Chapter IV: Denoising methods Applied for ICG signal Analysis

In our work, this method is based on the local least-squares polynomial approach, where the polynomial degree is controlled [12].

After testing the orders (from 1 to 10) and comparing them with the adaptive filters simultaneously, we found that the polynomial of degree 9 performs well, which reduces noises to the maximum.

The evaluation criteria step is essential to verify the technique performance. For this purpose, four metrics are calculated as defined in the following equations:

The error (Err) equation defined as follow:

$$\text{Err} = (d(i) - y(i)) \quad (16)$$

The signal to noise ratio output (SNR) expressed in dB, its equation defined as follow:

$$\text{SNR} = 10\log_{10} \left[\frac{\sum_i y^2(i)}{\sum_i (y(i) - d(i))^2} \right] \quad (17)$$

The signal to noise ratio input (SNR_i) expressed in dB which the input noise ranges is calculated from 0 dB to 20 dB:

$$\text{SNR}_i = 10\log_{10} \left[\frac{\sum_i x^2(i)}{\sum_i (\text{noise})^2} \right] \quad (18)$$

The mean square error (MSE) equation defined as follow:

$$\text{MSE} = \text{mean} (x(i) - y(i))^2 \quad (19)$$

Where $d(i)$ is the original signal, $x(i)$ is the noisy signal, $y(i)$ is the reconstructed signal.

III. Method 2

The second method used in the paper published in 2021 IEEE 6th International Conference on Computing, Communication and Automation (ICCCA) proceeding. It is based on a novel noise-reduction technique of filtering tool called singular value decomposition (SVD) Algorithm for ICG signal, where we compared it with LMS based

Chapter IV: Denoising methods Applied for ICG signal Analysis

adaptive filter, already explained in the previous method, which is used specially to eliminate the breathing artifact.

To evaluate the technique, a specific performance setting has been calculated: SE, RMSE, SNR and SNR improvement.

Singular value decomposition is a method that enables the factorization of a matrix. It provides complete orthogonality to supply a more visible view of a geometric signal processing structure based on the number of Singular values other than zero values placed on the matrix [13] [14].

It is also a noise reduction technique and other undesired signal components that recover ICG signals. It is based on the decomposition of the data space as an ICG data matrix into orthogonal subspaces.

The produced ICG signals are settled in a linearly structured matrix as Hankel-form matrix, which decomposes it into two subspaces signal and noise components contained in the data [15].

The most advantageous of the SVD technique is the energy-preserving orthogonal transformation that allows a high-resolution spectrum estimation and noise anomalies detection in the 2.4 GHz band. In point of view, the SVD aims to reduce original data using fewer dimensions that give a better approximation. It serves to make relationships between the elements that reconstruct the original data. It allows releasing the classification of data points according to the largest variation dimensions.

The LMS algorithm steps are defined above in method 1.

Our SVD study based on the following algorithm steps:

- The real matrix $A \in \mathbb{R}^{m \times n}$ transform to diagonal matrix Σ with a non-negative real numbers via the product of three simple matrices as defined in equation (20) [16] [17]:

$$A = U \Sigma V^T = \sum_{i=1}^{\min\{m,n\}} s_i u_i v_i^T \quad (20)$$

Chapter IV: Denoising methods Applied for ICG signal Analysis

Where U and V are an orthogonal matrices; u_i and v_i are singular vectors, S is the diagonal matrix ($m \times n$) with positive real entries, S_i are the non-zero diagonal elements organized in descending order.

- Adding white Gaussian noise to the ICG signal with Signal Noise Ratio input (SNR_i) with range 0 dB to 20 dB as shown in equation (21):

$$x(n) = d(n) + N(n) \quad (21)$$

Where $x(n)$ the noisy waveform, $d(n)$ is the ICG waveform, $N(n)$ is the noise added

- Construct Hankel matrix is represented in equation (22) [15]:

$$H = \begin{bmatrix} u_1 & \cdots & u_j \\ \vdots & \ddots & \vdots \\ u_i & \cdots & u_{i+j-1} \end{bmatrix}_{i \times j} \quad (22)$$

The dimension of the Hankel matrix is $i \times j$, represents the summation of clean ICG signals and random noises.

- Achieve U_i, S_i, V_i through SVD as defined in equation (23):

$$H = U \Sigma V^T = \sum_{i=1}^{\min\{m,n\}} S_i u_i v_i^T \quad (23)$$

- Make each singular value in a diagonal matrix S_i according to its column index to extract the breaking point.
- The clean Matrix constructed H_2' defined in equation (24) as follows [15]:

$$H_2' = U \Sigma' V^T \quad (24)$$

- Reconstruct denoise signals.

Chapter IV: Denoising methods Applied for ICG signal Analysis

Four metrics parameters are calculated to estimate the quality of the reconstructed signal and to evaluate the performance of the algorithm coded. These parameters are defined in equations as follows [7]:

- Square Error (SE):

$$SE = (d(n) - y(n))^2 \quad (25)$$

- Signal to Noise Ratio (SNR):

$$SNR \text{ (dB)} = 10 \log_{10} \left[\frac{\sum_n y^2(n)}{\sum_n (y(n) - d(n))^2} \right] \quad (26)$$

- Signal to Noise Ratio Improvement (SNR_{imp}):

$$SNR_{imp} \text{ (dB)} = 10 \log_{10} \left[\frac{\sum_n |x(n) - d(n)|^2}{\sum_n |y(n) - d(n)|^2} \right] \quad (27)$$

- Root Mean Square Error (RMSE):

$$RMSE = \frac{1}{L} \sum_n^L (d(n) - y(n))^2 \quad (28)$$

Where $d(n)$ is the original signal, $x(n)$ is the noisy signal, $y(n)$ is the reconstructed ICG signal, and L is the length of signal.

IV. Method 3

The signal processing and denoising methods are necessary for noises removal as respiration and motion artifacts, which have very low-frequency ranges of 0.04 Hz to 2 Hz and 0.1 Hz to 10 Hz respectively, to extract signal characteristics and different significant information from ICG signal that is employed in the medical field whether in earlier diagnosis or patients monitoring. In this study, we are discussed about the wavelets denoising concept basing on the scale-dependent thresholding which is used in two types of an Orthogonal Wavelet family that are Daubechies wavelets (db); created by Ingrid Daubechies⁶ in 1988; and Symlet (sym), applied on the ICG.

For this purpose, the wavelet coefficients are thresholded using Sureshrink, NeighBlock, and the classic thresholds as Rigrsure and Sqtwolog, they are all compared with the linear filters as well as with the LMS-based adaptive filtering algorithm. The calculation results of the estimation parameters show that the best denoising technique

Chapter IV: Denoising methods Applied for ICG signal Analysis

that performs well on noise reduction is the wavelets sym8 at level 5 and the most optimal thresholding method is that of Rigrsure with a mean error rate (MER) equal to 0.0001 %. This method shown the reliability of results, it is published under journal named *Traitement du Signal*. The following diagram presented in Figure 13 shows our processed methodology.

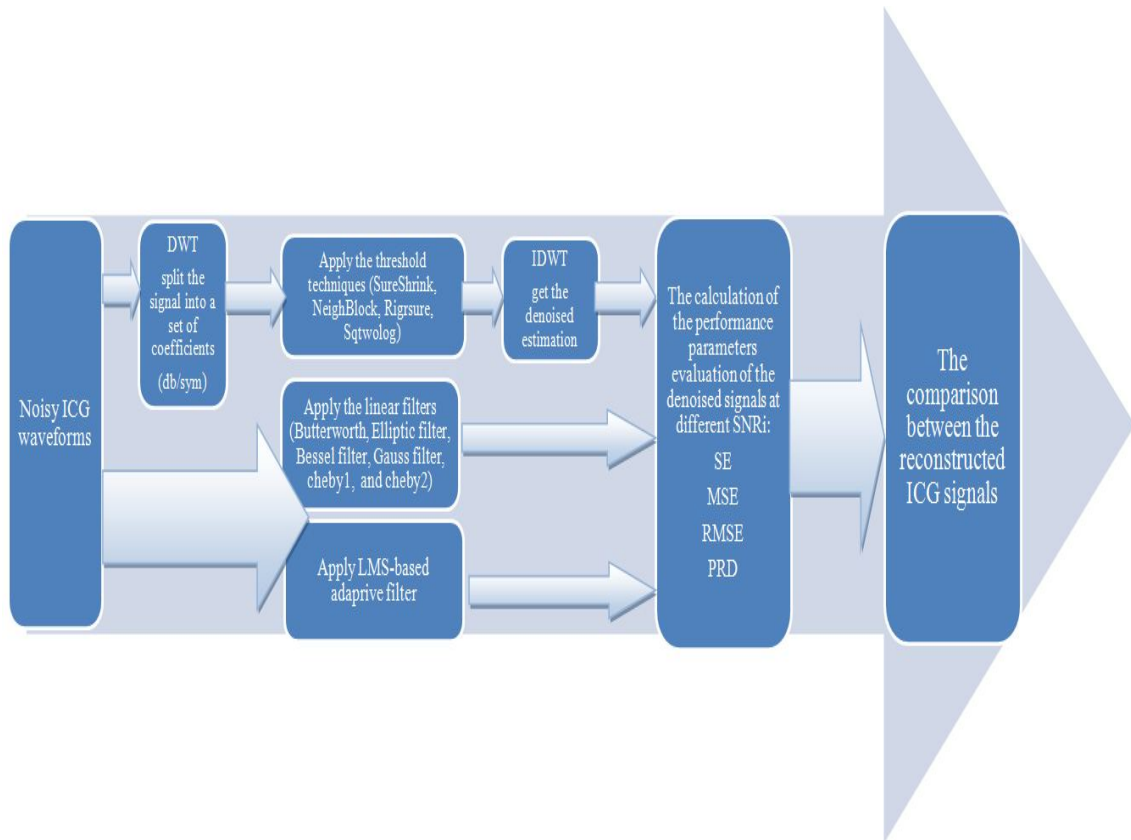


Figure 13: The interpretable diagram of our processed methodology.

The Wavelet analysis is a signal processing tool, despite that its mathematical underpinnings return to Joseph Fourier since the nineteenth century; where he made the basics of frequency analysis theory.

It is a method that measures the average fluctuations at different scales that have shown a significant decrease in noise and preserve the signal characteristics. In 1909, the wavelet was in the thesis of Alfred Haar. Their analysis methods have been developed and disseminated by Y. Meyer and others [18].

When the signal is transformed by the wavelet transform, the relevant information is extracted thanks to the signal analysis [19]; it came to solve the problem of the signal

Chapter IV: Denoising methods Applied for ICG signal Analysis

noises. Among the discrete wavelets, there is the sym26 which is used for the ICG signal denoising [20].

Five denoising methods were compared using different filters: The Savitzky-Golay filter was compared with the median filter, the band-pass filter, wavelet (db8) and the moving average filter. The results provide that the first one filter is the best [8].

A comparison between the ensemble empirical mode decomposition (EEMD), the optimal FIR filter, and the Symlet wavelet family (sym8) for the ICG denoising where this last one is the best [21].

The study of Choudhari proved that db4 is the most performing for denoising [22].

Chabchoub states that the decomposition level is that which gives the more sweet separation of signal and noise and he found that the db8 wavelet family is better than other wavelet families [7].

For the ICG denoising is necessary to pass by the multiscale decomposition, then the thresholding coefficients, after that the signal will be reconstructed using the inverse of Discrete Wavelet Transform (IDWT). There is no better threshold which is universal for a determination technique [23], that why there are multiple thresholds techniques as the classic thresholding and others like SureShrink and NeighBlock that are already used for ECG signal denoising and them showed reliability in the results and they had never used for denoising the ICG signal [24].

The used interest of the wavelet denoising is the preservation of signal characteristics and noise removal whatever the frequency content which is different from the smoothing that is used to remove high frequencies and keep the lower ones [23].

The study aims is to investigate the ICG signal denoising using linear filters that are tested as well as LMS adaptive filter and various thresholding techniques for wavelets such as SureShrink which is proposed by Donoho and Johnstone in 1995 [25], NeighBlock; local thresholding; Rigrsure, Sqtwolog; the universal thresholding; in order to have signal less noisy.

The orthogonal wavelets analysis decomposes the signal into shifted and scaled versions of the mother wavelet defined in equation (3) [26].

The wavelet transformation has two types: continuous wavelet transformation (CWT) and discrete wavelet transformation (DWT) that use the filter banks to decompose the signal into a coefficient component called Details, and Approximation [27].

Chapter IV: Denoising methods Applied for ICG signal Analysis

Its advantages include the possibility to select scales and dynamic positions to gain more reliability. The equation of the DWT is defined in equation (30).

$$\psi(x) = \begin{cases} 1 & \text{for } 0 << \frac{1}{2} \\ -1 & \text{for } \frac{1}{2} < x < 1 \\ 0 & \text{otherwise.} \end{cases} \quad (29)$$

$$X[\alpha, \beta] = \sum_{n=-\infty}^{+\infty} x[n] \psi_{\alpha, \beta}[n] \quad (30)$$

$$\psi_{\alpha, \beta}[n] = \frac{1}{\sqrt{\alpha}} [\psi_{(n-\beta)/\alpha}] \quad (31)$$

Where, α and β are the wavelet location parameters, $x[n]$ is the signal, n is the samples number, and $\psi(\cdot)$ is the mother wavelet [28].

The Figure 14 presents the DWT for multiscale wavelet decompositions where H_0 is an HPF output and G_0 is an LPF output $c_j[n]$ denote the approximation coefficients and $d_j[n]$ denotes the detail coefficients.

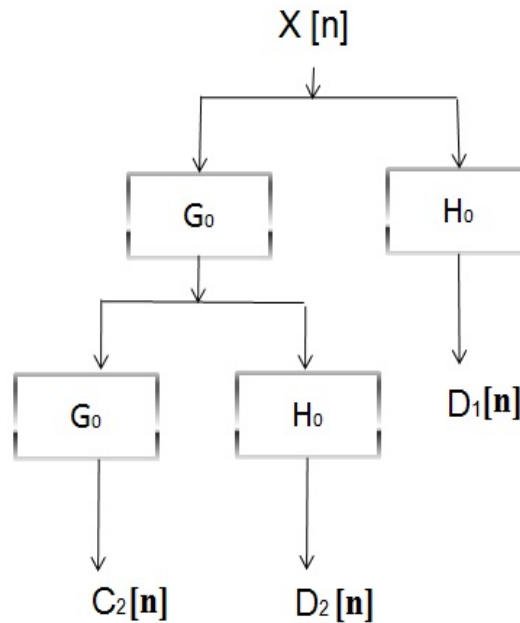


Figure 14: The signal wavelet decomposition.

Chapter IV: Denoising methods Applied for ICG signal Analysis

The thresholding hypothesis is based on the idea that the no modified coefficients are zero or almost zero, so the noise is on all the coefficients with a low level that allows us to differentiate between the wavelet coefficients with those that are noisy. The wavelet thresholding method was introduced by Donoho in 1993; it serves to threshold the wavelet coefficients by eliminating their noisy part [23].

The wavelet transform noiseless coefficients are indeed rare and the ones with low amplitude are set to zero, the wavelet thresholding name comes from the comparison which is made by the coefficient with a threshold to know if it is a part constitutive desirable or not of the original signal

The wavelet decomposes the signal into Approximations c_j that present the low frequencies where resides the most information of signal and in d_j details which represent the high frequencies.

The thresholding draws the significant coefficients from c_j , if they are lower than a threshold level λ , they will be equal to zero, this threshold depends on decomposition level which is called Sureshrink [25] [29] that is proposed by Donoho and Johnstone [25], and an inverse wavelet discrete transformation IDWT that leads to a less noisy signal reconstruction [23].

Among these other threshold methods, the classical thresholding such as Rigrsure which used Stein's unbiased risk principle (SURE), and Sqtwolog which used the universal threshold. The methods are respectively defined as follows:

$$th_i = \theta_i \sqrt{2 \log(N_i)} \quad (32)$$

$$\theta_i = \frac{\text{median } |\omega|}{0.6745} \quad (33)$$

Where,

θ_i is the mean absolute deviation and N_i is the length of the noisy signal, and ω is the wavelet coefficient to scale j .

$$th_i = \theta_i \sqrt{\omega_a} \quad (34)$$

Where,

θ is the standard deviation of noisy signal, and ω_a is the coefficient wavelet square.

Chapter IV: Denoising methods Applied for ICG signal Analysis

The neighbourhood block method, proposed by Cai and Silverman [30], is based on the calculation of the shrinkage factor within blocks of successive coefficients. It is applied to the group of adjacent coefficients, and is not applied for each coefficient and level. The use of multiple thresholds for all coefficients improves noise reduction performance [31].

The choice of the threshold can be chosen according to the local noise levels, this technique calculates a threshold value with the neighbourhood [30] [32], and is based on the following steps:

Step 1: Decomposition of the signal in coefficient with the DWT;

- Step 2: Carry out the coefficients in disjoint block $b_{i,j}$ for each level;
- Step 3: The shrinkage factor rule is chosen according to the local properties of the coefficient. It is defined in equation (35) as follows:

$$\beta_{i,j} = \max\left(0, \left(1 - \frac{\lambda L \theta^2}{S^2}\right)\right) \quad (35)$$

With,

$$\begin{aligned} L &= L_0 + 2L_1 \\ L_0 &= \frac{\log_2(n)}{2} \\ L_1 &= \max\left(1, \frac{L_0}{2}\right) \\ S^2 &= \sum_{j,k \in \beta_{i,j}} \theta_{i,j} \\ K &= 1, \dots, L_1 \end{aligned}$$

Where, i is the block, j is the level, $\lambda=4.5053$, and θ^2 is the variance of the extended block.

There are two thresholding approaches which are defined as follows [31]:

$$\text{Hard: } d_i = \begin{cases} d_i & \text{if } |d_i| > \lambda \\ 0 & \text{else} \end{cases} \quad (36)$$

Chapter IV: Denoising methods Applied for ICG signal Analysis

$$\text{Soft: } d_i = \begin{cases} d_i - \lambda & \text{for } d_i > \lambda \\ d_i + \lambda & \text{for } d_i < -\lambda \\ 0 & \text{else} \end{cases} \quad (37)$$

Simple wavelet thresholding is the hard thresholding but soft thresholding is more efficient, considered as the wavelet denoising (shrinkage) method, i.e., a non-linear process integrated in a linear denoising technique.

According to Donoho, the calculation of λ is based on Stein's unbiased risk principle (SURE) as follows [33]:

$$\lambda = \sqrt{2 \log M} \quad (38)$$

where, M coefficients numbers.

The linear filters used to denoise the ICG signal of 10 participants are:

- Butterworth
- Elliptical
- Bessel
- Gaussian
- Chebychev1
- Chebychev2

The addition of a high frequency component of 600 Hz to the signal was necessary for efficiency testing. The filters used a frequency bandwidth for cutoff ranging from 0.1 to 10 Hz and an order of 3. A comparison was made to identify the best of them. The performance of the denoising method was evaluated by calculating specific parameters to verify perfect reconstruction.

The adaptive filter, in particular the fundamental LMS adaptive algorithm, is widely applied in denoising biosignals. Hence, it is used for the respiratory elimination artifact. The LMS is simple in its implementation and is used to control the finite impulse response (FIR) filter at each use. Moreover, it is based on a feedback process to reduce the error $e(n)$ of the input signal $x(n)$ and the reconstructed signal $y(n)$ by adjusting its parameters: a higher order is chosen, weighting coefficients update $w(n+1)$ defined in

Chapter IV: Denoising methods Applied for ICG signal Analysis

equation (39) [2], and a predefined step size μ ($0 < \mu < (2/\text{FIR filter T-tap})$) at the beginning of the adaptive filtering process. If μ is too small, the algorithm will converge, so we took ($0 < \mu < 0.2$) and we added an HF component with a frequency of 600 Hz to the ICG reference signal to also test the efficiency of the filters.

$$w(n + 1) = w(n) + \mu e(n)x(n) \quad (39)$$

$$w(n) = [w_0(n), w_1(n), w_{k-1}(n)]^t \quad (40)$$

where, n^{th} is the weight coefficient vector, K is the input sample length, and $e(n)$ is the difference between the reference and the output signal.

Figure 15 shows the overall scheme of the wavelet denoising algorithm applied on ICG signal.

The transform wavelet method of ICG signal defined as follow: we added a high-frequency component of 600 Hz to ICG waveforms for efficiency testing, then applied two types of DWT (db/sym) that split signals into coefficients; Details and Approximation; where we used four types of thresholding techniques (Sureshrink, NeighBlock, Rigrsure, and Sqtwolog) for each type of DWT (db(2, 4, 6, 8),sym (2, 4, 6, 8)), also we tested each threshold technique and compared wavelet levels from level 1 to level 10. Finally we applied the inverse DWT to reconstruct the final signal.

Chapter IV: Denoising methods Applied for ICG signal Analysis

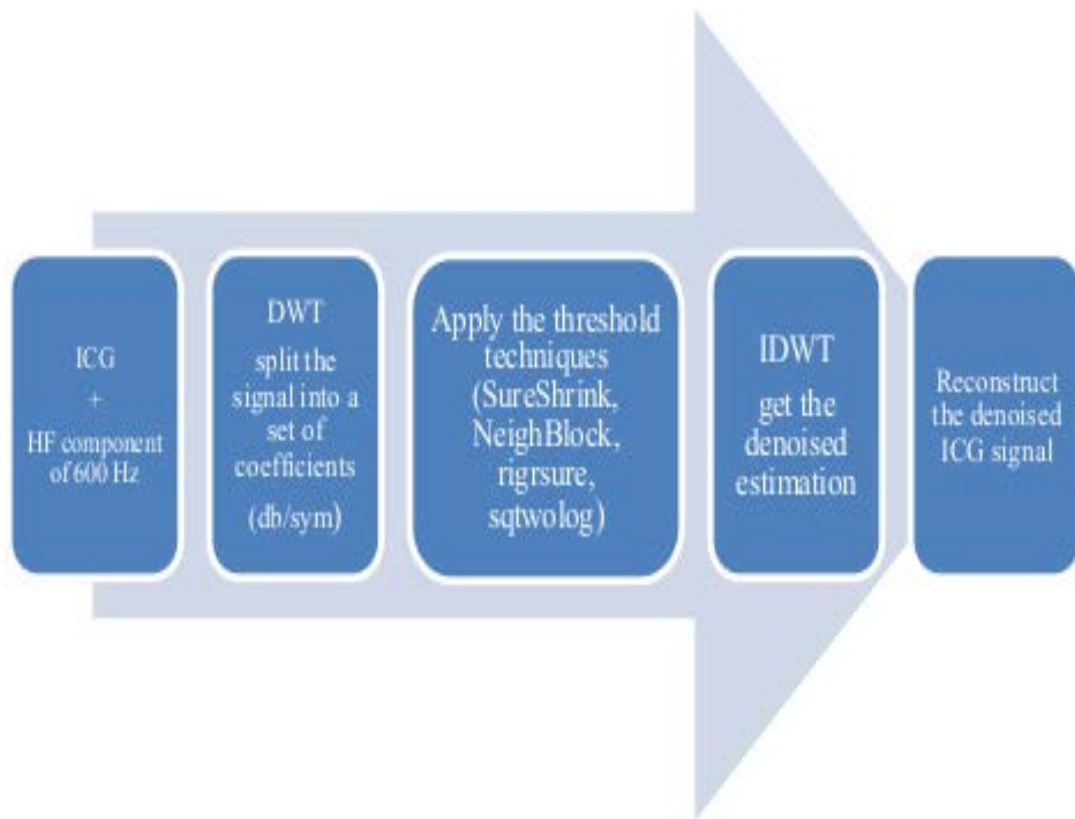


Figure 15: Schematic diagram method.

The study is based on a comparison between linear filters, LMS-based adaptive filter, and orthogonal wavelets such as Daubechies (db) and Symlet (sym) with order N (2, 4, 6, 8), which already used according to literature demonstration citing above the paper. The thresholding methods used are the classic threshold, Sureshrink, NeighBlock, which have been chosen according to T.T. Cai [34] [35], it has threshold criteria that exceed that of Rigrsure and Sqtwolog, we also used the Soft thresholding rule because it considered as the wavelet denoising method and “mIn” for rescaling that used for noise estimation at each wavelet level from 1 to 10. Our method based on the steps presented in the following diagram presented in Figure 16:

Chapter IV: Denoising methods Applied for ICG signal Analysis

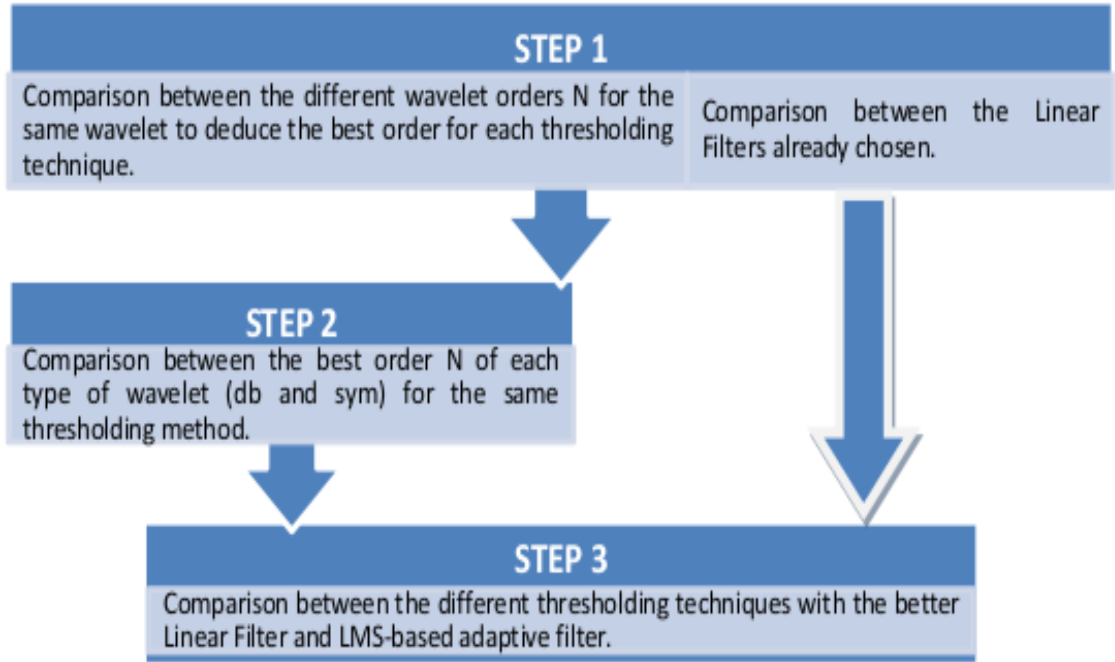


Figure 16: Interpretable diagram algorithm.

For the evaluation of the results of our comparisons, we based on the following parameters[34] [36], to verify the improvement of the reconstructed ICG signal: the square error (SE), the signal to noise ratio output (SNR) expressed in dB, the signal to noise ratio input (SNR_i) expressed in dB which the input noise range calculate thanks to equation (43) is from 0 dB to 35 dB, the root mean square error (RMSE), and the percent difference root mean square (PRD) expressed in % , their formulas are defined in the order as follow:

$$SE = (x(n) - y(n))^2 \quad (41)$$

$$SNR = 10 \log_{10} \left[\frac{\sum_n y^2(n)}{\sum_n (y(n) - x(n))^2} \right] \quad (42)$$

$$SNR_i = 10 \log_{10} \left[\frac{\sum_n x^2(n)}{\sum_n (\text{noise})^2} \right] \quad (43)$$

Chapter IV: Denoising methods Applied for ICG signal Analysis

$$\text{RMSE} = \frac{1}{L} \sum_n^L (x(n) - y(n))^2 \quad (44)$$

$$\text{PRD (\%)} = 100 \sqrt{\frac{\sum_n^L (x(n) - y(n))^2}{\sum_n^L x^2(n)}} \quad (45)$$

Where, $x(n)$ is the original signal, $y(n)$ is the reconstructed signal, and L is the signal length.

The best denoising method has the highest SNR, the lowest PRD, the lowest RMSE and the lowest reconstructed error.

V. Conclusion

In this chapter, we have presented the different denoising methods applied on our ICG signals to choose the best that perform better in terms of noise reduction. The denoising method is the significant step for diagnosis and monitoring of cardiovascular diseases, it helps medical persons to extract medical information. These methods are used to calculate hemodynamic parameters thanks to the feature point extraction from ICG waveform.

In the next chapter we will present all results obtained from denoising methods.

Chapter IV: Denoising methods Applied for ICG signal Analysis

REFERENCES

- [1] S. Podtaev, R. Stepanov, A. Dumler, S. Chugainov, and K. Tziberkin, 'Wavelet analysis of the impedance cardiogram waveforms', in *Journal of Physics: Conference Series*, 2012, vol. 407, no. 1, p. 012003.
- [2] F. Khraim, R. Pike, and J. Williams, 'Using non-invasive impedance cardiography to assess cardiac hemodynamic measures of persons with heart failure', *Canadian Journal of Cardiology*, vol. 30, no. 10, p. S371, 2014.
- [3] S. Mansouri, T. Alhadidi, S. Chabchoub, and R. B. Salah, 'Impedance cardiography: recent applications and developments', *Biomedical Research*, vol. 29, no. 19, pp. 3542–3552, 2018.
- [4] S. Kerai, 'The impedance cardiography technique in medical diagnosis', *Medical Technologies Journal*, vol. 2, no. 3, pp. 232–244, 2018.
- [5] X. Hu *et al.*, 'Adaptive filtering and characteristics extraction for impedance cardiography', *Journal of Fiber bioengineering and Informatics*, vol. 7, no. 1, pp. 81–90, 2014.
- [6] V. K. Pandey, P. C. Pandey, N. J. Burkule, and L. R. Subramanyan, 'Adaptive filtering for suppression of respiratory artifact in impedance cardiography', in *2011 Annual International Conference of the IEEE Engineering in Medicine and Biology Society*, 2011, pp. 7932–7936.
- [7] S. Chabchoub, S. Mansouri, and R. B. Salah, 'Impedance cardiography signal denoising using discrete wavelet transform', *Australasian physical & engineering sciences in medicine*, vol. 39, no. 3, pp. 655–663, 2016.
- [8] I. B. Salah and K. Ouni, 'Denoising of the impedance cardiographie signal (ICG) for a best detection of the characteristic points', in *2017 2nd International Conference on Bio-engineering for Smart Technologies (BioSMART)*, 2017, pp. 1–4.
- [9] A. Sharma, S. Toshniwal, and R. Sharma, 'Noise reduction technique for ECG signals using adaptive filters', *Int J Res Rev*, vol. 7, no. 2, pp. 187–191, 2014.
- [10] A. Singh and R. Mehra, 'Adaptive filter for ECG noise Reduction using RIs Algorithm', *IJERA*, vol. 3, pp. 1304–8, 2013.
- [11] J. Luo, K. Ying, P. He, and J. Bai, 'Properties of Savitzky–Golay digital differentiators', *Digital Signal Processing*, vol. 15, no. 2, pp. 122–136, 2005.

Chapter IV: Denoising methods Applied for ICG signal Analysis

- [12] N. Rastogi and R. Mehra, 'Analysis of Savitzky-Golay filter for baseline wander cancellation in ECG using wavelets', *Int. J. Eng. Sci. Emerg. Technol.*, vol. 6, no. 1, pp. 2231–6604, 2013.
- [13] B. Hadjer and K. Salim, 'A Novel SVD Noise Cancellation Algorithm for ICG Signal', in *2021 IEEE 6th International Conference on Computing, Communication and Automation (ICCCA)*, 2021, pp. 157–160 ,doi: 10.1109/ICCCA52192.2021.9666326.
- [14] K. Mridha, R. N. Shaw, and A. Ghosh, 'Intelligent Based Waste Management Awareness Developed by Transfer Learning', in *2021 IEEE 4th International Conference on Computing, Power and Communication Technologies (GUCON)*, 2021, pp. 1–5.
- [15] K.-C. Lee, J.-S. Ou, and M.-C. Fang, 'Application of SVD noise-reduction technique to PCA based radar target recognition', *Progress In Electromagnetics Research*, vol. 81, pp. 447–459, 2008.
- [16] D. C. Lay, S. R. Lay, and J. J. McDonald, *Linear algebra and its applications*. Pearson, 2016.
- [17] T. Roughgarden and G. Valiant, 'CS168: The Modern Algorithmic Toolbox Lecture# 9: The Singular Value Decomposition (SVD) and Low-Rank Matrix Approximations', *Online*], <http://theory.stanford.edu/~tim/s15/l/19.pdf>. Accessed:[29 June 2019], 2015.
- [18] M. Hadaś-Dyduch, 'Wavelets in the prediction of short-time series', *Mathematical Economics*, no. 11 (18), pp. 43–54, 2015.
- [19] O. Rioul and M. Vetterli, 'Wavelets and signal processing', *IEEE signal processing magazine*, vol. 8, no. 4, pp. 14–38, 1991.
- [20] T. Sebastian, P. C. Pandey, S. M. M. Naidu, and V. K. Pandey, 'Wavelet based denoising for suppression of respiratory and motion artifacts in impedance cardiography', in *2011 Computing in Cardiology*, 2011, pp. 501–504.
- [21] S. De Ridder, X. Neyt, N. Pattyn, and P.-F. Migeotte, 'Comparison between EEMD, wavelet and FIR denoising: Influence on event detection in impedance cardiography', in *2011 Annual International Conference of the IEEE Engineering in Medicine and Biology Society*, 2011, pp. 806–809.

Chapter IV: Denoising methods Applied for ICG signal Analysis

- [22] P. C. Choudhari and D. M. Panse, 'Denoising of radial bioimpedance signals using adaptive wavelet packet transform and Kalman filter', *IOSR J VLSI Signal Process*, vol. 5, pp. 1–8, 2015.
- [23] R. Rangarajan, R. Venkataramanan, and S. Shah, 'Image Denoising Using Wavelets—Wavelets & Time Frequency—', 2002.
- [24] M. AlMahamdy and H. B. Riley, 'Performance study of different denoising methods for ECG signals', *Procedia Computer Science*, vol. 37, pp. 325–332, 2014.
- [25] D. L. Donoho and I. M. Johnstone, 'Adapting to unknown smoothness via wavelet shrinkage', *Journal of the american statistical association*, vol. 90, no. 432, pp. 1200–1224, 1995.
- [26] R. M. Bodile and V. K. Talari, 'Removal of Power-Line Interference from ECG Using Decomposition Methodologies and Kalman Filter Framework: A Comparative Study.', *Traitement du Signal*, vol. 38, no. 3, 2021. <https://doi.org/10.18280/ts.380334>
- [27] A. Antoniadis, J. Bigot, and T. Sapatinas, 'Wavelet estimators in nonparametric regression: a comparative simulation study', *Journal of statistical software*, vol. 6, pp. 1–83, 2001.
- [28] L. Cohen, 'Time-frequency distributions-a review', *Proceedings of the IEEE*, vol. 77, no. 7, pp. 941–981, 1989. <https://dx.doi.org/10.1109/5.30749>
- [29] R. Cohen, 'Signal denoising using wavelets', *Project Report, Department of Electrical Engineering Technion, Israel Institute of Technology, Haifa*, vol. 890, 2012.
- [30] S. Podtaev, R. Stepanov, A. Dumler, S. Chugainov, and K. Tziberkin, 'Wavelet analysis of the impedance cardiogram waveforms', in *Journal of Physics: Conference Series*, 2012, vol. 407, no. 1, p. 012003.
- [31] S. Grimnes and O. G. Martinsen. *Bioimpedance Bioelectr. Basics* Third Ed., Oxford: Academic Press; 2015 [Chapter 1].
- [32] <http://www.abelprize.no/nyheter/vis.html?tid=69665> (accessed March 30, 2019).

Chapter IV: Denoising methods Applied for ICG signal Analysis

- [33] N. W. Kotanko P and L. F. Zhu, 'Curent state of bioimpedance technologies in dialiysis', *J. Med. Nephrology Dialysis Transpl*, vol. 23, pp. 808–812, 2008.<https://dx.doi.org/10.1093/ndt/gfm889>
- [34] T. T. Cai, 'Adaptive wavelet estimation: a block thresholding and oracle inequality approach', *The Annals of statistics*, vol. 27, no. 3, pp. 898–924, 1999. <http://dx.doi.org/10.1214/aos/1018031262>
- [35] T. T. Cai and B. W. Silverman, 'Incorporating information on neighbouring coefficients into wavelet estimation', *Sankhyā: The Indian Journal of Statistics, Series B*, pp. 127–148, 2001.
- [36] A. Khiter, A. B. Adamou-Mitiche, and L. Mitiche, 'Denoising Electrocardiogram Signal from Electromyogram Noise Using Adaptive Filter Combination.', *Rev. d'Intelligence Artif.*, vol. 34, no. 1, pp. 67–74, 2020.. <https://doi.org/10.18280/ria.340109>.

Chapter .V

I. Introduction

In this section we have presented and discussed all results obtained from our methods that are applied on ICG signals.

The first method presents the results obtained from the comparison made between adaptive filters and Savitzky-Golay (SG) that are applied on ICG signals for noise removal. The evaluation criteria step is crucial to verify the technique performance, where we use Err., SNR, SNR_i, and MSE.

The second method presents comparison results of two methods, the first is a novel noise-reduction technique called SVD singular value decomposition (SVD) and the second is LMS based adaptive filter. To evaluate the technique, specific metric parameters have been calculated: SE, RMSE, SNR and SNR_{imp}.

The third method present a results study that is based on the wavelets denoising concept, when we applied two types of an Orthogonal Wavelet family: Daubechies wavelets (db); and Symlet (sym); whereas, wavelet coefficients are thresholded using Sureshrink, NeighBlock, and the classic thresholds as Rigrsure and Sqtwolog, all are compared with the linear filters as well as with the LMS-based adaptive filtering algorithm. To verify the improvement of the technique, we are calculating SE, SNR, SNR_i, RMSE, and PRD.

II. Results of Method 1

The results of our simulations present in table 3 and Figure 19, whereas table 3 presents the results values of different denoising methods of SNR, and MSE at SNR_i equal to 10 dB. Figure 17 shows the error between the original and the reconstructed signal at different SNR_i levels for several denoising methods that applied to 10 subjects.

Chapter V: Results obtaining from Denoising Techniques

Table 3: SNR, MSE estimation parameters results after simulation for 10 subjects at SNRi 10 dB.

Step size	Evaluation parameters	Filters Techniques							
		LMS	RLS	NLM S	LLM S	SLM S	SRLM S	SSLM S	SG
$\mu = 0.004$	SNR(db)	-24.78			-24.78	-24.78	-24.78	-2.85	
	MSE	0.217		0.198	0.217	0.240	0.205	0.982	
$\mu = 0.008$	SNR(db)	-18.73		-12.64	-18.73	-18.73	-18.73	-0.0785	
	MSE	0.197		0.16	0.197	0.187	0.19	0.302	
$\mu = 0.01$	SNR(db)	-16.78		-10.6	-16.78	-16.78	-16.78	0.216	
	MSE	0.189		0.16	0.189	0.160	0.191	1.55	
	SNR(db)		3.022						10.09
	MSE		0.0502						0.0079

The application of filter algorithm methods has been investigated for suppressing artifacts from signals of 10 subjects. Our comparative study of the best filter performance which effectively reduces the noises from ICG waveforms, although adaptive filters decrease the error between original and reconstructed signal (see Figure 17), however it is not preserved well the information on the signals where their error calculated was high. The proposed Savitzky-Golay filter technique provides the optimum quality of the corrupted ICG signals, and it did not make any visible distortion of the waveform shape (see Figure 18).

Chapter V: Results obtaining from Denoising Techniques

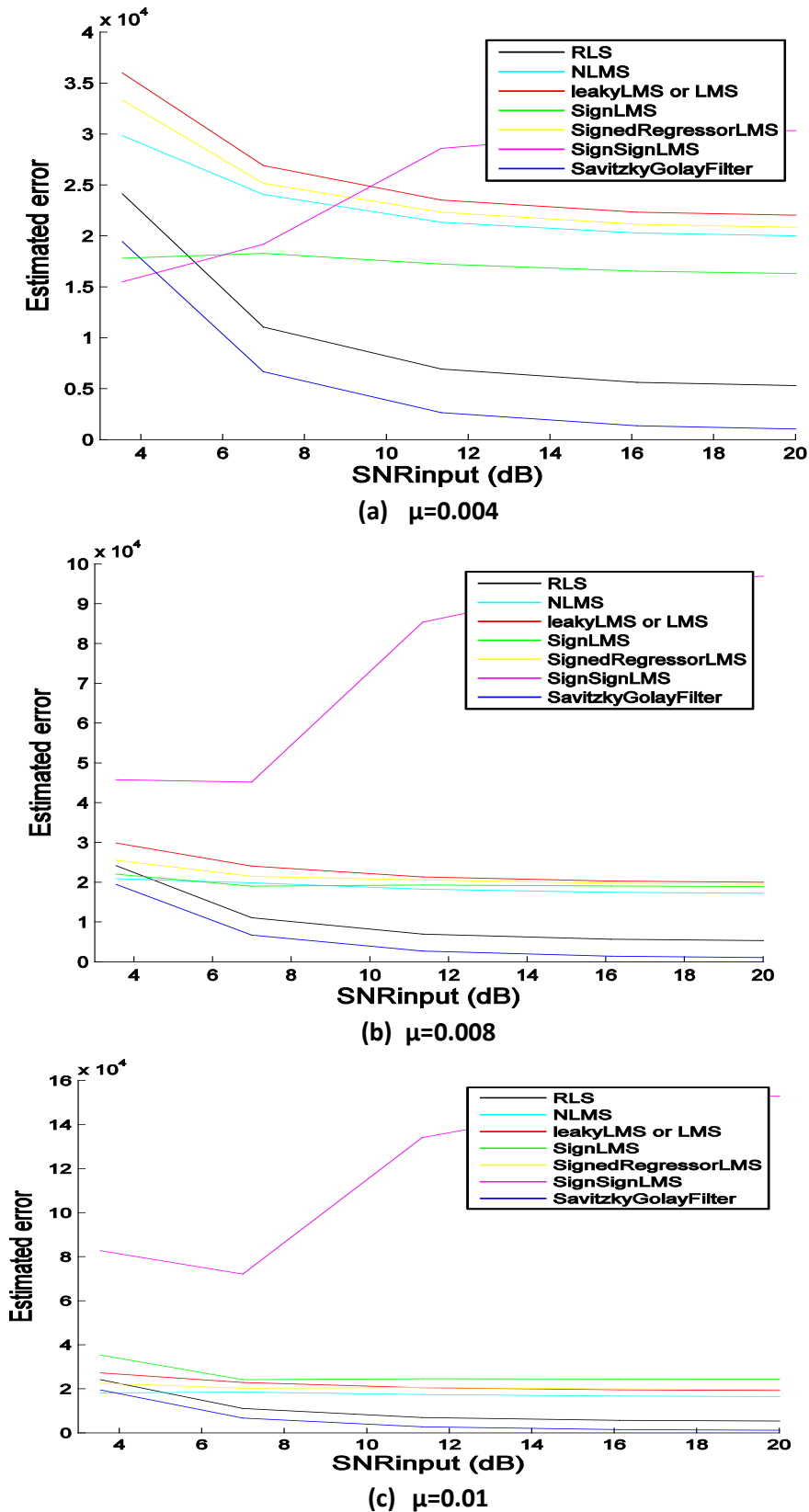


Figure 17: Estimated the error results from the original and reconstructed signal after applying the adaptive filters as well as SavitzkyGolay filters on 10 ICG signals at different SNR_i, where (a) with $\mu=0.004$, (b) with $\mu=0.008$, and (c) with $\mu=0.01$.

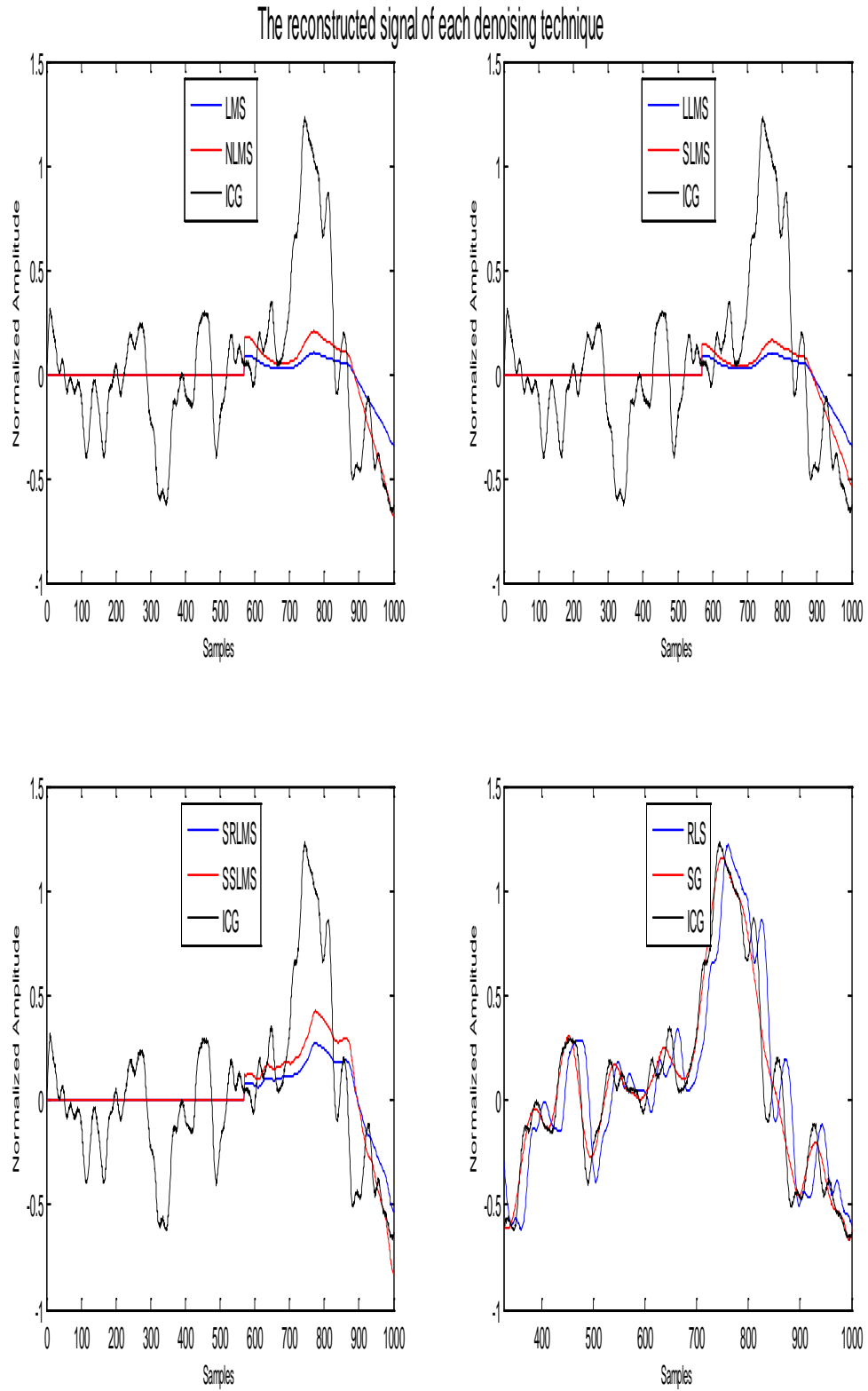


Figure 18: The reconstructed signal of each denoising technique.

Chapter V: Results obtaining from Denoising Techniques

To improve the effectiveness of the technique, we used a specific performance parameter for evaluation as Err, MSE, and SNR that measured and compared. We find that the best method has the lowest err values (see Figure 17), lowest MSE values, highest SNR values (table 3) is the Savitzky-Golay filter. We found that SNR and MSE for all 10 subjects are equal to 10.09 dB, 121.01 dB, and 0.0079 respectively.

The simulation results show that the Savitzky-Golay filter converges better than RLS algorithms and LMS types presented in Figure 16, and the NLMS algorithm gives better convergence characteristics than the LMS when table 3 informs that LLMS and LMS gave the same results. The adaptive filter gets its optimum value when the forgetting factor is from 0.98 to, and the step size is from 0 to 0.2 for convergence of the algorithm. The Savitzky-Golay filter method is the best denoising technique because it has the lowest error, it preserves the signal shape, and thus the information constitutes the signal. The morphology of the denoising ICG may be helpful in the medical field for diagnostic and continuous monitoring of cardiovascular diseases. The Savitzky-Golay filter method facilitates the extraction of cardiovascular indices.

- Validation step

The following tables present the mean error rate calculation at different SNR_i when the mean error is the average of all the cross-validation errors. It should be close to zero.

Table 4: Estimated MER results from the original and reconstructed signal after applying the adaptive filters with $\mu = 0.01$, as well as Savitzky-Golay filters on 10 ICG signals at different SNR_i.

Mean error rate (MER) % of each methods	SNR _i (dB)							
	0	2	4	6	8	10	15	20
LMS	0.032165	0.032324	0.032378	0.032397	0.032404	0.032407	0.032408	0.032409
NLMS	0.024433	0.024752	0.024859	0.024897	0.024911	0.024917	0.024919	0.02492
LLMS	0.032165	0.032324	0.032378	0.032397	0.032404	0.032407	0.032408	0.032409
SLMS	0.0019094	0.0010087	0.0012842	0.0013816	0.001418	0.001432 6	0.001439	0.001442
SRLMS	0.030629	0.029472	0.028374	0.028331	0.02864	0.028507	0.028223	0.028001
SSLMS	0.0076973	0.013639	0.019279	0.019499	0.01791	0.018596	0.020051	0.021193
RLS	0.0060667	0.0059313	0.0058553	0.0058125	0.005788 4	0.005774 9	0.0057673	0.005763
SG	0.0003827 9	0.0003877 1	0.0003904 7	0.0003920 3	0.000392 9	0.000393 4	0.0003936 7	0.0003938 3

Chapter V: Results obtaining from Denoising Techniques

Table 5: Estimated MER results from the original and reconstructed signal after applying the adaptive filters with $\mu=0.004$, as well as Savitzky-Golay filters on 10 ICG signals at different SNRi.

Mean error rate (MER) % of each methods	SNRi (dB)							
	0	2	4	6	8	10	15	20
LMS	0.036804	0.036868	0.036889	0.036897	0.0369	0.036901	0.036901	0.036902
NLMS	0.033711	0.033839	0.033882	0.033897	0.033903	0.033905	0.033906	0.033906
LLMS	0.036804	0.036868	0.036889	0.036897	0.0369	0.036901	0.036901	0.036902
SLMS	0.024015	0.024342	0.024452	0.024491	0.024505	0.024511	0.024514	0.024515
SRLMS	0.03619	0.035727	0.035288	0.035271	0.035394	0.035341	0.035228	0.035139
SSLMS	0.020859	0.018482	0.016227	0.016139	0.016774	0.0165	0.015918	0.015461
RLS	0.0060667	0.0059313	0.0058553	0.0058125	0.005788 4	0.005774 9	0.0057673	0.005763
SG	0.0003827 9	0.0003877 1	0.0003904 7	0.0003920 3	0.000392 9	0.000393 4	0.0003936 7	0.0003938 3

Table 6: Estimated MER results from the original and reconstructed signal after applying the adaptive filters with $\mu =0.008$, as well as SavitzkyGolay filters on 10 ICG signals at different SNRi.

Mean error rate (MER) % of each methods	SNRi (dB)							
	0	2	4	6	8	10	15	20
LMS	0.033711	0.033839	0.033882	0.033897	0.033903	0.033905	0.033906	0.033906
NLMS	0.027526	0.027781	0.027867	0.027897	0.027908	0.027913	0.027915	0.027916
LLMS	0.033711	0.033839	0.033882	0.033897	0.033903	0.033905	0.033906	0.033906
SLMS	0.0081321	0.0087864	0.0090068	0.0090846	0.0091138	0.0091255	0.0091306	0.009133
SRLMS	0.032483	0.031557	0.030678	0.030644	0.030892	0.030785	0.030558	0.03038
SSLMS	0.0018215	0.002932	0.0074435	0.0076196	0.006348 4	0.006897 4	0.0080611	0.0089753
RLS	0.0060667	0.0059313	0.0058553	0.0058125	0.0057884	0.0057749	0.0057673	0.005763
SG	0.0003827 9	0.0003877 1	0.0003904 7	0.0003920 3	0.0003929	0.0003934	0.0003936 7	0.0003938 3

We noticed from Table 4, Table 5, and Table 6 that SSLMS did not give us any useful information, and LMS and LLMS gave us the same values. However, when comparing the LMS types filters results when μ equal to 0.01, 0.004 and 0.008, we deduced that the best result is when μ equal to 0.01.

We observed that the SG denoising method performs better than the other adaptive filters for the entire SNRi levels.

Chapter V: Results obtaining from Denoising Techniques

Souhir Chabchoub [1] found that db8 wavelet has the lowest mean error rate for different SNRi compared to the several denoising methods of Ridder [2], it equal to 0.3 % at 0 dB, 0.1 % at 5 dB, 0.01 % at 10 dB, and 0.14 % at 15 dB. According to our results, we find that the mean error rate of the best denoising technique equal to 0.00038 %. Besides, we saw that our results are more suitable when compared with the literature review.

III. Results of method 2

In this method, we present a comparison between LMS and SVD, whereas the two denoising techniques are applied on ICG signals for ten healthy subjects. Figure 19, Figure 20, and Figure 21 show the denoising results.

We see that the SVD preserves to the maximum the shape of the signal with minimal distortion, while Figure 22 presents the performance evaluation criteria for all subjects at different SNRi. Therefore, we observed that SVD has the minimum SE, RMSE, and maximum SNR and SNR_{imp} .

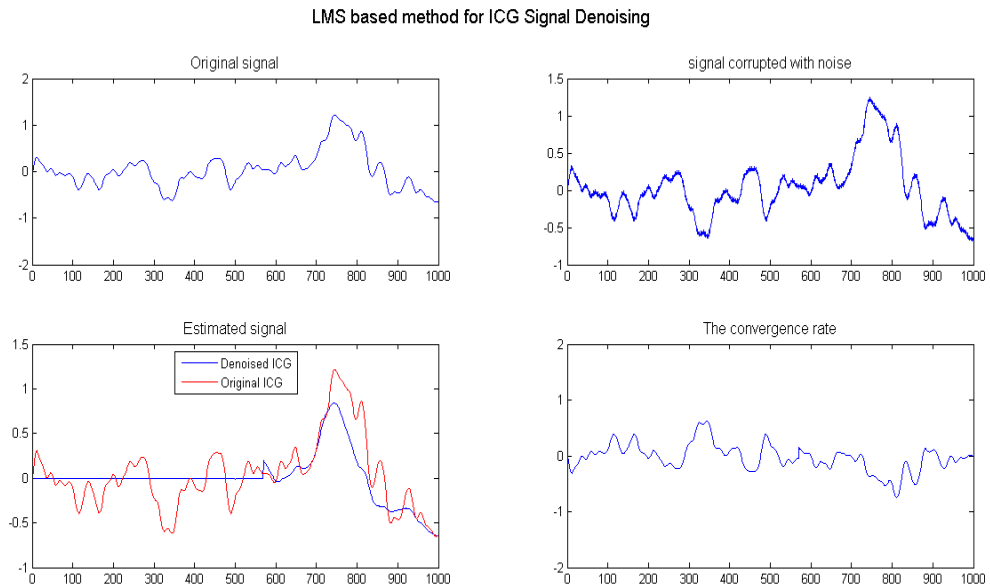


Figure 19: LMS based method for ICG signal denoising.

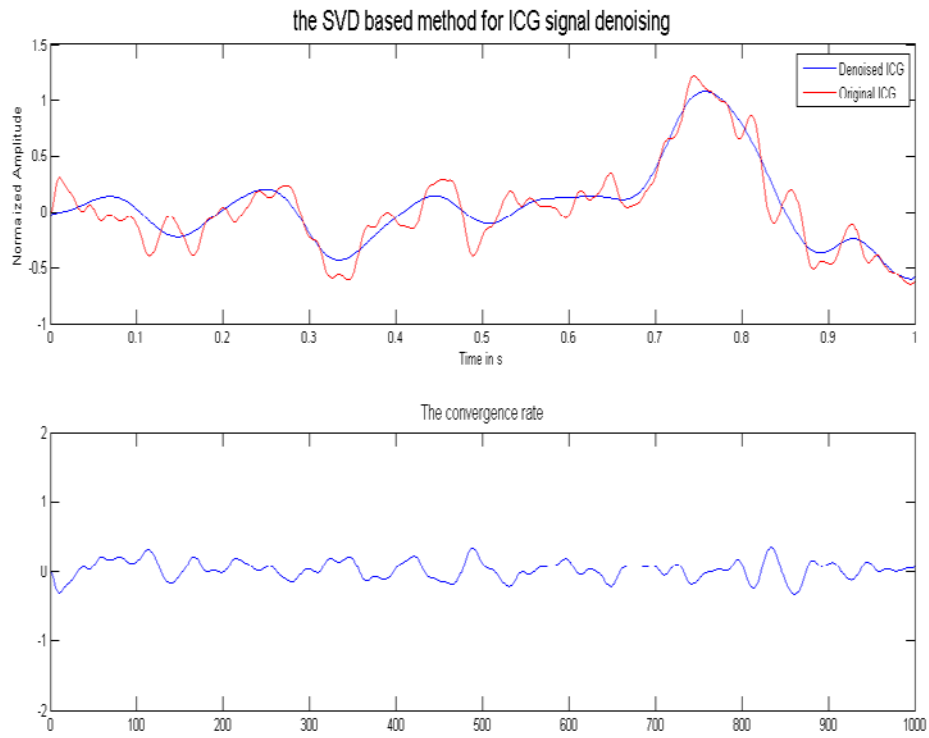


Figure 20: SVD based method for ICG signal denoising.

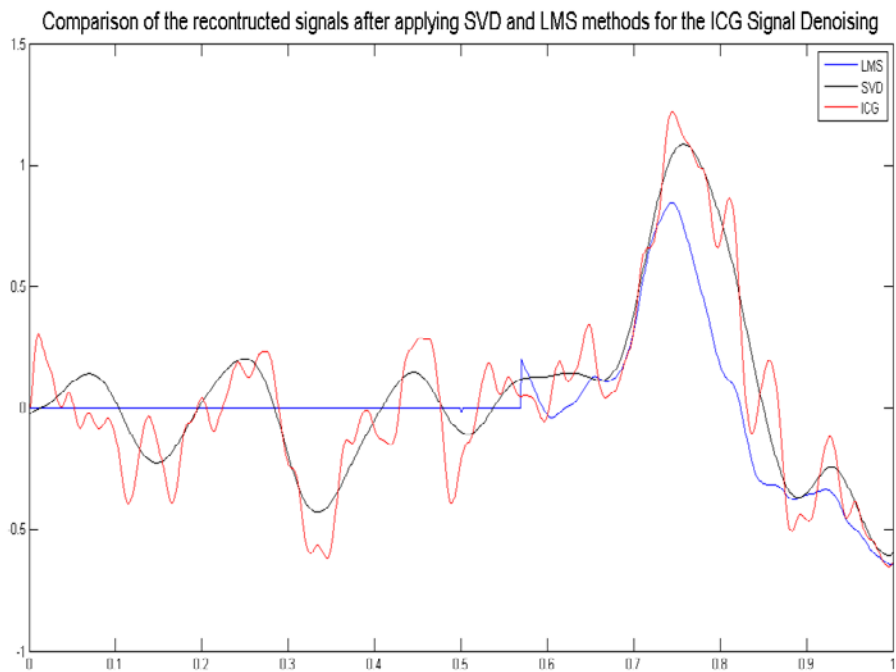


Figure 21: Comparison between two methods: SVD and LMS for the denoising of the ICG signal.

Chapter V: Results obtaining from Denoising Techniques

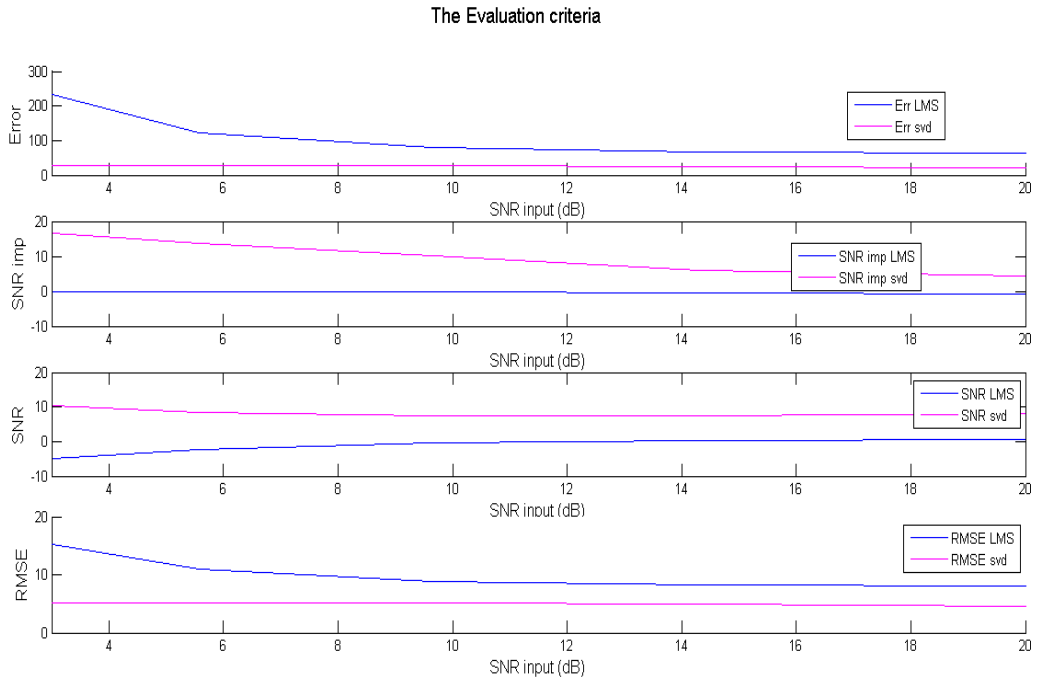


Figure 22: The estimation parameters evaluation for all 10 subjects.

- *Discussion*

We applied two techniques to noise removal from ICG waveforms of 10 participants; they did not make any visible distortion of the waveform shape when the first is the LMS-based adaptive filtering and the second is the SVD.

To verify the effectiveness of methods, we calculated and compared between performance evaluation criteria as SE, RMSE, SNR and SNR_{imp} , where the better who has a minimum of SE, RMSE, and maximum SNR and SNR_{imp} . The results are shown in Figure 22.

Chapter V: Results obtaining from Denoising Techniques

Table 7: The C Point Coordinates of The Original Signal and The Reconstructed Signals of The LMS and The SVD Techniques.

Participants	ICG signals	Axes	
		X	Y (Normalized Amplitudes)
P1	Original	0.744	1.219
	SVD	0.76	1.086
	LMS	0.746	0.8439
P2	Original	0.577	1.195
	SVD	0.586	0.7994
	LMS	0.582	0.7926
P3	Original	0.439	1.19
	SVD	0.455	1.077
	LMS	0.571	0.2512
P4	Original	0.597	1.3555
	SVD	0.599	1.151
	LMS	0.593	0.5945
P5	Original	0.809	1.274
	SVD	0.824	1.174
	LMS	0.799	0.7974
P6	Original	0.558	1.064
	SVD	0.528	0.9329
	LMS	0.571	0.7514
P7	Original	0.825	1.471
	SVD	0.833	1.326
	LMS	0.791	1.077
P8	Original	0.702	1.737
	SVD	0.719	1.454
	LMS	0.691	0.9627
P9	Original	0.548	1.334
	SVD	0.568	1.184
	LMS	0.571	0.7434
P10	Original	0.548	1.264
	SVD	0.53	1.11
	LMS	0.573	0.6433

Table 7 presents C Point coordinates (X and Y) of the original signal and the reconstructed signals of both techniques. We observe that the SVD preserves better the amplitude (Y) of point C than the LMS for all participants.

According to the simulation results, the SVD method is the best denoising technique because it preserves the shape of the signal; it gives a better approximation for data reduction compared to the LMS filter (see Table 7 above).

The results have shown efficiency for the entire data. We conclude that SVD performs well and is more reliable than LMS, which is a classical filter and already used in state of the art by Pandey [3] and Hu [4].

IV. Results of method 3

In this party, we have presented a comparison between the selected denoising techniques, whereas, the first purpose is to apply the linear filters. The second purpose is to denoise the ICG signal using LMS-based adaptive filters that had been chosen because it has shown reliability in Hu *et al.* [4] and Rahma *et al.* [5] studies.

The third purpose is to choose the best threshold (SureShrink, Neighblock, Rigrsure, Sqrtwolog) for two types of discrete wavelet families (Daubechies, Symlet).

Our study used different thresholds to demonstrate that the right choice of thresholding affects the obtained results' effectiveness. Hence, Neighblock never applied for ICG waveforms. Linear filters were applied to the ICG signals of 10 participants. The results are presented in Table 8.

Table 8: Estimation parameters of linear filters applied to 10 subjects.

Filters	SE	RMSE	PRD	SNR
Butter	46.2660	0.2842	66.9836	4.4693
Elliptic	50.5032	0.2967	69.1668	3.8837
Gaussian	5.5373	0.0938	31.2531	13.8792
Bessel	210.0218	0.7360	185.1752	1.4735
Chebychev1	51.3537	0.2992	69.7024	3.8104
Chebychev2	198.89	0.6241	121.1752	2.321

According to the results in Table 8, the filter with the highest performance is the Gaussian filter; it has a minimum SE of about 5.5373, a minimum RMSE value of about 0.0938, a minimum PRD value of about 31.2531 and a maximum SNR of about 13.8792. Therefore, it did not fulfil the objective of our analysis for assessing accuracy.

High values were obtained; hence the use of the LMS adaptive filter and discrete wavelets is of paramount importance. We added White Gaussian Noise with SNRi ranging from 0 to 35 dB to the signals to choose the best threshold technique.

Figure 23a-d explains exactly the different comparisons made and the results obtained for 10 subjects. In addition, Figure 23 shows a comparison between Daubechies (db) and Symlet (sym) with the order N (2, 4, 6, 8) in relation to threshold techniques.

First, we found that db2 is better than db (4, 6, 8) in Sureshrink, db4 is better than db (2, 6, 8) in Neighblock, db4 is better than db (2, 6, 8) in Rigrsure, and db8 is better than db (2, 4, 6) in Sqrtwolog. Second, sym2 is better than sym (4, 6, 8) in Sureshrink, sym4 is

Chapter V: Results obtaining from Denoising Techniques

better than sym (2, 6, 8) in Neighblock, sym8 is better than sym (2, 4, 6) in Rigrsure, and sym8 is better than sym (2, 4, 6) in Sqtwolog. Thirdly, after comparing two types of wavelets in each threshold technique, we found that the best are: db4 in Neighblock, sym8 in Rigrsure, and sym 8 in Sqtwolog. Next, the results obtained were compared with the Gaussian filter and the LMS adaptive filter at different SNRi. The results presented in Figure 24 were found using parameter estimation calculations.

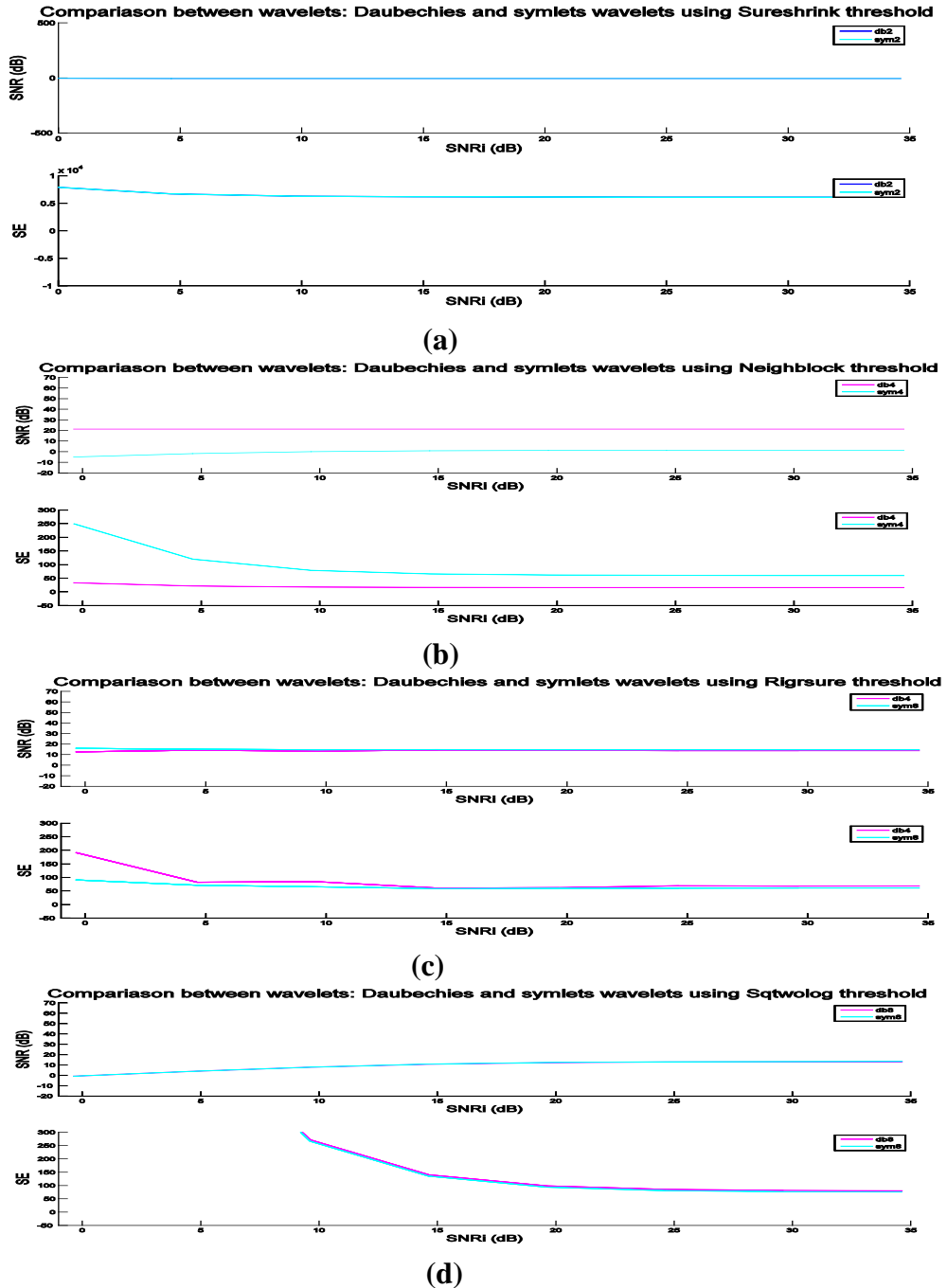


Figure 23: Comparison results between different types of thresholds at different SNRi values.

Comparison between Gaussian Filter, adaptive LMS filter and the different wavelet thresholding methods at frequency 600 Hz

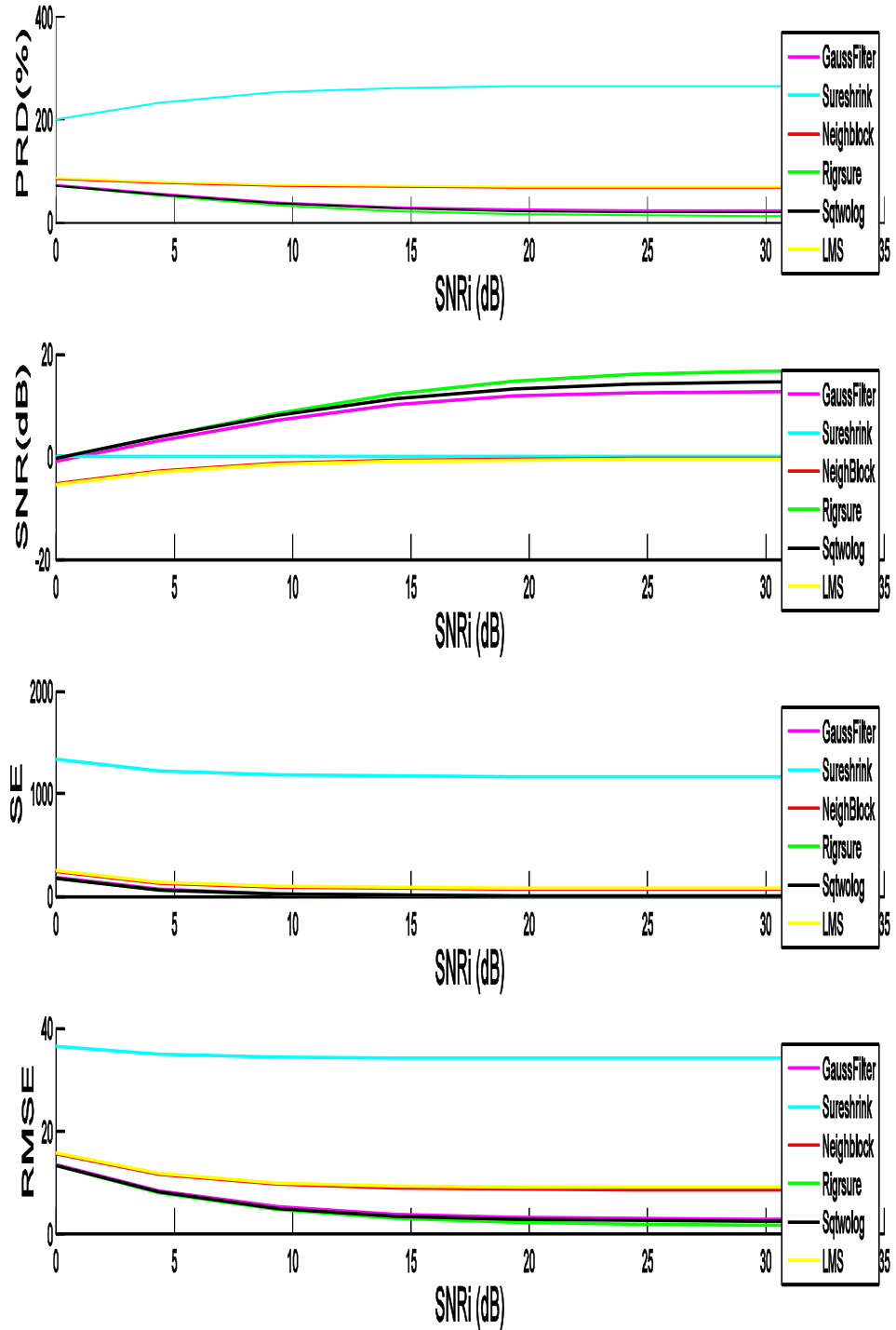


Figure 24: Comparison results of performance parameters evaluation for Gaussian filter, LMS adaptive filter and various wavelets thresholds at different SNRi values.

Chapter V: Results obtaining from Denoising Techniques

- *Discussion*

This study is based on a performance study using linear filters: Bessel; Butterworth, Gaussian, Elliptic, Chebychev1, and Chebychev2 with third order; the LMS adaptive filter, as well as orthogonal wavelets such as Daubechies (db) and Symlet, used with four thresholding techniques such as Sureshrink, NeighBlock, Rigrsure, Sqrtwolog. The evaluation of all comparison results is a necessary step which was carried out by calculating SE, SNR, RMSE, and PRD.

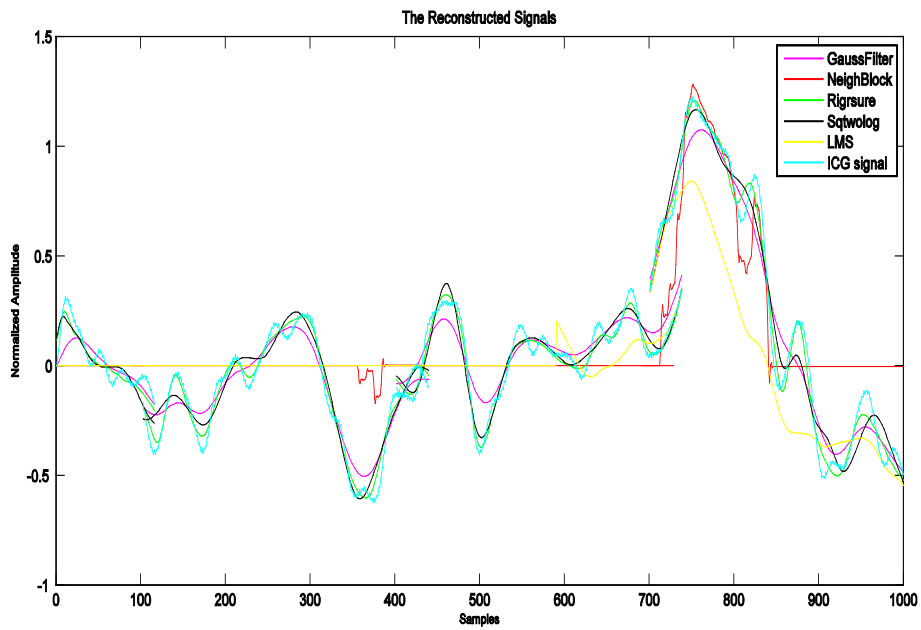
In a first step, a comparison between several linear filters, the results of which are presented in Table 8. In addition, another comparison of orthogonal wavelets of different N-order (2, 4, 6, and 8) was performed.

Although the best selected wavelets were taken from the literature, namely db and sym, which are the most applied to this type of signal, they were compared with multiple thresholding techniques (Figure 23 a-d) such as NeighBlock db4, Rigrsure sym8 and Sqrtwolog sym8.

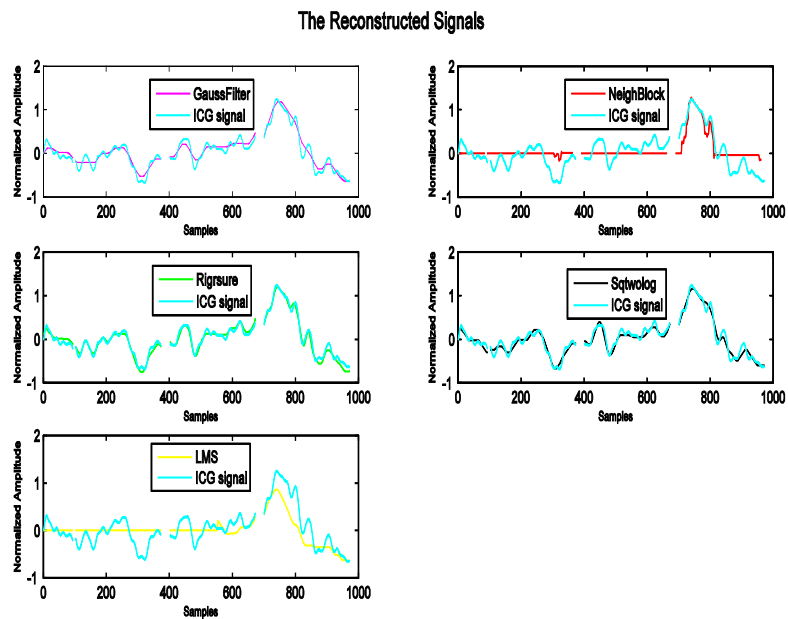
Next, they were also compared with the best linear filter which is the Gaussian filter and the LMS adaptive filter. The results show that the best one has a minimum value of PRD, RMSE, SE, and it has the maximum value of SNR (Figure 24).

According to the results obtained in the simulation, the best denoising method for the ICG signal that preserves the characteristics of the original waveform is the rigidity at level 5 of the sym8 wavelet with minimal degradation of the ICG signal shape. Figures 25 and Figure 26 show reconstructed samples for subject 1.

Chapter V: Results obtaining from Denoising Techniques



(a)



(b)

Figure 25: The ICG signal reconstructed after each technique applied for subject 1 for each technique.

Chapter V: Results obtaining from Denoising Techniques

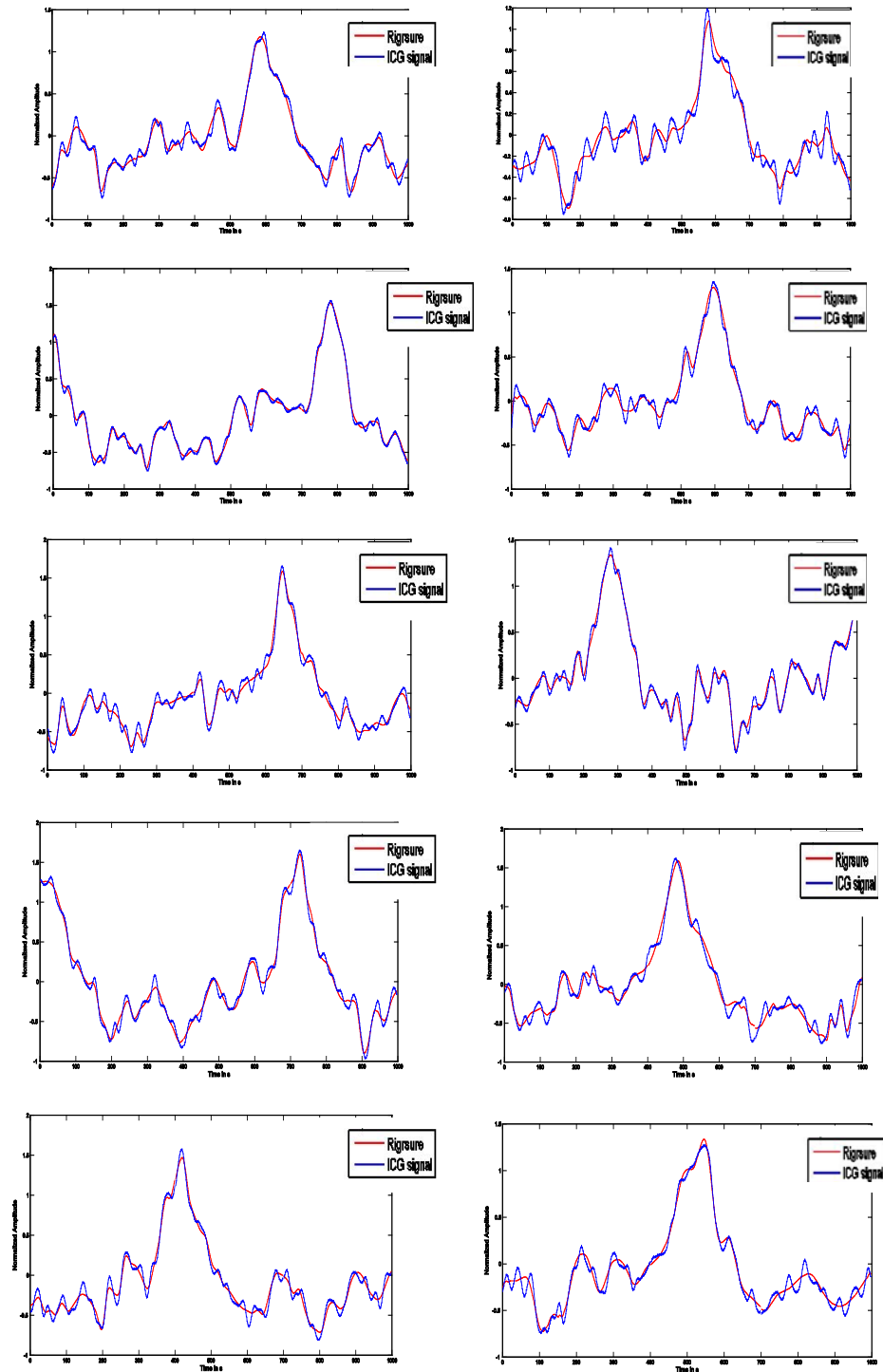


Figure 26: The ICG signal samples reconstructed after applying the best denoising technique for all participants: subjects 1 to 10.

The advantage of this performance study is to reduce the noise and artefacts, which cause distortions in the ICG wave, to a maximum and to preserve the shape of our ICG signal, i.e. the peak $\max(dZ/dt)_{\max}$ of the ICG signal which is present at point C which

Chapter V: Results obtaining from Denoising Techniques

is important in clinical decision making and monitoring of cardiovascular diseases. The peak amplitude C of the original signal and the reconstructed signal after using each denoising technique was calculated to evaluate the results. Pan-Tompkins algorithm [6] was used to detect the C peak. Table 9 lists the results obtained:

Table 9: Detection of peak amplitudes C (Ohms) from original noise-free ICG signals.

Participants	Original C peak amplitude	C peak amplitudes after using denoising methods				
		Gaussian filter	LMS	Neighborhood (db4)	Rigrsure (sym8)	Sqwtolog (sym8)
P1	5021	4999	3429	4433	5001	4047
P2	4337	4337	4276	4336	4463	4743
P3	4959	2911	4049	4054	4654	4053
P4	4351	3357	4127	4353	4112	4357
P5	5401	4493	5106	4490	5287	4490
P6	5002	2511	3663	3870	5089	4294
P7	4756	3609	3383	3382	4665	3606
P8	4246	3197	4014	4424	4102	4009
P9	4486	5408	3021	4067	4365	4869
P10	4596	3395	4942	3447	4623	4396
Mean	4716	3842	4000	4087	4716	4286

According to the results in the above Table 9, the best denoising method is the one that preserve the C peak amplitudes with minimal degradation. We observe that the mean C peak amplitudes of Rigrsure (sym8) equal to the mean C peak amplitudes of the original signal is about 4.716 Ohms. Moreover, for Gaussian filter is about 3.842 Ohms, 4 Ohms for LMS, 4.087 Ohms for Neighborhood, and 4.286 Ohms for Sqwtolog (sym8).

Chapter V: Results obtaining from Denoising Techniques

Table 10: Mean error rate (%) of denoising methods for 10 subjects at different SNR_i (ranging from 0 to 35 dB).

Methods	SNR _i							
	0	5	10	15	20	25	30	35
LMS	0.02855	0.02855	0.02855	0.02855	0.02855	0.02855	0.02855	0.02855
Gaussian	0.00352 23	0.004156 9	0.004512 7	0.004713 3	0.004826 2	0.004889 4	0.004925	0.004945 2
Neighblo ck db4	10.1783	10.1796	10.1801	10.1803	10.1804	10.1804	10.1804	10.1805
Rigrsure sym8	6.2976e -05	8.8323e- 05	0.000191 18	0.000241 63	0.000270 19	0.000285	0.000293 76	0.000297 96
Sqtwolo g sym 8	9.0362e -05	0.000117 34	0.000212 62	0.000263 96	0.000294 01	0.000310 66	0.000320 04	0.000324 41

The results of the mean error rate listed in Table 10 provide better accuracy than the Ridder [2] and Chabchoub [1] methods at different SNR_i, especially for the best thresholding technique, the Rigrsure of sym 8. For an SNR_i of 0 dB, the minimum MER value for the Chabchoub and Ridder methods is equal to 0.3 % and 7.3 %, respectively. For 10 dB, the minimum MER value for the Chabchoub and Ridder methods are equal to 0.01% and 0.7 %, respectively. In this study, the minimum MER value is equal to 0.00006 % in 0 dB and 0.0001 % in 10 dB.

Chapter V: Results obtaining from Denoising Techniques

V. Conclusion

In this chapter, the results of the three methods have discussed several filter techniques for denoising, which are used in the biomedical signal processing field for artifacts removal from ICG signals.

The obtained results of method 1 indicate that the Savitzky-Golay filter with the polynomial of degree 9 is the most suitable method for ICG signals denoising that present better results than adaptive filters described in the simulation results.

The Savitzky-Golay filter attenuates the strong variations; it can use to remove noises making it relevant for medical applications.

The obtained results of method 2 show that the singular values decomposition preserves better the shape of waveforms than LMS-based adaptive.

The two techniques have been evaluated using the denoising performance evaluation criteria presented in the simulation results.

The best method can remove noises that make it relevant for medical applications. Thus, the most suitable choice that preserves the signal better is that of SVD that facilitates the study of beat-to-beat variation.

The obtained results of method 3 present a comparison between the LMS adaptive filter, the Gaussian filter and wavelet families (Daubechies and Symlet) using different threshold techniques such as Sureshrink, NeighBlock, Rigrsure and Sqtwolog to find the best technique for denoising the ICG signal.

The calculation results of the performance parameters evaluation show that the best denoising technique that performs well on noise reduction is the wavelets of sym8 at level 5, and the most optimal thresholding technique is that of Rigrsure with a mean error rate equal (MER) to 0.0001%.

The proposed method has shown the reliability of results more than the other methods that can help us later to extract precisely significant information to diagnose earlier and monitor cardiovascular disorders.

REFERENCES

- [1] S. Chabchoub, S. Mansouri, and R. B. Salah, ‘Impedance cardiography signal denoising using discrete wavelet transform’, *Australasian physical & engineering sciences in medicine*, vol. 39, no. 3, pp. 655–663, 2016.
- [2] S. De Ridder, X. Neyt, N. Pattyn, and P.-F. Migeotte, ‘Comparison between EEMD, wavelet and FIR denoising: Influence on event detection in impedance cardiography’, in *2011 Annual International Conference of the IEEE Engineering in Medicine and Biology Society*, 2011, pp. 806–809.
- [3] V. K. Pandey, P. C. Pandey, N. J. Burkule, and L. R. Subramanyan, ‘Adaptive filtering for suppression of respiratory artifact in impedance cardiography’, in *2011 Annual International Conference of the IEEE Engineering in Medicine and Biology Society*, 2011, pp. 7932–7936.
- [4] X. Hu *et al.*, ‘Adaptive filtering and characteristics extraction for impedance cardiography’, *Journal of Fiber bioengineering and Informatics*, vol. 7, no. 1, pp. 81–90, 2014.
- [5] Rahman, Z.U., Mirza, S.S., Krishna, K.M. (2019). Adaptive Noise Cancellation Techniques for Impedance Cardiography Signal Analysis. *International Journal of Innovative Technology and Exploring Engineering (IJITEE)*, 8(9): 2278-3075. DOI: 10.35940/ijitee.I7531.078919
- [6] J. Pan and W. Tompkins, ‘Real time algorithm detection for QRS’, *IEEE Trans. Eng. Biomed Eng*, vol. 32, no. 3, pp. 230–236, 1985. <https://doi.org/10.1109/TBME.1985.325532>

Chapter .VI

I. Introduction

The impedance cardiography [1] is widely used, mainly in clinical applications; it is devoted for non-invasively cardiac functions. The ICG signal is an interesting indicator for the monitoring and diagnosis of cardiovascular diseases [2], it is based on the application of an alternative electric field at the level of the thorax [3].

The aortic blood volume and its velocity variations cause changes in impedance which subsequently causes a voltage difference, where the dZ/dt is the first derivative that presents the maximum rate of ICG waveform [4] [5].

The recuperated ICG signal is affected by noises like respiratory in the range of 0, 4 to 2 Hz and motion artifacts in the range of 0, 1 to 10 Hz [6] that cause baseline drift, power frequency interference, myoelectricity interference [7].

It is crucial to use artifact suppression methods as filtering, adaptive filtering, ensemble averaging, coherent ensemble averaging, and wavelet-based methods [8] [9] [10] to estimate the constitutive characteristics points of the waveform in order to calculate the hemodynamic parameters such as Stroke volume (SV), and Cardiac Output (CO) as and others defined in equations below [1] [6], for the diagnosis and detection of cardiovascular diseases.

$$SV = \rho_b (L |Z_o|)^2 (dZ/dt)_{max} LVET \quad (1)$$

$$CO = \text{stroke volume} \times \text{heart rate} \quad (2)$$

$$PEP = |T_Q - T_B| \quad (3)$$

Where ρ is the resistivity, Z_0 is the base impedance, (dZ/dt) is the 1st derivate of ICG, LVET is the left ventricular ejection time, between B point and X point, PEP is the time

interval (T) between Q point of ECG signal and B point of ICG signal, and the values of heart rate expressed in (L / min) for man and woman respectively are 5.6 and 4.9.

In this context at the first step, our study presents and describes the background of automatic detection methods that are shown to be efficient; they are evaluated using the Doppler echocardiography. In the second step, we are based on a new algorithm to detect B, C and X points by using a simple mathematical model based on two bells to study ICG signals for 26 cycles; the pre-ejection and the ejection waves.

The cycles of ICG signals are recorded from healthy subjects with a sampling frequency equal to 1000 Hz. The code is developed under MatLab. The configuration of the measurement is based on a Tetrapolar system with four electrodes with contact skin, where two inject a signal, and the other recuperate the potential.

The results significantly improve the efficacy and accuracy of LVET estimation for beat-to-beat estimation under conditions.

II. Background of Detection Methods

The detection of the ICG signal characteristic points is a critically step, for that the components of the signal have been presented in (Figure 27) where the point A coincides with Q of electrocardiogram signal (ECG), the point B corresponds to the opening of the aortic valve, the point C represents the maximal velocity of the blood it is the maximum point on the curve, corresponding to the ventricular contraction [11], it can be measured using the ultrasonic technique [5], the point X is the local minimum, corresponds to the 2nd sound (B2) of the phonocardiogram signal (PCG) [11] and closing the aortic valve [12], the last point is the point O coincides with the mitral valve opening, corresponds to the maximum deviation after X and the opening of the mitral valve, when the lowest left and right lowest points of C are respectively B and X [8] .

The points A and O no longer provide meaningful information for clinical uses, for that reason, the researchers are based only on the B, C, and X detection [8].

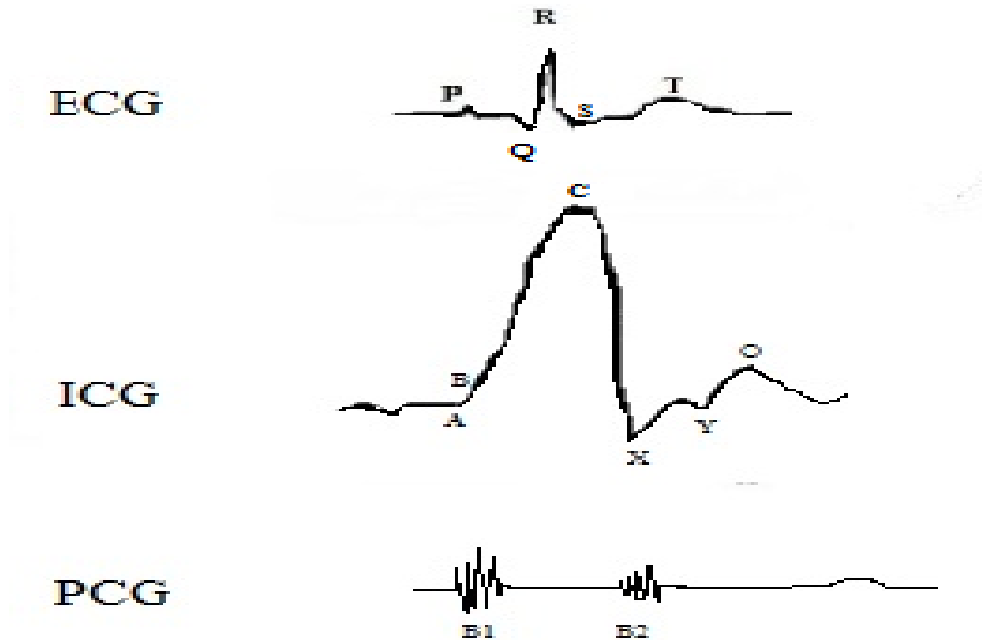


Figure 27: The characteristic feature points of the ICG waveform.

DeMarzo and his colleagues [4] have applied the impedance cardiography method as well as the Doppler technique for Stroke volume computation, where they used HYPER GRAPHTM computer-based impedance cardiograph connected with electrodes for ICG signal data recovery and echocardiography Model SONOS 1500 (Hewlett-Packard Packard Company) for recovering Doppler data, they applied a regression analysis, hereafter, they showed that the electrodes positioning on thorax and the position of the patients during examination affects negatively on measurement reliability. In another Dromer study [13], a more developed SFLC algorithm is applied for the performance estimation of the proposed technique for a beat to beat estimation of B, C, X points, they used this modified algorithm for both Least Mean Square (LMS) and Recursive Least Squares (RLS) algorithm. Gerard Cybulski¹ and Piotr Piskulak [14] used a new technique for automatic detection called Form Factors (FF) which is a quantitative method for evaluating signals. It allows more precision. It performs a classification of either artefact (1) normal (0). They discovered that the FF gives very good results for the

Chapter VI: Feature Point Extraction from ICG waveform

study of QX segments by contribution to the QQ segments. The different FFs are tested in several studies [15] [16] [17], where Q is the point on the electrocardiogram (ECG) signal. The previous article of this study was made by Augustyniak in 1997 [15].

The several equations of the FF are presented as follows, which it is favourable to use more than one for better automatic recognition of the artefacts [4]:

$$FF_1 = \frac{GA}{LA} \quad (4)$$

$$FF_2 = \frac{L}{2\sqrt{nS}} - 1 \quad (5)$$

$$FF_3 = \frac{SU}{SA} \quad (6)$$

$$FF_4 = \frac{\sum_{n=1}^n |x_{i+1} - x_i|}{n-1} \quad (7)$$

$$FF_5 = \sqrt{\frac{\sum_{n=1}^n (x_{i+1} - y_i)^2}{n-1}} \quad (8)$$

Where GA is the number of samples that are above average, LA is the number of samples that are below average, L is the circumference of the QX segment, S is the relative area of the QX segment, SU is the lower surface of the interval (QX), and SA is the upper surface of the interval (QX).

There is a function developed under Matlab by Giuseppe Cardillo [18] based on an area under the curve (AUC) calculation.

The various techniques proposed for characteristic points detection of the ICG signal are applied on a non-processed signal in order to test the sensitivity and reliability of the estimation and the identification of these points on the waveform as the study made by Naidu in 2014 [8], he showed that point C is on the ICG segment in the third of the R-R interval of the ECG signal, where R is taken as a reference peak to select the ICG signal cycles, the max peak is the C point, in case of finding more than one maximum point especially in the case of abnormal patients; otherwise cardiac; it is enough to pick the highest peak, when the point B is on the ICG segment which is the fifth of the C-C interval, the lowest value named valley point where the difference between the two-points C and valley point named the peak-to-peak height (Hpp). Point

B is the deviation preceding point C, it locates by sweeping back the first difference to " valley point ", looking for a sign change from the point corresponding to 0.32 Hpp below the point C, and if the sign is absent, point B is located at 0.72 Hpp below point C. Point X locates on the ICG segment that is the third of C-C, scanning from point T, to search for the lowest value, where the ECG signal T point is a third party segment of R-R, which is localised by sweeping from point R [8].

The evaluation technique is done by calculating SV and other indices with the Doppler echocardiography method to compare them with those calculated by the ICG method.

Kubicek et al. (1970) proposed to identify the point B from the low line about 15% of the max value [19].

Ono et al (2004) proposed to identify the B point from the low line about 40 %, and 80% of the max value through the baseline-upstroke intersection [20].

Shyu et al. (2004) identified points B and X by the quadratic spline wavelet method, which showed that point B is detectable in the 6th level and X in the 4th level [21].

Zhao et al. (2006) proposed the wavelet bior3.3 method to identify points B and X which are detected in the 4th level [22].

Bartnik and Reynolds (2011) have proposed to identify the point X which is in the 2nd noise (B2) of the phonocardiogram tracing (PCG) [23].

Carvalho et al (2011) have proposed to identify the characteristic points of the first four derivatives of the ICG waveform where B is estimated thanks to the baseline-upstroke intersection, they deduced that the point X is identified in the 1st derivative, found in the interval from 0.75 of the R-T interval [24].

Arbol et al (2016) proposed to identify point B from the 3 rd derivative of the 300 ms signal before point C [25].

Hu et al (2014) used a quadratic spline wavelet to identify B, C, and X points [26].

To avoid illusions about point location on ICG signals morphologies; the ECG signal measurement in real-time is essential to estimate the cycles correctly.

The technique proposed in the Bagal study [27] is on wavelet-based scale-dependent thresholding described by Pandey (2007) has been used for noises removal due to breathing, he showed that in the interval R-C [20-65]%, the point B is found with the

Chapter VI: Feature Point Extraction from ICG waveform

min value before point C, in the case of several similar points, it enough to calculate the first difference. In the first third of the C-C interval, X and O are located, when the 1st point is the lowest and the 2nd is the highest point.

The wavelet transform of Bior3.3 and Mexican Hat with a new thresholding technique used by Liu Shan [7] [28] is defined as following:

$$\hat{h}_{ij} = \begin{cases} \text{Sign}(d_{ij}) * \sqrt{d_{ij}^2 - T_j^2}, & |d_{ij}| \geq T_j \\ 0, & |d_{ij}| < T_j \end{cases} \quad (9)$$

Where T_j : is the value of threshold on the j^{th} scale, d_{ij} is the i^{th} coefficient value on the j^{th} scale, and \hat{h}_{ij} is the i^{th} coefficient value on the j^{th} scale after threshold.

They based on the designation of max, all 100 points which are equal to a group; in other words, a cycle; the max of every 100 points is point C [29], point B is minimums from 40 points of point C, and point X is the first negative point after point C; it represents the end of the ventricular ejection. Snajdarova et al.[5] have developed an application called the ICG studio software application to clarify and facilitate detection. Nicholas et al. [30] dedicated their study to performing a comparison between a peak detection algorithm based on phase estimation; where the signals have taken in silico or in vivo are filtered through the linear pass-band filter from the 6th onwards to reduce the computation time with a bandwidth that is determined to avoid shape distortion; and the 6th order Morlet wavelet and transformed Hilbert which uses the Fourier transform (FT) to produce a 90° phase shift of a filter.

- *Discussion*

The evaluation of the automatic detection technique is with the Sensitivity, Positive Predictive, and Detection Error calculation as defined in the following equations [14]:

$$\text{Sensitivity} = \text{TP}/(\text{TP}+\text{FD}) \quad (10)$$

$$\text{Positive predictivity} = \text{TP}/(\text{TP}+\text{MD}) \quad (11)$$

$$\text{Detection error} = (\text{FD}+\text{MD})/(\text{TP}+\text{FD}) \quad (12)$$

Where FD is the Failure Detection based on the detection of the points for these true points. The technique did not allow us to detect a localised point by visual examination, MD is the Misdetection that is used to detect the points for these bad points or incorrect ones; the points detected by the technique does not correspond to a visually detected point, and TP is the True Points that visually detects points for these correct points. As well as other parameters as Mean Error, Root Mean Square Error, Correlation Coefficient, the Mean Values of the intervals and Standard Deviation of the Error and intervals.

The overall mean method, filter method, template method and wavelet transform method are used when the first one improves results of feature extraction are given less precision than others [7].

The 6th order Morlet wavelet, Hilbert transforms, and peak detection algorithm was considered advantageous in their ability to detect the phase that examines the development of oscillation over time [30].

The comparison between the new thresholding technique created by Liu Shan, the hard-thresholding model and the soft, shows that this method controls the deviation between the reconstructed and original signal wavelet coefficients but its disadvantage is that it cannot oscillate the signal, and it keeps the amplitude stable before and after processing [28].

The Bagal method cited above is compared with the Naidu, Kubicek, and Ono methods showed reliability. The method of Nicholas et al. [30] sensitive to noises, and has a slow calculation time, where Morlet's wavelets gives phase at a known moment, thanks to the power of higher frequency computation, as long as Hilbert uses the notion of the weighted average using the Fourier transform, then in the case of high noises, the technique gives reliable results than standard methods.

The results of these researches showed good agreement, where the points detection techniques are satisfactory for beat-to-beat estimation under conditions, especially for modified algorithms that give an accurate estimate of heart rate.

III. A novel algorithm for B C X Points extraction

Our study is based on the calculation of LVET that presents left ventricular ejection time between B point and X point, with normal range varying from around 0.30 to 0.39

Chapter VI: Feature Point Extraction from ICG waveform

second. Our purpose is to avoid illusions about points' location on ICG signals that negatively affect LVET calculation and subsequently on SV. In this context, our algorithm methodology is based on a mathematical model for automatic detection methods for LVET measurement.

To denoise the recuperated ICG signal, we used a butter filter with order 3 and cutOff frequency equal to 10 Hz. The detection of the ICG signal characteristic points is a critical step. However, to detect the BCX point, we based on a simple mathematical model based on the summation effect of the processes on the $dZ|dt$ waveform and the associated ICG parameters. The first is the pre-ejection wave, and the second is the ejection wave [31].

The model uses two bells to study ICG signals.

The system is based on the time expressed in second (s) of the pic C (t_{max}) and their amplitudes (Amp_C), t_0 which is the intersection of the signal with the line zero, it is tightly halfway from the maximum time (t_{max}) to the minimum time (t_{min}), where the first one is of the point C and the second for the point X.

We use the model of Ermishkin and calculate the ejection signal using the following equations [30]:

$$b = \left[\frac{t_0}{t_0 - t_{max}} \right]^2 \quad (13)$$

$$c = \frac{b}{t_0} \quad (14)$$

$$A = \frac{Amp_C}{e^{-ct_{max}} \times t_{max}^{(b-1)} \times \sqrt{(b)}} \quad (15)$$

The ejection signal defined in (5)

$$S_1 = A \times e^{-ct} \times t^b \times \left[\frac{b}{t} - c \right] \quad (16)$$

with,

$$t = [0.001: 1/fs: 1] \quad (17)$$

where, fs is the sampling frequency equal to 1000, S_1 is the ejection signal.

Chapter VI: Feature Point Extraction from ICG waveform

Our approach based on the calculation of the preejection signal defined in (18) from the original x_1 (ICG) and the ejection signal, where we use the minimum time of the point X defined in (19):

$$S = x_1 - S_1 \quad (18)$$

$$t_{min} = 2t_0 - t_{max} \quad (19)$$

To detect the maximum peak C, we used the findpeaks function with MinPeakHeight and threshold equal to 0.8. B point presents the local minimum; it identifies before point C that we used the findpeaks function with minpeakdistance and threshold equal to 14. We applied the index in each little peak and chose the last one on the pre-ejection wave that coincided with the point before peak C in the ICG waveform. The point X is the local minimum after point C that coincided with the first minimum on the ejection wave Table 11 presents t_0 , the amplitudes and times of point C:

Chapter VI: Feature Point Extraction from ICG waveform

Table 11: The ICG parameters used for our algorithm.

Number of simples	t_0 (s)	Point C	
		Amplitudes (Amp_C)	Times (t_{max} (s))
1	0.603	1.2942	0.485
2	0.615	1.1795	0.486
3	0.372	1.042	0.242
4	0.4	1.2994	0.285
5	0.688	1.1286	0.574
6	0.426	1.5993	0.294
7	0.841	1.5756	0.72
8	0.65	1.3355	0.505
9	0.442	1.3751	0.298
10	0.428	1.2156	0.316
11	0.43	1.3384	0.31
12	0.824	1.476	0.714
13	0.596	1.4237	0.482
14	0.414	1.2473	0.289
15	0.649	1.3194	0.54
16	0.489	1.2927	0.362
17	0.311	1.2567	0.184
18	0.603	1.2444	0.495
19	0.367	1.2001	0.244
20	0.835	1.094	0.706
21	0.574	1.1539	0.466
22	0.629	1.2005	0.532
23	0.68	1.1647	0.549
24	0.496	1.2762	0.367
25	0.843	1.295	0.714
26	0.642	1.0397	0.512

Chapter VI: Feature Point Extraction from ICG waveform

- Results and discussion

Figure 28 presents the location of characteristic points from the ICG signal and the two their waves of ejection and pre-ejection for cycles. However, we extracted the point C that corresponds to the maximum peak in the ejection and original waveform, X presents the lowest peak in ejection waveform after point C, and B is the lowest peak in the pre-ejection signal before point C. Our approach is applied for 26 ICG cycles and their ejection and pre-ejection waveforms. We follow the same technique to detect the features extraction B and X for the other cycles as presented, also we calculate the LVET. The results are presented in Table 12.

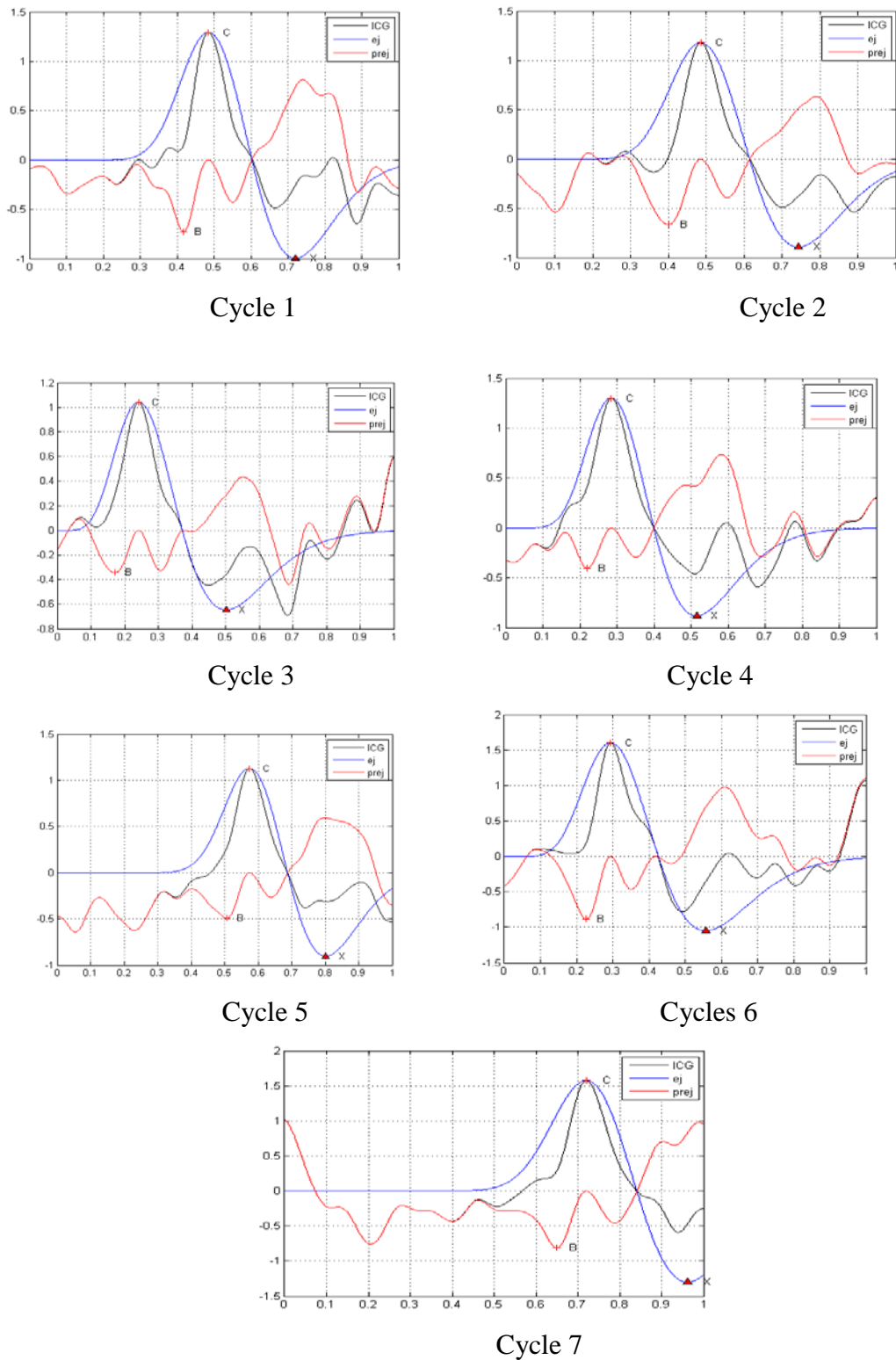


Figure 28: Extraction of the BCX point from ejection, pre-ejection and original signal for cycles from 1 to 7.

Chapter VI: Feature Point Extraction from ICG waveform

Table 12: The LVET calculation for each cycle of ICG signal.

Number of cycles	LVET (s)	Point B		Point X	
		Amplitudes (Amp_C)	Times (t_{max} (s))	Amplitudes (Amp_C)	Times (t_{max} (s))
1	0.304	-0.72512	0.417	-0.99496	0.721
2	0.344	-0.66218	0.4	-0.8895	0.744
3	0.331	-0.34328	0.171	-0.64608	0.502
4	0.295	-0.40213	0.22	-0.87985	0.515
5	0.296	-0.49222	0.506	-0.90377	0.802
6	0.331	-0.88576	0.227	-1.0493	0.558
7	0.312	-0.81042	0.65	-1.2995	0.962
8	0.389	-0.69368	0.401	-0.98891	0.79
9	0.377	-0.68028	0.209	-0.88203	0.586
10	0.322	-0.43309	0.218	-0.85334	0.54
11	0.313	-0.56678	0.237	-0.91703	0.55
12	0.29	-0.54022	0.644	-1.2345	0.934
13	0.299	-0.5384	0.411	-1.1011	0.71
14	0.332	-0.46239	0.207	-0.82759	0.539
15	0.291	-0.37287	0.467	-1.0533	0.758
16	0.33	-0.58918	0.286	-0.90995	0.616
17	0.323	-0.47617	0.115	-0.71492	0.438
18	0.29	-0.37597	0.421	-0.97853	0.711
19	0.322	-0.21194	0.168	-0.75956	0.49
20	0.32	-0.40652	0.644	-0.88946	0.964
21	0.301	-0.35746	0.381	-0.89626	0.682
22	0.291	-0.23598	0.435	-0.97642	0.726
23	0.345	-0.61341	0.466	-0.89912	0.811
24	0.326	-0.51668	0.299	-0.89788	0.625
25	0.329	-0.76577	0.643	-1.055	0.972
26	0.362	-0.47478	0.41	-0.79191	0.772

The LVET calculation is used to evaluate our methodology of characteristic point extraction of ICG signals. We observe that some LVET values are around 0.29 of a few cycles, but if we evaluate the mean of LVET, we find that the LVET is in the normal range, wherever the results are satisfactory.

IV. Conclusion

The hemodynamic parameters related to the process of heart mechanical activities must be calculated thanks to the estimation of the characteristic points on the ICG signal, for this purpose, we noted, that it is important to find an effective means to push towards a correct detection to not disclose the clinical diagnosis.

The automatic detection techniques are reliable, but the difference between them is the computational complexity, which varies from one method to another. They are applicable for the processed or unprocessed signal. Therefore, that will be used to solve the ambiguity caused by ICG signal morphology for the diagnosis and monitoring of cardiovascular diseases.

In this paper, the first step based on presentations and descriptions on the possibility of evaluating the performance ICG features extraction, which is based on the ECG signal simultaneous measurement, because the R wave is the reference peak used by several researchers to estimate A, B, C points.

However, at the second step, we used a model based on two bells; ejection and pre-ejection wave, and then applied a new algorithm of detection technique to calculate the LVET of the ICG signal without needing the R peak. This hybridization technique can confirm the calculation of the LVET from the two bells without calculating it from the original ICG waveform.

Our approach can evaluate the performance of the features points' extraction, and predict the typical ICG shape if the error exists, thanks to the early phase of the ventricular systole.

We established a new detection method that identifies precisely the localization of the patterns for not disclosing the clinical diagnosis and the monitoring of cardiovascular diseases. It allows us to estimate the heart mechanical activities process of the patient.

REFERENCES

- [1] S. Kerai, 'The impedance cardiography technique in medical diagnosis', *Medical Technologies Journal*, vol. 2, no. 3, pp. 232–244, 2018. , Doi:10.26415/2572-004X-vol2iss3p232-244.
- [2] L. Guohua, Z. Daimo, T. Xiaodan 'A new theory of impedance blood flow chart [J]'. *Chinese Journal of Medical Physics*, vol. 1 no. 4, pp.:201- 204, 1996.
- [3] J. M. Gayes, 'Transthoracic electrical bioimpedance: a noninvasive measurement of cardiac output.', *Journal of Post Anesthesia Nursing*, vol. 4, no. 5, pp. 300–305, 1989.
- [4] A. P. DeMarzo, R. M. Lang, R. Priemer, and C. E. Korcarz, 'Computer method of predicting the reliability of impedance cardiography stroke volume measurements', in *Computers in Cardiology 1995*, 1995, pp. 497–500. DOI: 10.1109/CIC.1995.482710
- [5] M. Snajdarova, S. Borik, and I. Cap, 'Features extraction from impedance cardiography signal', in *2017 11th International Conference on Measurement*, 2017, pp. 225–228. DOI: 10.23919/MEASUREMENT.2017.7983577.
- [6] V. K. Pandey and P. C. Pandey, 'Cancellation of respiratory artifact in impedance cardiography', in *Proc. 27th Annual Conference on Engineering in Medicine and Biology*, 2005, pp. 5503–5506. DOI: 10.1109/IEMBS.2005.1615729
- [7] S. Liu, K. Yue, H. Yang, L. Liu, X. Duan, and T. Guo, 'Study on cardiac impedance signal feature point extraction', in *2017 IEEE 3rd Information Technology and Mechatronics Engineering Conference (ITOEC)*, 2017, pp. 790–793. DOI: 10.1109/ITOEC.2017.8122460
- [8] S. M. M. Naidu, U. R. Bagal, P. C. Pandey, S. Hardas, and N. D. Khambete, 'Detection of characteristic points of impedance cardiogram and validation using Doppler echocardiography', in *2014 Annual IEEE India Conference (INDICON)*, 2014, pp. 1–6. DOI: 10.1109/INDICON.2014.7030596
- [9] V. K. Pandey, 'Suppression of artifacts in impedance cardiography', Ph. D Thesis 2009, Indian Institute of Technology Bombay, India, 2009.

- [10] D. W. Kim, C. G. Song, and M. H. Lee, 'A new ensemble averaging technique in impedance cardiography for estimation of stroke volume during treadmill exercise.', *Frontiers of Medical and Biological Engineering: the International Journal of the Japan Society of Medical Electronics and Biological Engineering*, vol. 4, no. 3, pp. 179–188, 1992.
- [11] D.-W. Kim, 'Detection of physiological events by impedance', *Yonsei Medical Journal*, vol. 30, no. 1, pp. 1–11, 1989.
- [12] R. P. Patterson, 'Fundamentals of impedance cardiography', *IEEE Engineering in Medicine and Biology magazine*, vol. 8, no. 1, pp. 35–38, 1989. DOI: 10.1109/51.32403.
- [13] O. Dromer, O. Alata, and O. Bernard, 'Improvements of scale fourier linear combiner for impedance cardiography analysis', in *2010 Annual International Conference of the IEEE Engineering in Medicine and Biology*, 2010, pp. 4331–4334..DOI: 10.1109/IEMBS.2010.5627082
- [14] G. Cybulski and P. Piskulak, 'The use of different measures of signal shape for automatic identification of artefacts in impedance cardiography', in *Computing in Cardiology 2014*, 2014, pp. 969–972.
- [15] P. Augustyniak, 'The use of shape factors for heart beats classification in Holter recordings', in *Computers in Medicine Conf*, 1997, vol. 47.
- [16] K. Malinowska 'The evaluation of the development of cross-sectional shape of the fibers' (in Polish: Ocena stopnia rozwinięcia kształtu przekrojów poprzecznych włókien). *Przegląd włókienniczy*, no.4: pp. 190-4,1975.
- [17] D. Csetverikov, 'Basic algorithms for digital image analysis: a course', *Institute of Informatics, Budapest, Hungary*, 1999.
- [18] G. Cardillo, 'ROC curve: compute a Receiver Operating Characteristics curve', *Natick (MA): Math-Works*, 2008.
- [19] W. G. Kubicek, R. P. Patterson, and D. A. Witsoe, 'Impedance cardiography as a noninvasive method of monitoring cardiac function and other parameters of the cardiovascular system', *Annals of the New York Academy of Sciences*, vol. 170, no. 2, pp. 724–732, 1970.DOI : 10.1111/j.1749-6632.1970.tb17735.x
- [20] T. Ono *et al.*, 'Beat-to-beat evaluation of systolic time intervals during bicycle exercise using impedance cardiography', *The Tohoku journal of experimental*

Chapter VI: Feature Point Extraction from ICG waveform

- medicine*, vol. 203, no. 1, pp. 17–29, 2004. Available at: <https://doi.org/10.1620/tjem.203.17>. <https://doi.org/10.1620/tjem.203.17>
- [21] L.-Y. Shyu, Y.-S. Lin, C.-P. Liu, and W.-C. Hu, ‘The detection of impedance cardiogram characteristic points using wavelet transform’, *Computers in biology and medicine*, vol. 34, no. 2, pp. 165–175, 2004. DOI: 10.1016/S0010-4825(03)00040-4.
- [22] Z. Shuguang, F. Yanhong, Z. Hailong, and T. Min, ‘Detection of impedance cardioaraphy’s characteristic points based on wavelet transform’, in *2005 IEEE Engineering in Medicine and Biology 27th Annual Conference*, 2006, pp. 2730–2732. DOI: 10.1109/IEMBS.2005.1617035.
- [23] D. Bartnik and B. Reynolds, *Impedance cardiography system and method*. Google Patents, 2011.
- [24] P. Carvalho, R. P. Paiva, J. Henriques, M. Antunes, I. Quintal, and J. Muehlsteff, ‘ROBUST CHARACTERISTIC POINTS FOR ICG’, 2011. DOI:10.5220/0003134901610168.
- [25] J. R. Árbol, P. Perakakis, A. Garrido, J. L. Mata, M. C. Fernández-Santaella, and J. Vila, ‘Mathematical detection of aortic valve opening (B point) in impedance cardiography: A comparison of three popular algorithms’, *Psychophysiology*, vol. 54, no. 3, pp. 350–357, 2017. DOI:10.1111/psyp.12799
- [26] X. Hu *et al.*, ‘Adaptive filtering and characteristics extraction for impedance cardiography’, *Journal of Fiber bioengineering and Informatics*, vol. 7, no. 1, pp. 81–90, 2014. Doi:10.3993/jfbi03201407.
- [27] U. R. Bagal, P. C. Pandey, S. M. M. Naidu, and S. P. Hardas, ‘Detection of opening and closing of the aortic valve using impedance cardiography and its validation by echocardiography’, *Biomedical Physics & Engineering Express*, vol. 4, no. 1, p. 015012, 2017.
- [28] S. Liu, Y. Li, X. Hu, L. Liu, and D. Hao, ‘A novel thresholding method in removing noises of electrocardiogram based on wavelet transform’, *Journal of Information & Computational Science*, vol. 10, no. 15, pp. 5031–5041, 2013.
- [29] S. M. M. Naidu, P. C. Pandey, and V. K. Pandey, ‘Automatic detection of characteristic points in impedance cardiogram’, in *2011 Computing in Cardiology*, 2011, pp. 497–500.

Chapter VI: Feature Point Extraction from ICG waveform

- [30] N. Mitrou, A. Laurin, T. Dick, and J. Inskip, 'A peak detection method for identifying phase in physiological signals', *Biomedical Signal Processing and Control*, vol. 31, pp. 452–462, 2017. DOI : 10.1016/j.bspc.2016.07.001
- [31] V. V. Ermishkin, V. A. Kolesnikov, E. V. Lukoshkova, and R. S. Sonina, 'Simulation of pathologic changes in ICG waveforms resulting from superposition of the preejection and ejection waves induced by left ventricular contraction', in *Journal of Physics: Conference Series*, 2013, vol. 434, no. 1, p. 012007.

Chapter .VII

I. Introduction

In this chapter, we aimed to develop a new application automatic access that helps the medical person to make a good diagnosis earlier. The Impedance cardiography (ICG) technique is applied to measure cardiac function. The ICG is non-invasive, easy to use, cheaper and safe, enabling the estimation of time's intervals and cardiac indices.

The digital processing field used on our signals helps doctors to provide all necessary medical information to establish a speed and reliable diagnosis.

Our plan is based on the optimization care quality and the speediness of diagnosis, whatever their geographical location, we carried out to two criteria: The storage of information, and the manipulation of data through an application of automatic access in real time.

In this party, three different environments are used: Matlab, MySQL, and Java Netbeans, which allowed the development of a new application, presented in Figure 29 that is easy, fast, and reliable and helps the clinics to analysed ICG and electrocardiogram (ECG) signals and diagnose if there are any abnormalities in heart functions, either locally or remotely. This work is presented in 2022 3rd International Conference on Electrical and Electronics Engineering ICEEE 2022.

The work is carried out under a 64-bit win 7. Three softwares are installed on the operating system:

- Java Netbeans IDE 7.3: allows you to deploy the web applications. The OpenSource licence of NetBeans makes it possible to develop and deploy Swing graphics applications, Applets, JSP / Servlets, J2EE architectures. It is easy to use in an extremely customizable environment. The NetBeans IDE is based on a robust kernel. The NetBeans Platform can also be used to develop your own Java applications [1].
- Matlab: is Matrix laboratory present interactive software developed by Math Works Inc. It exists in Dos, Windows, and UNIX environments, aimed for digital signal processing. In this study, we have used the Matlab R2014a version that allows a speed visualisation of results, modelling, simulation, and design of complex digital systems [2].

Chapter VII: Telemedicine Application of ICG Signals

- WAMP / EASYPHP (MySQL) for web development, it allows you to create web applications with Apache2, MySQL database and PHPMyAdmin to easily manage your databases [3] [4].

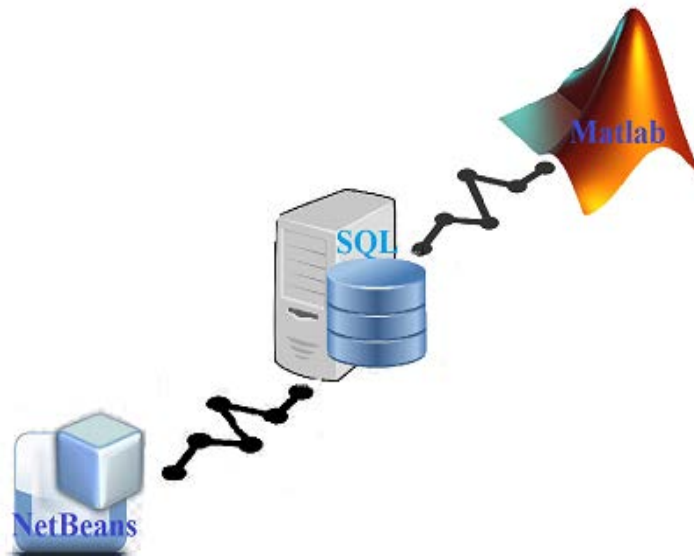


Figure 29: The principle of our developed application.

II. Network Background

Figure 30a presents architecture with a LAN (Local Area Network). It has two machines, a remote server, an RJ45 cable, and a modem that acts as an access point. Figure 30b presents architecture with an extended topology called WAN (Wide Area Network). For the purpose to have remote access to the server; which is located at the central hospital, for example, that has a specialised line with a high speediness connection; from different clinics located in different places installed our application.

Chapter VII: Telemedicine Application of ICG Signals

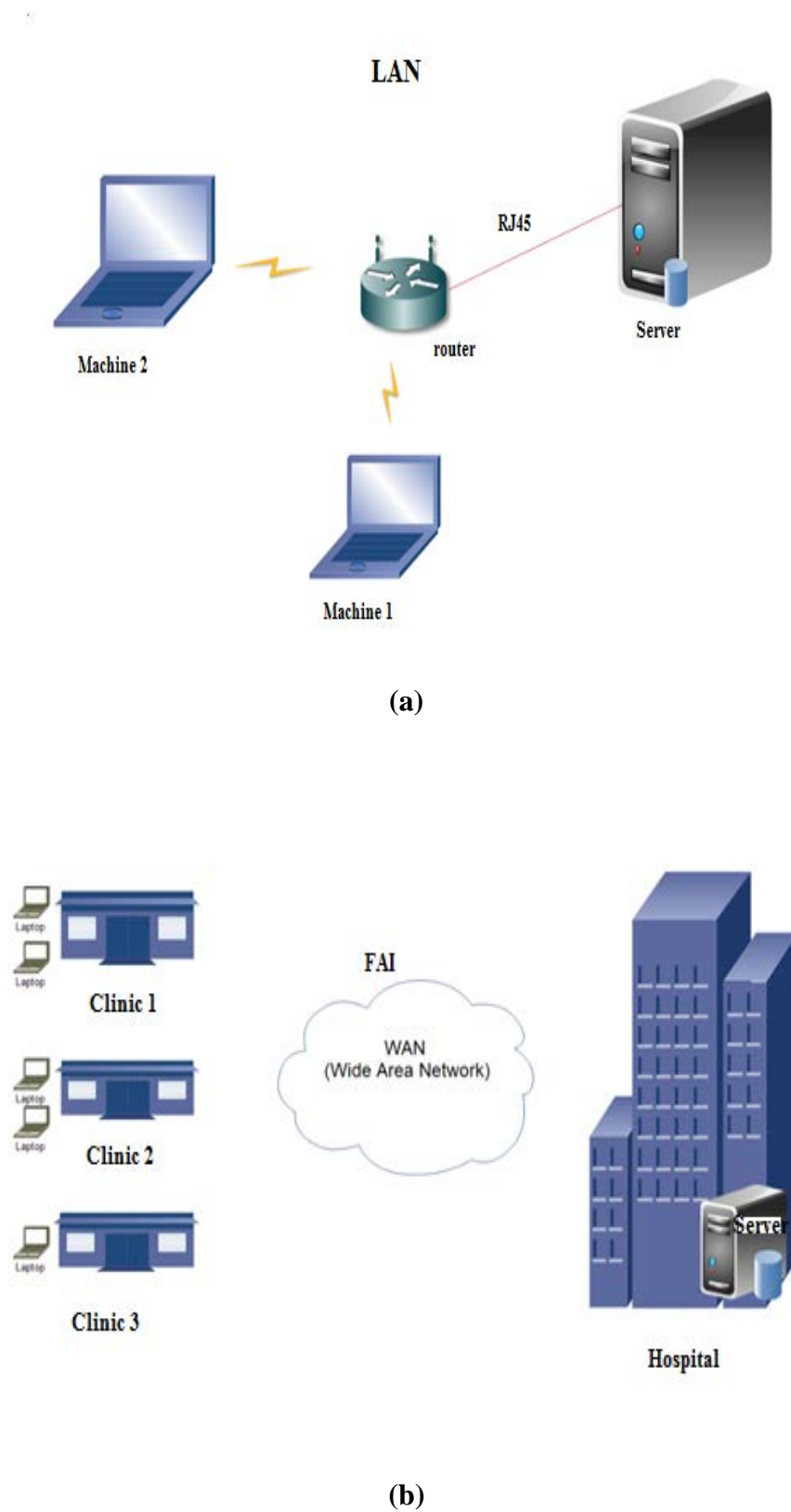


Figure 30: (a) The local area network topology, (b) The wide area network topology.

III. Our Developed Application

- In a treatment room where machine one is available, installed Matlab there is:

To calculate the hemodynamic parameters and time intervals such as stroke volume (SV), thoracic fluid content (TFC), cardiac output (CO), heart rate variability (HRV), left ventricle ejection time (LVET), and preejection period (PEP) are defined in the following equations [6]:

$$TFC = \frac{1}{Z_0} \quad (1)$$

$$SV = V_c \sqrt{LVET * \left(\frac{1}{Z_0}\right) \left(\frac{dZ}{dt}\right)_{max}} \quad (2)$$

$$CO = HR * SV \quad (3)$$

$$PEP = |T_Q - T_B| \quad (4)$$

Where, V_c is the intrathoracic blood volume expressed in mL, LVET is the left ventricle ejection time between B and X points of the ICG signals, Z_0 : basic thoracic impedance, $(dZ/dt)_{max}$ is the maximum on the ICG signal curve, HR is the heart rate, and PEP is the time interval (T) between Q point of ECG signal and B point of ICG signal.

We must apply a features point extraction algorithm for ICG signal and ECG signal: We applied our algorithm on signals of ten healthy subjects, when we recorded and analysed ECG and ICG signals with a sampling frequency equal to 1000 Hz. We filtered the ECG signal using the low pass filter and high pass filter, we used an algorithm of detection of PQRS. It is based on the detection of the point R and the point-by-point methods for the other points.

To denoise ICG signal from artifacts due to motion or respiration of subjects, we applied butter filter with order three. The Pan-Tompkins algorithm [6] is used to identify

Chapter VII: Telemedicine Application of ICG Signals

point C, whereas B and X are the local minima located before and after C, respectively. All results are displayed in the Matlab console and saved directly to the MySQL server using a simple program. We are based on two ways, where the first is a small application developed under Netbeans to send the figures of the ICG and ECG signals analysis to the MySQL server. The second is a Matlab program aimed to send the saved figures to the server automatically.

- MySQL server is a remote server that has our database (DB).
- Java Netbeans: An application under Netbeans installed on the user's workstation, allowing access to information.

For a remote server, we used WAMP / EASYPHP to create the database. In our project, we adjust the privilege of our database to open a communication with another machine (customers). Then, we use PHPMyAdmin MySQL to create the fifth table (ecg, icg, icg_signal, results, users). Under Matlab, we have implemented two programs: the first for the digital processing of the ICG signal, and the second for sending the results (features characteristics points, time intervals, and cardiac indices), thanks to the fastinsert function, after their processing, to a table (results) under a specific database (database) in the MySQL server under WAMP or ESAYPHP, As explained above, a small application is developed to send the ICG/ECG figures to the server under a table (icg_signal).

The Java Netbeans application has five interfaces with its function (login, menu, users, signals and results). This part is used to visualise and display the data already processed in the treatment room (which contains the Matlab software for the segmentation of ICGs signals), and also to enter various information of patients and users, the latter is identified by a password and a user ID for confidentiality reasons.

The purpose of this application is to provide the user with all the necessary information, which helps him to establish a fast and reliable estimate. This application is a real-time automatic access application used to optimise the quality of care and the speed of diagnosis regardless of their geographical location, and is carried out according

to two important criteria: the storage of information and the manipulation of data thanks to the connection between softwares.

- **MySQL connection with Matlab**

The fundamental objective set behind this part is to establish a connection between two environments: "Matlab and MySQL server" to store the information extracted from digital processing of the ICG/ECG signal. Before proceeding with any treatment, compatibility between the systems used is mandatory. This compatibility facilitates the achievement of the following tasks (see Figure 31):

1. Installation of ODBC driver;
2. The incorporation of the "database" that has already been created under MySQL in Matlab;
3. Confiscation of information in the MySQL connector window (name, server IP address), to test the connection;
4. Connection of the database.

Chapter VII: Telemedicine Application of ICG Signals

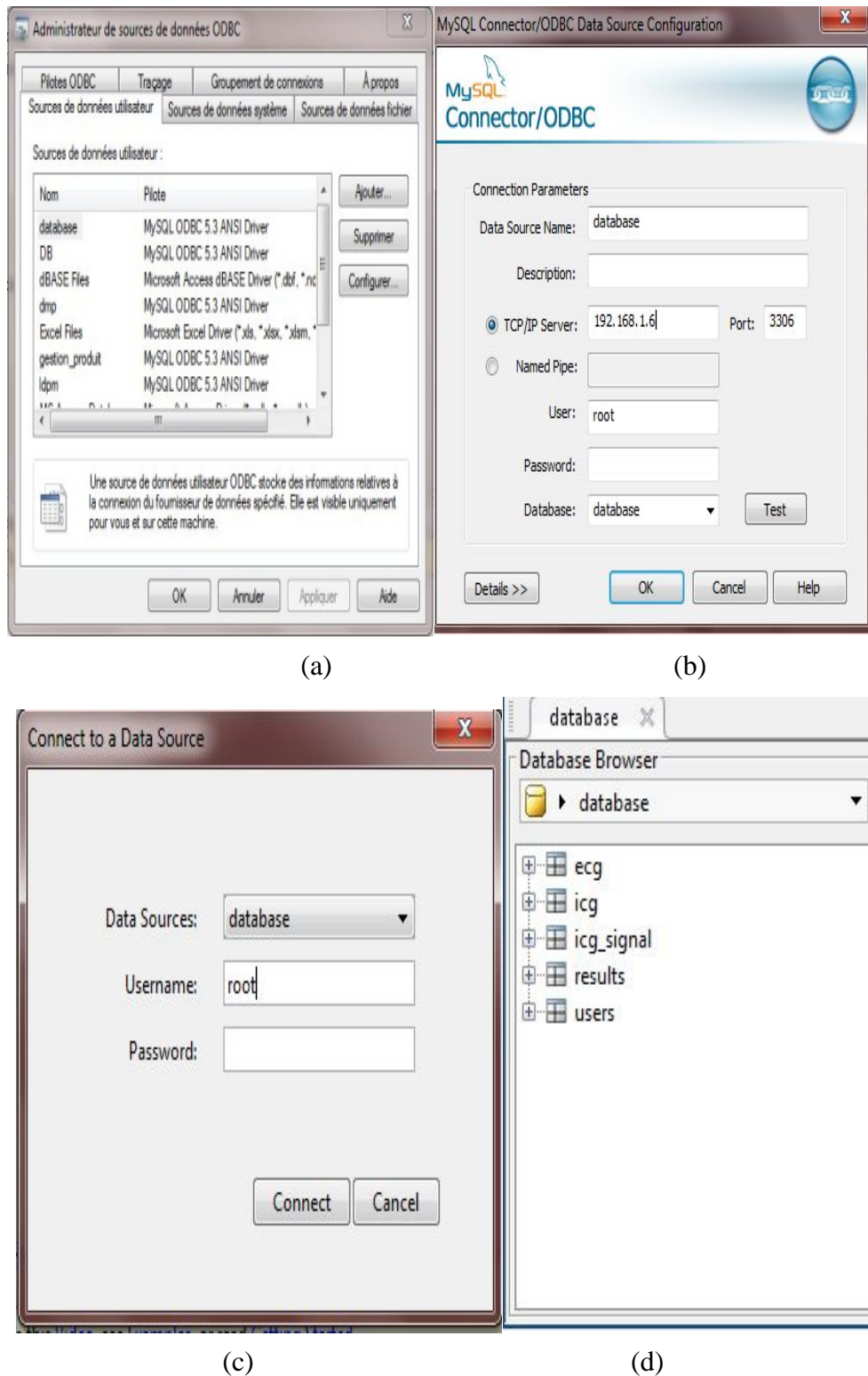


Figure 31: The connection of Matlab and MySQL. (a) connect to database, (b) enter the IP address and port number, (c) test the connection, (d) MySQL database appeared in Matlab.

- **MySQL connection with Java Netbeans**

To establish MySQL & Java Netbeans connection, you must install a "MySQL JDBC Driver" compatible with the machine used, and then follow the following steps:

1. Connect Netbeans with MySQL: determine the server address. (A public but fixed address).
2. Connect Netbeans with the "database" database
3. Creation of graphical interfaces.
4. Connect Netbeans with DB tables (so that the content of the tables will be visible in the interfaces created using java Netbeans).

IV. Results and Discussions

Tables below (Table13, Table14 and Table15) present some results of the ICG and ECG signals after processing in Matlab.

Chapter VII: Telemedicine Application of ICG Signals

Table 13: Feature points extraction for ECG signal.

Code of patient	Number of cycle	Times (second (s))				Amplitudes			
		P	Q	R	S	P	Q	R	S
1	7	0.262	0.339	0.304	0.327	0.0088	0.0010	0.4118	-0.4421
2	1	0.432	0.532	0.471	0.494	0.0043	0.0001	0.4148	-0.4475
3	1	0.276	0.3851	0.318	0.341	0.0069	-0.0021	0.42100	-0.4579
4	5	0.315	0.452	0.358	0.381	0.0042	-0.0056	0.4140	-0.4395
5	6	0.549	0.638	0.589	0.612	0.0077	-3.6 e-005	0.4130	-0.4451
6	2	0.559	0.663	0.598	0.621	0.0064	0.0010	0.4235	-0.4548
7	5	0.257	0.431	0.299	0.323	0.0068	-0.0064	0.4301	-0.4448
8	6	0.506	0.569	0.547	0.57	0.0111	0.0045	0.4026	-0.4309
9	5	0.314	0.388	0.353	0.376	0.0073	-0.0004	0.4293	-0.4497
10	1	0.34	0.478	0.383	0.407	0.0096	0.0005	0.4044	-0.4315

Table 14: Feature points extraction for ICG signal.

Code of patient	Number of cycle	Times (s)			Amplitudes		
		B	C	X	B	C	X
1	7	0.282	0.431	0.63	-0.1484	0.9576	-0.4985
2	1	0.482	0.587	0.795	0.0291	0.9033	-0.4306
3	1	0.317	0.455	0.656	0.0765	1.1106	-0.4501
4	5	0.362	0.486	0.702	-0.1304	1.1794	-0.4881
5	6	0.565	0.731	0.869	-0.0235	1.2501	-0.3251
6	2	0.582	0.735	0.904	-0.1073	1.1986	-0.3129
7	5	0.31	0.45	0.635	-0.1947	1.2849	-0.6462
8	6	0.51	0.69	0.82	-0.1631	1.1887	-0.2146
9	5	0.283	0.495	0.64	-0.2785	1.2444	-0.2432
10	1	0.368	0.532	0.702	-0.1617	1.2004	-0.4751

Chapter VII: Telemedicine Application of ICG Signals

Table 15: Time intervals and hemodynamic parameters values.

Code of patient	Number of cycle	HRV (ms)	LVET (s)	PEP (s)	SV (ml)	TFC (s)	CO (ml/ms)
1	7	835	0.348	0.0570	83.339	1.3525	69.58
2	1	835	0.313	0.05	102.57	1.3557	85.64
3	1	801	0.339	0.0681	85.144	1.348	68.20
4	5	776	0.34	0.090	87.885	1.323	68.19
5	6	826	0.304	0.073	120.26	1.334	99.33
6	2	769	0.322	0.081	127.91	1.333	98.36
7	5	802	0.325	0.0121	75.427	1.303	60.49
8	6	804	0.31	0.059	114.24	1.326	91.85
9	5	783	0.35	0.105	94.74	1.328	74.18
10	1	789	0.334	0.11	96.76	1.338	76.34

Application under netbeans decomposed into interfaces as follow:

- Login interface

Security is necessary for any application to assure access to its functions. For this purpose, we have created an authentication mechanism (see Figure 32) for the user with a correct user ID and password.

- Menu interface

The user can manage the database as he wants according to their choice (see Figure 33) (User, Signals, and Results).

- Users interface

The bottom users in Figure 34 is a simple mechanism, grouped into a simple interface that stores the different user IDs and passwords of users who have the right to access medical information and who also have the right to read and write.

- The ICG images storage

A small application developed under Java Netbeans is used to record images automatically under the MySQL server in a table (icg_signal). This interface presented in Figure 35 allows us to enter the ID, the patient's code, and the number of cycles, and then click on the browse button to bring the image. The latter will be stored in the table under MySQL.

- Signals interface

The following interface (see Figure 36) presents the characteristic points of ICG and ECG signals for several cycles and patients according to ID, patient code, and the number of cycles. As well as the images display different signals after their treatments according to the ID.

- Results interface

The following interface presented in Figure 37 shows the display of the results after the processing of the ICGs and ECGs signals from different subjects. The doctor can read and print the values presented in the interface. Each value has a normal range for a healthy person without suffering from any cardiac disease.

For example:

- Left ventricle ejection time (LVET) varying from 0.30 to 0.39 second
- Preejection period (PEP) varying from 0.05 to 0.12 second
- Stroke volume (SV) varying from 70 to 150 ml.

Thanks to this information that can be print, the doctor or any medical person can estimate if the subject has cardiovascular disease or not.

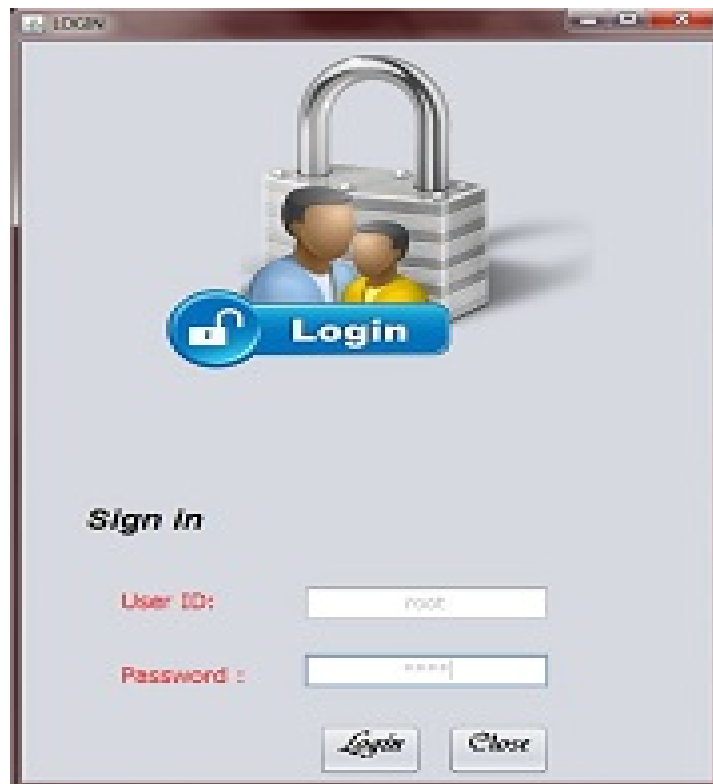


Figure 32: Login interface.

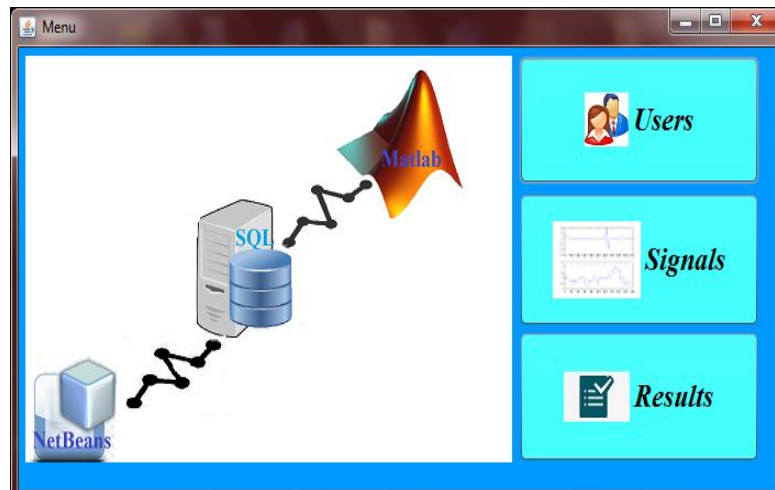
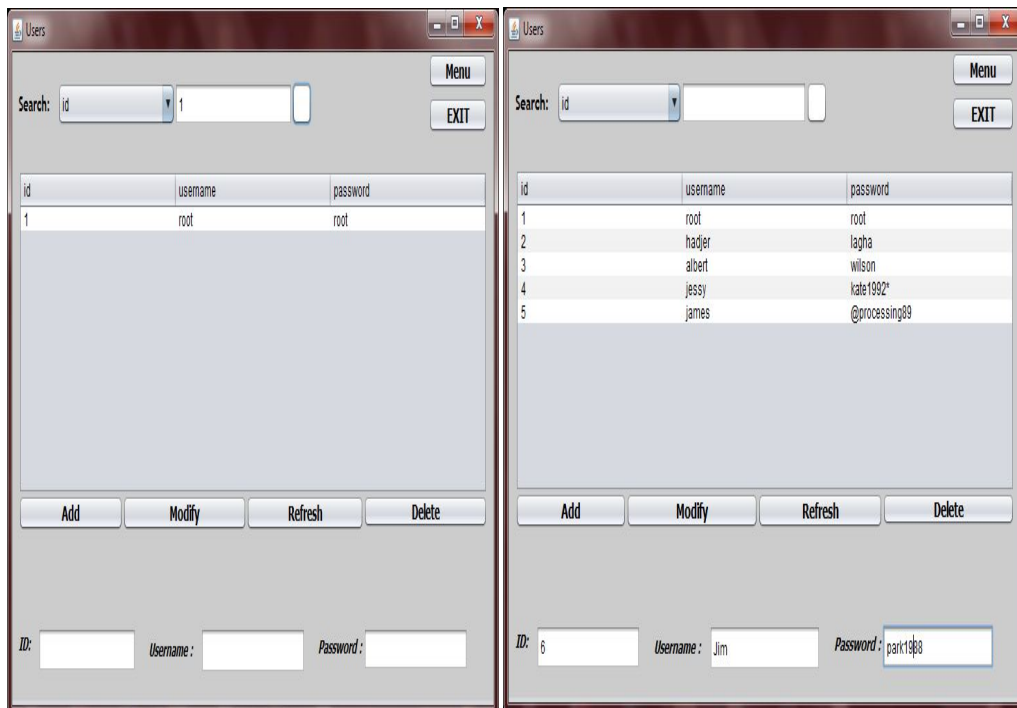


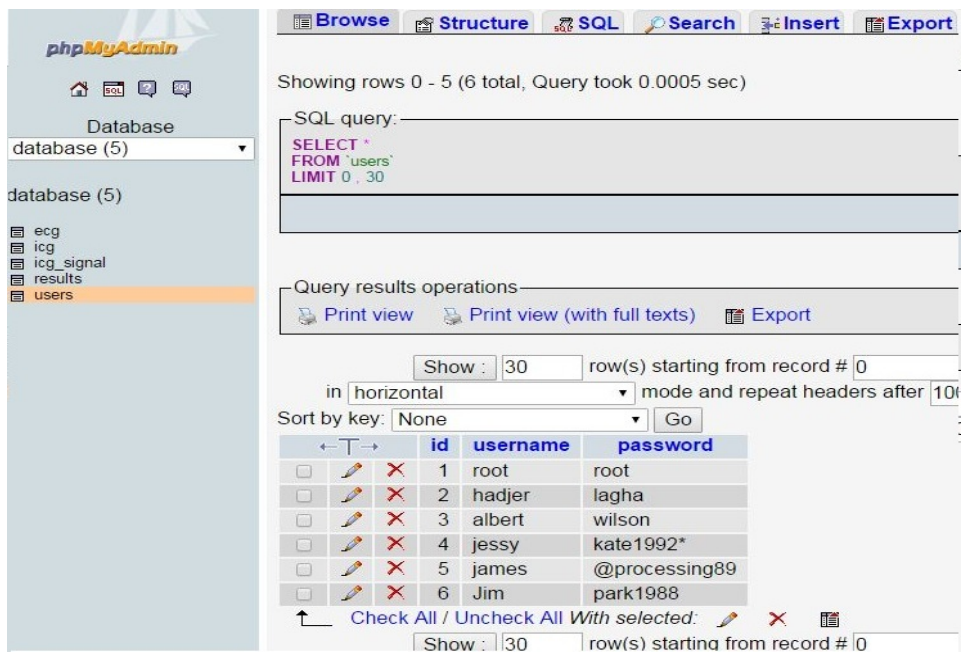
Figure 33: Menu interface.

Chapter VII: Telemedicine Application of ICG Signals



(a)

(b)



(c)

Figure 34: User's management interface; (a) search according to id, (b) add bottom option from the user interface, (c) add option saved to the server under the database.

Chapter VII: Telemedicine Application of ICG Signals

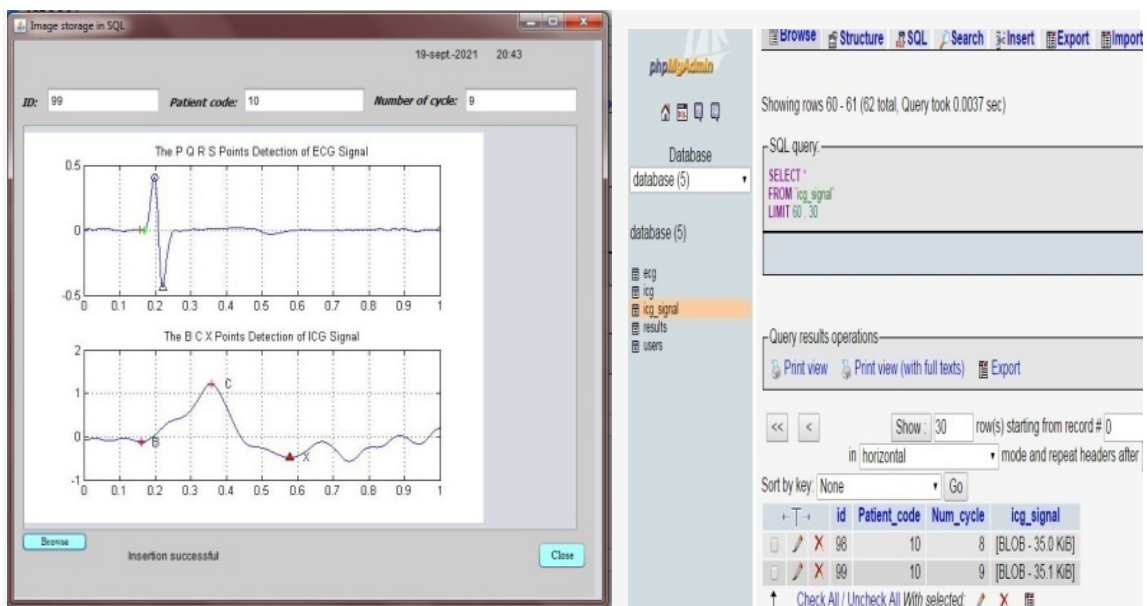
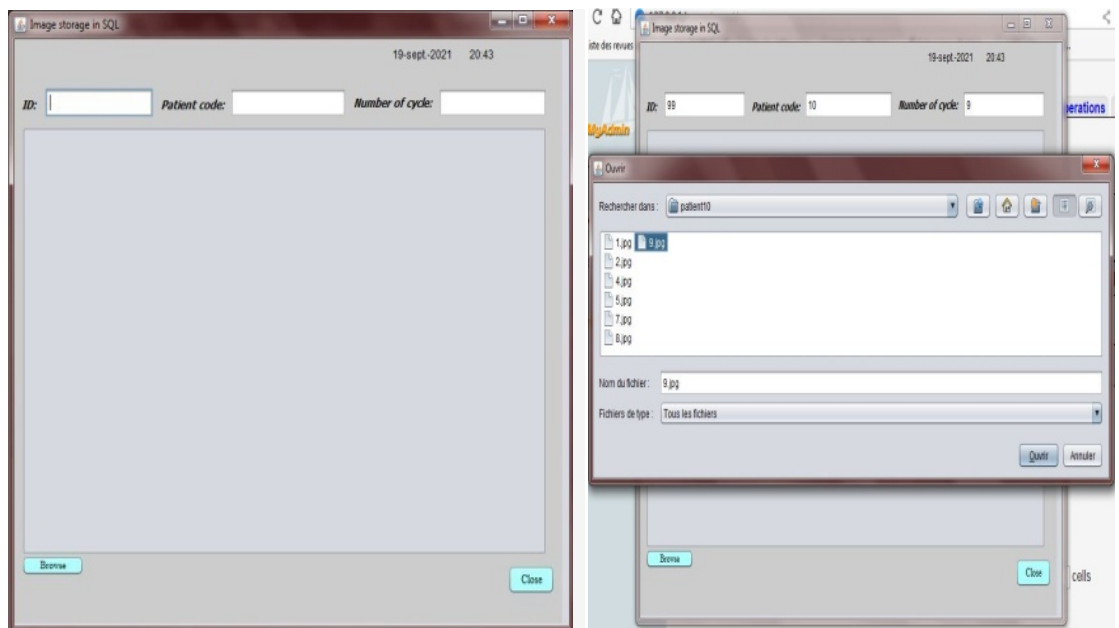
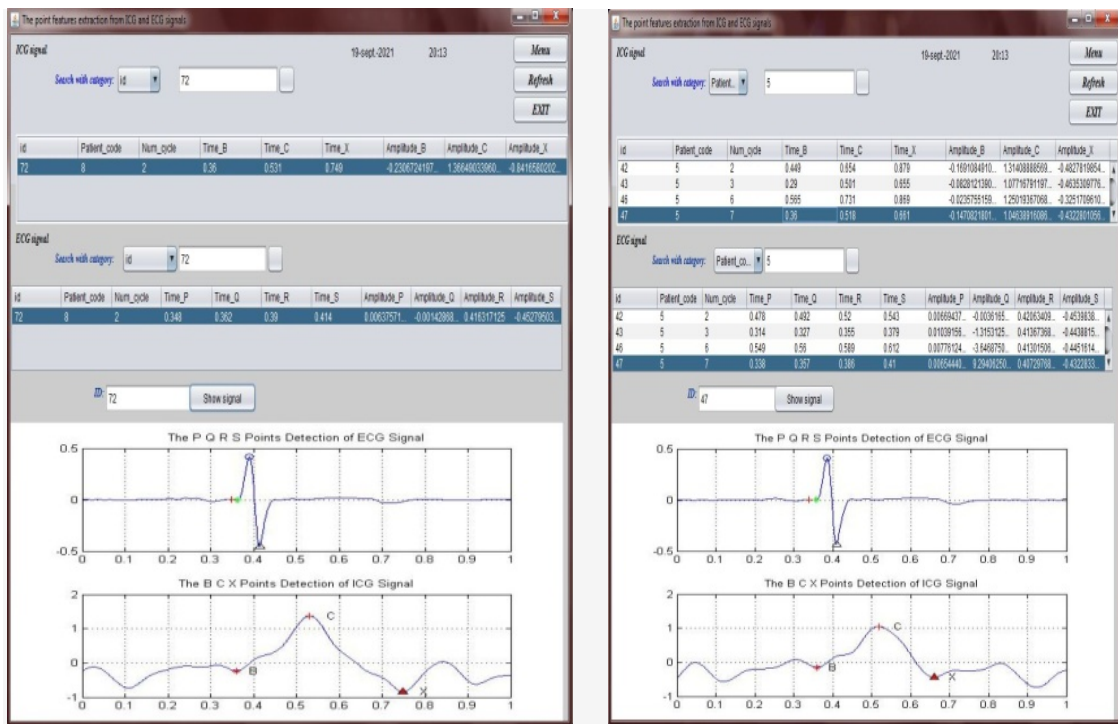


Figure 35: (a), (b), (c) and (d) The images storage interface from Netbeans to the MySQL database in table 'icg_signal'.

Chapter VII: Telemedicine Application of ICG Signals



(a)

(b)

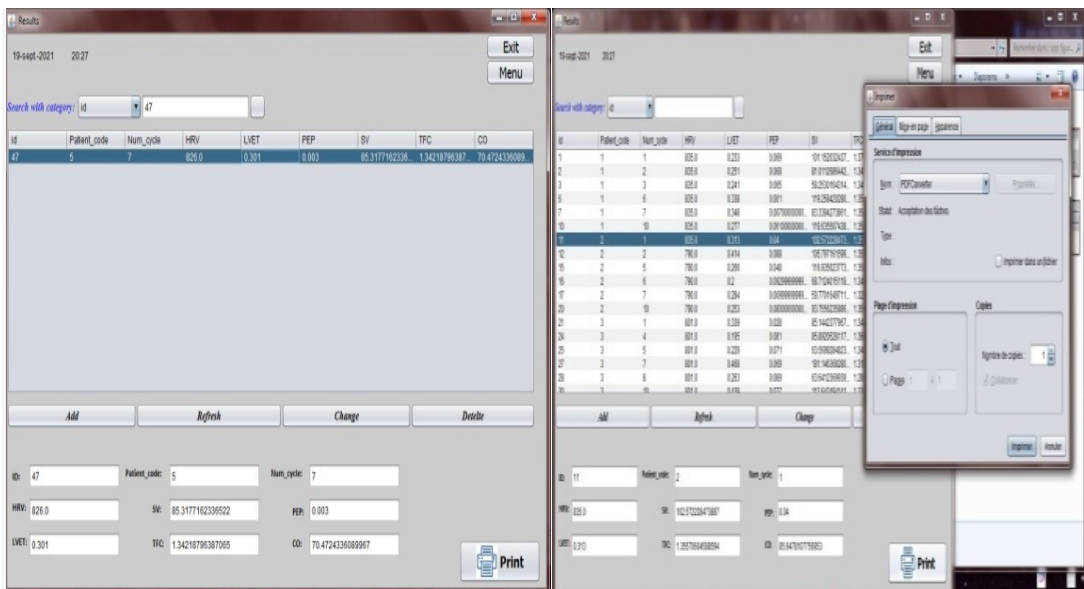


(c)

(d)

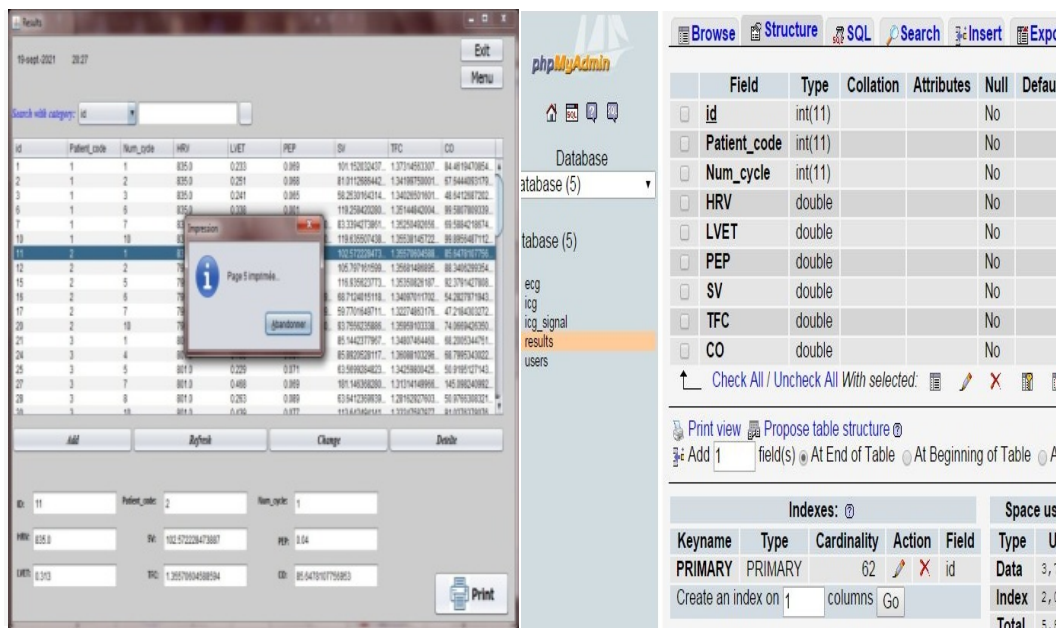
Figure 36: Signals interface. (a) search option with category id, (b) tables in the interface that presents the characteristics points of ICG and ECG signal processing in Matlab, (c) ecg table in the server, (d) icg table in the server.

Chapter VII: Telemedicine Application of ICG Signals



(a)

(b)



(c)

(d)

Figure 37: The Results interface. (a) search with category id, (b) print option, (c) complete impression of the results presented in textfields, (d) results table.

V. Conclusion

In this paper, we have presented several parties, where we present characteristic points BCX algorithm detection of the cardiography impedance signal (ICG) to measure various cardiac indices and calculate the time intervals as SV, CO, LVET and PEP.

The results obtained seem very satisfactory and help the patient's condition analysis. We have also presented another algorithm that allows us to record the values of the ICG signal obtained after its processing in the MySQL server, in parallel, a simple application that allows the insertion of the ICG images directly into the server.

This app helps physicians diagnose each patient by cardiac time interval and hemodynamic parameters either locally or remotely.

For future work, we can implement this algorithm and application to develop cardiography impedance systems more sophisticated for the non-invasive diagnosis and medical monitoring of patients.

REFERENCES

- [1] T. Boudreau, J. Glick, S. Greene, V. Spurlin, and J. J. Woehr, *NetBeans: the definitive guide: developing, debugging, and deploying Java code*. O'Reilly Media, Inc., 2002.
- [2] Matlab, S.: Matlab. The MathWorks, Natick, MA. (2012).
- [3] MySQL, A.B.: MySQL. (2001).
- [4] D. Ipswich, 'Setting up a WAMP server on your windows desktop', *Technology Now at Smashwords*, 2011.
- [5] H. Benabdallah and S. Kerai, 'Respiratory and Motion Artefacts Removal from ICG Signal Using Denoising Techniques for Hemodynamic Parameters Monitoring.', *Traitement du Signal*, vol. 38, no. 4, 2021.
- [6] A. Rana and K. K. Kim, 'Cardiac disease detection using modified Pan-Tompkins algorithm', *Journal of Sensor Science and Technology*, vol. 28, no. 1, pp. 13–16, 2019.

General Conclusion

General Conclusion

In this thesis, we have presented several monitoring methods, and we have shown the best choice of the best method according to the risk rate of the patient. Thus, we are based on the Bioimpedance that is one of the non invasive techniques. It consists of the analysis of the electrical impedance of biological tissues to diagnose and study the physiological and pathological state.

Nowadays, the most popular diseases are cardiovascular, for this reason, we are focused on impedance cardiography signals (ICG) that helps us to monitor and to detect the disorder earlier for diagnosis. It is non-invasive, low cost and simple in its implementation in the medical field especially in intensive unit care. The ICG method is promising in monitoring cardiac contraction and functional status.

We are presented with several denoising techniques such as SG, linear filter, adaptive filter and wavelets to noise cancellation from ICG signal, and we have chosen the best that perform better than others for each party.

To verify the effectiveness of the denoising technique we are based on the calculation of the denoising performance evaluation criteria.

We have discussed the possibility of evaluating the performance of ICG features extraction, which is based on the ECG signal simultaneous measurement, because the R wave is the reference peak used by several researchers to estimate A, B, C, X, and O points.

The automatic detection techniques are reliable, but the difference between them is the computational complexity, which varies from method to another.

They are applicable for the processed or unprocessed signal. The performance evaluation of the characteristic points on ICG waveforms helps us to measure time cardiac intervals as LVET.

Thus it allows us to calculate several cardiac indices as SV and CO cited above that are related to the heart mechanical activities process.

General Conclusion

In our detection algorithm we have based on two bells without using the reference of peak R, where it showed efficiency in results.

For this purpose, it is imperative to find an effective means to establish a correct detection method that identifies precisely the localization of the patterns for not disclosing the clinical diagnosis and the monitoring of cardiovascular diseases for patient health.

Finally, we have presented our application for automatic access that helps physicians diagnose each patient by cardiac time interval and hemodynamic parameters either locally or remotely.

To conclude we can say that our thesis purpose is the determination of cardiovascular parameters from the cardiac impedance signal by a non-invasive method with the creation of an application that helps doctors to diagnose and monitor their patients from distance via telemedicine.

CONFERENCES AND PUBLICATIONS

Conferences

- Member of the organizing committee and participation in the “8ème journée Doctorale de Génie Biomedical” (JD-GBM’2018) (paper titled: The Electrical Bioimpedance in Medical Diagnosis).
- International congress on health sciences and medical technologies 2018 (ICHSMT’18) (paper titled: The impedance Cardiography Technique in Medical Diagnosis)
- Member of the organizing committee and participation in the “9ème journée Doctorale de Génie Biomedical (JD-GBM’2019)” (paper titled: The performance Study of ICG Signal Denoising Methods)
- International congress on health sciences and medical technologies 2019(ICHSMT’19) (paper titled : Detection of A, B, C, X and O Patterns in ICG waveform for Stroke Volume and Cardiac Output Measurement).
- The “8ème journée de la maintenance biomédicale « biosmart&bioengineering » 2019” (paper titled :Case Study on the Adaptive LMS Filter and SVD Denoising Methods for Impedance Cardiography Signal)
- First international conference on innovation in biomechanics and biomaterials (ICIBAB2019) (paper titled: A comparative Study between the linear Filters for The ICG Signal Denoising).
- 3 rd international conference Biosciences 2019 Biotechnology and cancer (paper titled: The Electrical Bioimpedance Technique in Cancer Diagnosis)
- 2nd international conference on electronics and electrical engineering (IC3E’2020) (paper titled :A Novel Noise Reduction Technique Applied on ICG Waveform)
- 2021 IEEE IAS 6th International Conference on Computing, Communication and Automation (ICCCA) (paper titled : A Novel SVD Noise Cancellation Algorithm for ICG Signal) selected as the best paper.
- 2022 3rd International Conference on Electrical and Electronics Engineering (ICEEE 2022) (paper titled : Automatic Access Application of ICG and ECG Signals) selected as the best paper.

AD Webinars

- Scholarly book publishing with springer nature: insights on currente Book Trend-Algeria 2020
- How to easily find the results you are looking for on Springer Nature-Algeria 2020

Citations of published articles

- BENABDALLAH, hadjer, and S. Kerai. “The Impedance Cardiography Technique in Medical Diagnosis”. *Medical Technologies Journal*, Vol. 2, no. 3, Sept. 2018, pp. 232-44, doi:10.26415/2572-004X-vol2iss3p232-244.
- ICG Signal Noise Cancellation Algorithms for Non-invasive Hemodynamic Monitoring , by *Hadjer BENABDALLAH, Salim KERAI* , in press in *International Journal of Medical Engineering and Informatics*.

CONFERENCES AND PUBLICATIONS

- <https://www.inderscience.com/info/ingeneral/forthcoming.php?jcode=ijmei>
- Benabdallah, H., Kerai, S. (2021). Respiratory and motion artefacts removal from ICG signal using denoising techniques for hemodynamic parameters monitoring. *Traitement du Signal*, Vol. 38, No. 4, pp. 919-928. <https://doi.org/10.18280/ts.380401>

Abstract

The non-invasive ICG technique comes to solve the complex problem of measurement and analyzing heart diseases based on the thoracic electrical impedance change assessment that is due to blood velocity and resistivity changes to estimate several hemodynamic monitoring parameters. This type of signal is altered by artefacts' which distort the significant information of the signal. This distortion will cause clinicians to misdiagnose or monitor the pathological state of patients, for whom it is important to find techniques to eliminate noises without destroying the varied morphology of the signal. For this reason, our three denoising methodologies are based on several comparative studies between different tools of denoising concepts that aim to find the best automatic detection technique that is applied to 10 subjects. All these algorithms are implemented to develop an application of automatic access that help clinics to analyze ICG and electrocardiogram (ECG) signals, either locally or remotely. This application aims to make available all necessary information to doctors that help them to establish a fast and reliable diagnosis either locally or remotely. This application is automatic access to the real-time application used to optimize the quality of care and speed of diagnosis, whatever their geographical location. It is performed according to two criteria: information storage and data manipulation. This application is based on three softwares: Java Netbeans, Matlab, and WAMP / EASYPHP (MySQL) for web development.

Keywords-- ICG, ECG, Hemodynamic monitoring, Non-invasive, Denoising concept, Automatic detection, Automatic access application.

Résumé

La technique non invasive d'ICG vient pour résoudre le problème de la complexité de la mesure et de l'analyse des maladies cardiaques, basant sur l'évaluation de changement d'impédance électrique thoracique qui est dus aux changements de vitesse et de résistivité du sang afin d'estimer plusieurs paramètres de surveillance hémodynamiques. Ce type de signal est altéré par des artefacts qui ruinent l'information significative du signal. Cette distorsion pousse les cliniciens vers un mauvais diagnostic et une mauvaise surveillance de l'état pathologique des patients, dans lesquels il est important de trouver des techniques pour éliminer les bruits sans détruire la morphologie de notre signal. Pour cette raison, nos trois méthodologies de débruitage sont basées sur plusieurs études comparatives entre différents outils de concepts de débruitage qui visent essentiellement à trouver la meilleure technique de détection automatique appliquée à 10 sujets sains. Tous ces algorithmes sont mis en œuvre pour développer une application d'accès automatique qui aide les cliniques à analyser les signaux ICG et électrocardiogramme (ECG), soit localement, ou à distance. Cette application a pour objectif de mettre à disposition des médecins toutes les informations nécessaires pour les aider à établir un diagnostic rapide et fiable soit localement soit à distance. Cette application est un accès automatique en temps réel permettant d'optimiser la qualité des soins et la rapidité du diagnostic, quelle que soit leur situation géographique. Elle est réalisée selon deux critères : le stockage de l'information et la manipulation des données. Cette application est basée sur trois logiciels : Java Netbeans, Matlab, et WAMP/EASYPHP (MySQL) pour le développement web.

Mots clés-- ICG, ECG, Surveillance hémodynamique, Non invasif, Concept de débruitage, Détection automatique, Application d'accès automatique.

المخلص

تأتي تقنية ICG السطحية لحل مشكلة تعقيد قياس وتحليل أمراض القلب، بالاعتماد على تقييم التغيرات في المعاوقة الكهربائية الصدرية التي ترجع إلى التغيرات في سرعة ومقاومة الدم من أجل تقدير عدة مؤشرات مراقبة الدورة الدموية. يتم تغيير هذا النوع من الإشارات من خلال الآثار التي تدمر المعلومات المهمة للإشارة. يدفع هذا التشويه الأطباء نحو التشخيص الخاطئ والمراقبة السيئة للحالة المرضى، حيث من المهم إيجاد تقنيات للقضاء على الضوضاء دون تدمير الشكل الخارجي للإشارة. لهذا السبب، تستند منهجياتنا الثلاثة لتقليل الضوضاء على العديد من الدراسات المقارنة بين أدوات مفهوم تقليل الضوضاء المختلفة التي تهدف بشكل أساسي إلى إيجاد أفضل تقنية للكشف التلقائي المطبقة على 10 أشخاص أصحاء. يتم تنفيذ كل هذه الخوارزميات لتطوير تطبيق وصول تلقائي يساعد العيادات على تحليل وتخطيط القلب ECG إما محلياً أو عن بُعد. يهدف هذا التطبيق إلى تزويد الأطباء بجميع المعلومات اللازمة لمساعدتهم إشارات ICG على إجراء تشخيص سريع وموثوق. هذا التطبيق هو وصول تلقائي في الوقت الحقيقي لتحسين جودة الرعاية وسرعة التشخيص، بغض النظر عن موقعهم الجغرافي. يتم تنفيذه وفقاً لمعيارين: تخزين المعلومات ومعالجة البيانات. يعتمد هذا التطبيق على ثلاثة

برامج: Java Netbeans و Matlab و Wamp/EASYPHP (MySQL)

الكلمات الرئيسية -- ICG, ECG, مراقبة الدورة الدموية، مفهوم عدم التوغل، مفهوم تقليل الضوضاء، الكشف التلقائي، تطبيق الوصول التلقائي.